**Point by point response to the reviews**

I am happy to note that the authors finally acknowledge in their rebuttal that the extraction technique used is not really appropriate for analyzing intact polar lipids (IPLs) as it may cause changes in the distribution, especially with respect to the abundance of the relatively labile phospholipids. They now state in their manuscript "Soxhlet extractions, rather than for example microwave assisted Bligh-Dyer extractions, were chosen at the time because it was the only feasible way to handle the double 142mm filters. Extraction protocol surely can affect IPL distributions; as shown by Lengger et al. (2012) for smaller sediment samples." (lines 196-197). This is a bit weird since the Bligh Dyer extraction technique method was already published in 1959 and it remains unclear why this method could not be used on GFF filters. A quick search reveals that these kind of extractions were already described in 1997 (Macnaughton et al., Journal of Microbiological Methods, 31 19-27) so "at that time" is inappropriate phrasing. They should also specify what kind of effects this extraction technique has on IPL distributions, specifically on the abundance of phospholipids. The effects of their unconventional extraction method should be taken into account in interpreting the data in the whole manuscript.

Different extraction protocols will lead to different results, no matter which sample is analyzed or what the targeted analyte is; this is common knowledge in organic geochemistry. At the same time, there is probably not THE single extraction protocol that is superior to all others when we consider the great chemical diversity of compounds found in environmental samples, let alone the different sample matrices encountered. This said, most established protocols are reasonably good compromises, and so is soxhlet extraction, as long as the limitations are acknowledged. While in environmental chemistry standardization may be useful and practicable, organic geochemists have for decades used non-standardized protocols that are tailored to the sample matrix as well as to the infrastructure available in the respective laboratories. Likewise, the use of a different mass spectrometers or chromatographic separation techniques will probably have similar or greater effects as the criticized choice of an extraction protocol, as already shown for much simpler compounds in numerous round robin tests (for the paleo sea surface proxies TEX86 and UK37, Rosell-Melé et al., 2001, G3 2:2000GC000141Schouten et al., 2009, G3 10:Q03012; Schouten et al., 2013, G3 14:5263-5285;). This approach may limit quantitative comparisons with datasets produced in different laboratories, but certainly not within a coherent sample set with identical methods, as done in our study. It is imperative among organic geochemists to acknowledge these differences and keep these in mind when interpreting the resulting data.

In fact, we have acknowledged that there may be issues with soxhlet extraction technique – hardly "unconventional" - but stand by our use of soxhlet extractions for the very large filters needed to collect particles at low seawater concentrations in the deep ocean: our "at that time" is entirely appropriate. We have pointed this fact out in the revised manuscript. It is true that the Bligh-Dyer protocol has been around for decades, as we know, but as used by other investigations with much smaller and/or freeze-dried samples, it simply will not work for large, seawater saturated filters. We have published papers over two decades using soxhlet for large filters (originally the filters were even larger) (e.g., Wakeham et al., 1995, DSR-I 42:1749-

1771; DeLong et al., 1998, AEM 64:1133-1138; Wakeham et al., 2004, Chem.Geol. 205:427-442; Wakeham et al., 2007, OGC 38:2070-2097; Schubotz et al., 2009, EM 11:2720-2734; Sáenz et al., 2011, OGC 42:1351-1362; Rush et al., 2012, OGC 53:80-87; Close et al., 2014, DSR-I 85:15-34). The referenced Macnaughton paper does not actually address the efficiency of soxhlet extractions, certainly not for large filters (Macnaughton used 0.25 cm sq filters vs the 2x147 (158 cm sq) mm filters we had), and actually did not measure IPLs. At the start of a soxhlet extraction, the solvent mixture is DCM:MeOH:water as in the Bligh-Dyer protocol (chloroform is no longer used for health reasons). The temperature of the DCM:methanol azeotrope in the soxhlet extraction is 35°C compared to 40°C or 60°C in microwave or ultrasonication protocols, and 80°C and 120°C in the ASE protocol of Macnaughton et al., so elevated temperature is not an issue. We do not see any reason why phospholipid compositions would be adversely affected. Further, to our knowledge there has not been a comprehensive comparison of extraction techniques that involved soxhlet vs. other protocols for the large samples and for the wide range of lipids we analyzed (in addition to those reported here), so we are unable to comment on this, except to say that more sensitive analytical techniques coming on-line may reduce to need for such large filter volumes.

I still read in the abstract "Abundant non-phosphorus 44 "substitute" lipids within the OMZ suggest that the indigenous microbes might be phosphorus limited (P 45 starved) at ambient phosphate concentrations of 1 to 3.5 µM, although specific microbial sources for many 46 of these lipids still remain unknown." The authors cannot talk about "abundant" because their extraction method does not allow to say anything about the abundance of one type of IPLs over another type of IPL as their extraction method leads to a bias in the distribution (especially if it relates to phospholipids. If the authors fail to build this concept into their manuscript, it remains flawed. I welcome the changes that have been made to Figure 4 (representation of minor IPLs) although (as indicated earlier) their extraction technique will have a substantial impact on the relative abundance of the phospholipids. In all tables and figures the authors present in this manuscript they have to mention in the legend or footnote that the extraction technique used has led to a discrimination of the phospholipids. Otherwise, presenting these data is not scientifically correct.

We reject the use of terms such as "flawed" or "scientifically incorrect". By the same criteria, much of the organic geochemical data and papers produced in the past decades were "flawed and incorrect", because they did not always with "the ideal" analytical protocol, especially when measured by modern standards.

As to this further comment on extraction, we have no evidence - nor is there any in the literature that we know of – that shows biases due to using soxhlet extraction, and in any event, we have noted in the revised manuscript that potential biases cannot be absolutely ruled out. Therefore, we have no reason not to be able to compare compound abundances within our sample set. We are confident that our results are not "flawed" or "scientifically incorrect". Nevertheless, we exchange "abundant" with "the presence" in the abstract.

It is also nice that the authors now provide data on the analyses of the mixtures of standards over time (the new. Fig. S1). However, the legend of the figure should explain what is shown in the first panel: is it the response of all IPLs comprising the standard mixture? Furthermore, they should specify the initial composition of the three standard mixtures in much more detail (concentration of the specified IPLs). The authors also report relative abundances of specific IPLs (e.g. GDGTs with a variety of polar head groups) but these IPLs are not represented by any of the IPL standards they use in their Standard Mix. How, are they able to derive mass spectrometric response factors for these IPLs. An explanation is required.

The plot in new Fig. S1 shows the slope of standards measured in different concentrations. We modified the figure caption to make this clearer. We only show select IPL standards to illustrate how response factors change over time. As stated in the methods section and shown in Suppl. Table 2 we used the commercially available standard 'Main phospholipid *Thermoplasma acidophilum*' as IPL-GDGT standard. These analyses were done at a time where we did not yet have our own standards for 1G-GDGT and 2G-GDGT, which we currently use besides the 'Main phospholipid *Thermoplasma acidophilum*' standard.

**List of relevant changes:**

Line 43 in the abstract: Changed "Abundant" to the "The presence of"

Changed caption of Suppl. Fig. 1: Fluctuations in (A) absolute and (B) relative responses of select commercially available IPL standards over time. The values represent the slope of standards measured in different concentrations (usually 100 pg to 10 ng injected on column). Standard Mix A, B and C represents newly prepared standard mixtures. The standard mix used in this study was from November 2015.

# Intact polar lipids in the water column of the Eastern Tropical North Pacific: Abundance and structural variety of non-phosphorus lipids

Florence Schubotz [1*], Sitan Xie [1,¶], Julius S. Lipp [1], Kai-Uwe Hinrichs [1], Stuart G. Wakeham[2]

[1]MARUM and Department of Geosciences, University of Bremen, 28359 Bremen, Germany

[2]Skidaway Institute of Oceanography, Savannah, GA 31411, USA

[¶]Current address: Wai Gao Qiao Free Trade Zone, 200131 Shanghai, China

[*]Corresponding author. MARUM, University of Bremen, Leobener Str. 13, Room 1070, 28359 Bremen, Germany. Tel: +49-421-218-65724. Fax: +49-421-218-65715. E-mail: schubotz@uni-bremen.de

**Keywords:** intact polar lipids, phospholipids, glycolipids, betaine lipids, ether lipids, oxylipins, phospholipid substitution, oxygen minimum zone

**Abstract**

Intact polar lipids (IPLs) are the main building blocks of cellular membranes and contain chemotaxonomic, ecophysiologic and metabolic information, making them valuable biomarkers in microbial ecology and biogeochemistry. This study investigates IPLs in suspended particulate matter (SPM) in the water column of the Eastern Tropical North Pacific Ocean (ETNP), one of the most extensive open ocean oxygen minimum zones (OMZ) in the world with strong gradients of nutrients, temperature and redox conditions. A wide structural variety in polar lipid head group composition and core structures exists along physical and geochemical gradients within the water column, from the oxygenated photic zone to the aphotic OMZ. We use this structural diversity in IPLs to evaluate the ecology and ecophysiological adaptations that affect organisms inhabiting the water column, especially the mid-depth OMZ in the context of biogeochemical cycles. Diacylglycerol phospholipids are present at all depths, but exhibit highest relative abundance and compositional variety (including mixed acyl/ether core structures) in the upper and core OMZ where prokaryotic biomass was enriched. Surface ocean SPM is dominated by diacylglycerol glycolipids that are found in photosynthetic membranes. These and other glycolipids with varying core structures composed of ceramides and hydroxylated fatty acids are also detected with varying relative abundances in the OMZ and deep oxycline, signifying additional non-phototrophic bacterial sources for these lipids. Betaine lipids (with zero or multiple hydroxylations in the core structures) that are typically assigned to microalgae are found throughout the water column down to the deep oxycline but do not show a depth-related trend in relative abundance. Archaeal IPLs comprised of glycosidic and mixed glycosidic-phosphatidic glycerol dibiphytanyl glycerol tetraethers (GDGTs) are most abundant in the upper OMZ where nitrate maxima point to ammonium oxidation, but

increase in relative abundance in the core OMZ and deep oxycline. The presence of non-phosphorus "substitute" lipids within the OMZ suggest that the indigenous microbes might be phosphorus limited (P starved) at ambient phosphate concentrations of 1 to 3.5 μM, although specific microbial sources for many of these lipids still remain unknown.

Deleted: Abundant

## 1. Introduction

Oxygen Minimum Zones (OMZ) are permanently oxygen-deficient regions in the ocean defined by $O_2$ concentrations <20 μM. They occur in areas where coastal or open ocean upwelling of cold, nutrient-rich waters drive elevated levels of primary production and the subsequent respiration of organic matter exported out of productive surface waters consumes oxygen faster than it is replaced by ventilation or by mid-depth lateral injections of oxygenated water. Low oxygen levels cause habitat compression, whereby species intolerant to low levels of oxygen are restricted to oxygenated surface waters (Keeling et al., 2010; Rush et al., 2012). But even these low levels of oxygen permit vertical migration of some zooplankton taxa into hypoxic waters (e.g., Seibel, 2011; Wishner et al., 2013). Oxygen depletion stimulates diverse microbial life capable of utilizing alternative electron acceptors for respiration under microaerobic conditions (e.g., Ulloa et al., 2012; Tiano et al., 2014; Carolan et al., 2015; Kalvelage et al., 2015; Duret et al., 2015). Important prokaryote-mediated processes within OMZs include denitrification and the anaerobic oxidation of ammonium (anammox), which together may account for 30-50% of the total nitrogen loss from the ocean to the atmosphere (Gruber, 2008; Lam and Kuypers, 2011). Modern day OMZs comprise ~8% of global ocean volume (Karstensen et al., 2008; Paulmier and Ruiz-Pino, 2009; Lam and Kuypers, 2011), but any expansion in the coming decades as a consequence of global warming and increased stratification (Stramma et al., 2008; Keeling et al., 2010) would have profound effects on marine ecology, oceanic productivity, global carbon and nitrogen cycles, the biological pump and sequestration of carbon (Karstensen et al., 2008; Stramma et al., 2010; Wright et al., 2012). A better understanding of the effect of low-$O_2$ on marine biogeochemistry and microbial ecology is thus warranted.

The Eastern Tropical North Pacific Ocean (ETNP), situated off the west coast of Mexico and Central America, hosts one of the largest OMZs in the open ocean, extending halfway across the Pacific Ocean and comprising ~41% of global OMZs (Lavín and Fiedler, 2006; Fiedler and Talley, 2006; Paulmier and Ruiz-Pino, 2009). By comparison, OMZs of the Eastern Tropical South Pacific Ocean off Peru and Chile and in the Arabian Sea are ~14% and ~8%, respectively, of global OMZs. In the ETNP, a sharp permanent pycnocline develops where warm, saline surface waters lie on top of a shallow thermocline, producing a highly stratified water column. Moderate primary production, dominated by picoplankton, depends on oceanic upwelling and wind mixing of coastal waters but is generally limited by the lack of micronutrient dissolved iron (Franck et al., 2005; Pennington et al., 2006). Remineralization, ~70% of which is microbially mediated (Cavan et al., 2017), of particulate organic carbon exported out of surface waters consumes oxygen at rates that cannot be balanced by ventilation across the pycnocline and by sluggish lateral circulation, leading to $O_2$ levels <2 μM at depths between ~100 and ~800 m. Abundances of micro- (Olson and Daly, 2013) and macro-zooplankton (Wishner et al., 2013; Williams et al., 2014) that are high in surface waters are reduced in the OMZ, and those macrozooplankton that are diel vertical migrators survive in the OMZ with reduced metabolic rates (Maas et al., 2014; Cass and Daly, 2015). Microbial abundances and activities for both heterotrophic and chemoautotrophic metabolisms are high in both surface waters and within the OMZ, but again with reduced metabolic rates in the OMZ (Podlaska et al., 2012). A strong nutricline indicates microbial nitrogen cycling involving co-occurring nitrification, denitrification and anammox (Rush et al., 2012; Podlaska et al., 2012), perhaps contributing up to 45% of the global pelagic denitrification (Codispoti and Richards, 1976). Microbial communities are mainly comprised of proteobacteria, with increasing contributions of archaea in deeper waters. Yet, on

89 average ca. 50% of the prokaryotic communities within the OMZ of the ETNP remained uncharacterized
90 (Podlaska et al., 2012).

91 Intact polar lipids (IPLs) are the main building blocks of cellular membranes and may be used to
92 characterize abundance and physiology of aquatic microorganisms from all three domains of life. IPLs
93 represent a diverse range of molecular structures, including phosphatidyl, glycosidic, phospho-glycosidic,
94 and amino acid polar head groups linked to glyceryl-acyl and glyceryl-*O*-alkyl apolar moieties. IPL
95 distributions have been documented in surface waters of the Eastern Subtropical South Pacific (Van Mooy
96 and Fredricks, 2010), the Western North Atlantic Ocean (Van Mooy et al., 2006; 200; Popendorf et al.,
97 2011a), the South Pacific Ocean (Kharbush et al., 2016), the Mediterranean Sea (Popendorf, et al., 2011b),
98 the North Sea (Brandsma et al., 2012), lakes (Bale et al., 2016), the Western English Channel (White et
99 al., 2015) and throughout the water columns of stratified water bodies (Ertefai et al., 2008; Schubotz et
100 al., 2009; Wakeham et al., 2012; Pitcher et al., 2011; Xie et l., 2014; Basse et al., 2014; Sollai et al., 2015).
101 Surface waters are typically dominated by nine IPL classes. Three diacylglycerol glycolipids,
102 monoglycosyl (1G-), diglycosyl (2G-) and sulfoquinovosyl diacylglycerol (SQ-DAG), are main IPLs
103 found in all thylakoid membranes of phototrophs, including those of cyanobacteria (Siegenthaler et al.,
104 1998)[1]. Three betaine lipids, diacylglyceryl homoserine (DGTS), hydroxymethyl-trimethyl-*β*-alanine
105 (DGTA) and carboxy-*N*-hydroxymethyl-choline (DGCC), are also generally abundant. Betaine lipids
106 are widely distributed in lower plants and green algae (Dembitsky, 1996) and are thus usually assigned to

[1] Elsewhere in the literature 1G-DAG, 2G-DAG, and SQ-DAG are also termed MGDG, DGDG and SQDG. However, we have opted to retain the 1G-DAG, 2-DAG, etc. nomenclature as other IPLs discussed throughout also contain monoglycosyl- and diglycosyl-moieties (e.g., 1G-GDGT and 2G-GDGT). Likewise, we retain the nomenclature PC-DAG, PE-DAG, and PG-DAG for phospholipids elsewhere termed PC, PE, PG.

eukaryotic algae in the ocean (Popendorf, et al., 2011a), but DGTS was recently also found in bacteria when phosphorus is limited (Yao et al., 2015; Sebastian et al. 2016). Three common detected phospholipids are diacylglycerol phosphatidyl choline (PC-DAG; often simply referred to elsewhere as PC), phosphatidyl ethanolamine (PE-DAG, often PE), and phosphatidyl glycerol (PG-DAG, often PG), all of which have mixed eukaryotic or bacterial sources in the upper water column (Sohlenkamp et al., 2003; Popendorf, et al., 2011a). Microbial source assignments have been broadly confirmed by isotope labeling studies (Popendorf, et al., 2011a). In oxygen-deficient subsurface waters IPL distributions are more diverse and other phospholipids such as diacylglycerol phosphatidyl (*N*)-methylethanolamine (PME-DAG), phosphatidyl (*N,N*)-dimethylethanolamine (PDME-DAG) and diphosphatidyl glycerol (DPG) increase in abundance; these IPLs occur in a number of bacteria that may inhabit low oxygen environments (Schubotz et al., 2009; Wakeham et al., 2012). Dietherglycerol phospholipids and glycosidic ceramides with unidentified sources have also been detected (Schubotz et al., 2009; Wakeham et al., 2012), the latter have been recently observed to be abundant in phosphorus-limited diatoms (Hunter et al., 2018). IPLs that are unique to marine archaea are comprised of glycerol dialkyl glycerol tetraethers (GDGT) core lipids with various glycosidic, diglycosidic and mixed phospho-glyco polar head groups (e.g., Schouten et al., 2008; Pitcher et al., 2011; Zhu et al., 2016; Elling et al., 2017). Abundances of archaeal IP-GDGTs vary considerably with depth, but are typically elevated in zones of water column oxygen depletion, especially where ammonium oxidizing thaumarchaea are abundant (Pitcher et al., 2011; Schouten et al., 2012; Sollai et al., 2015).

IPL can also be indicators of metabolic and physiologic status. Many organisms remodel their IPL composition when faced with environmental stressors such as changes in pH, salinity, temperature or

availability of nutrients (Zhang and Rock, 2008; Van Mooy et al., 2009; Meador et al., 2014; Carini et al., 2015; Elling et al., 2015). Replacing phospholipids with non-phosphorus containing substitute lipids is an important mechanism when facing nutrient phosphate starvation in oligotrophic surface waters where phosphate concentrations may be as low as nanomolar levels. Cyanobacteria replace PG-DAG with SQ-DAG (Benning et al., 1993; Van Mooy et al., 2006) and microalgae and some bacteria replace PC-DAG with DGTS (Geiger et al., 1999; Van Mooy et al., 2009; Popendorf, et al., 2011b) due to their similar ionic charge at physiological pH. Heterotrophic marine bacteria can replace PE-DAG with either 1G-DAG or DGTS (Carini et al., 2015; Sebastian et al., 2016; Yao et al., 2015). Notably, substitute lipids are also biosynthesized under micromolar concentrations of phosphate (Bosak et al., 2016).

Here, we use IPL distributions in suspended particulate matter (SPM) to characterize eukaryotic, bacterial and archaeal communities inhabiting the water column of the ETNP. This study is an extension of that of Xie et al. (2014), which focused on the distribution of core and intact polar archaeal and bacterial tetraether lipids at two stations investigated here (stations 1 and 8). The water column of the ETNP comprises distinct biogeochemical zones based on oxygen concentrations and IPL distributions reflect the localized ecology. Abundant non-phosphorus substitute lipids within the core of the OMZ suggest phosphorus limitation of the source microorganisms even at micromolar concentrations of phosphate. Overall our results provide deeper insight into the broad community composition and the physiologic state of microorganisms inhabiting OMZs.

## 2. Methods

### *2.1 Sample collection and CTD data*

149 Suspended particulate matter (SPM) samples were collected at four stations (distance to shore:
150 400~600 km; Fig 1) along a northwest-southeast transect (Station 1: 13° 01.87'N，104° 99.83'W; Station
151 2: 11° 99.96' N，101° 22.82' W; Station 5: 10° 68.94' N，96° 34.12' W; and Station 8: 8° 99.46'N，
152 90°00.18'W) in the ETNP during the R/V *Seward Johnson* cruise in November 2007 (R/V *Seward Johnson*
153 Cruise Scientists, 2007). Station 1 in the Tehuantepec Bowl is an area of relatively low primary
154 productivity (e.g., 0.05 mg Chl-*a*/$m^2$; (Fiedler and Talley, 2006; Pennington et al., 2006) whereas Station
155 8 in the Costa Rica Dome is moderately productive (1 mg Chl-*a*/$m^2$). All stations are characterized by a
156 strong thermocline/pycnocline/oxycline (at 20-50 m depths depending on location) and a profound and
157 thick OMZ (down to ~2 μM $O_2$ between ~300-800 m depth). Station 1 is a reoccupation of the Vertical
158 Transport and Exchange II/III site from the early 1980's (Lee and Cronin, 1984; Martin et al., 1987;
159 Wakeham and Canuel, 1988; Wakeham, 1987, 1989).
160 Seawater was filtered *in-situ* using submersible pumps (McLane Research Laboratories WTS-142
161 filtration systems) deployed on the conducting cable of the CTD/rosette that measured temperature,
162 conductivity, oxygen, fluorescence/chlorophyll-*a* and transmissivity during pump deployments and
163 during pumping. Filtered water volumes ranged between 130 and 1800 L (Suppl. Table 1). Pumps
164 were fitted with two-tier 142 mm diameter filter holders: a 53 μm mesh Nitex "prefiltration" screen to
165 remove larger eukaryotes and marine snow aggregates and a double-stacked tier of ashed glass fiber filters
166 (142 mm Gelman type A/E, nominal pore size 0.7 μm). IPL concentrations we report represent minimum
167 values to reflect potentially inefficient collection of 0.7 μm particles by GFFs. Since pore size of the
168 filters may also decrease during filtration the recovered material may vary dependent on filtration time.

169 Following pump recovery, GFF filters and Nitex screens were wrapped in pre-combusted foil and stored
170 frozen at -20°C until extraction.
171
172 *2.2 Elemental, pigment and nutrient analysis*
173 Particulate organic carbon (POC) and total particulate nitrogen (TN) were measured on 14 mm-
174 diameter subsamples of each glass fiber filter (GFF) prior to lipid extraction; therefore, POC and TN
175 concentrations reported here are only for <53 µm material. The plugs were acidified in HCl vapor in a
176 desiccator for 12 hours to remove inorganic carbon. Elemental analysis was performed with a
177 ThermoFinnigan Flash EA Series 1112 interfaced to a ThermoFinnigan Delta V isotope ratio mass
178 spectrometer at the Skidaway Institute Scientific Stable Isotope Laboratory. Organic carbon and
179 nitrogen contents were calibrated against internal laboratory chitin powder standards which in turn had
180 previously been cross-calibrated against USGS 40 and 41 international standards.
181 Chlorophyll-*a* (Chl-*a*) and pheopigment concentrations were measured on-board the ship (Olson and
182 Daly, 2013). Seawater samples (100 – 500 ml) from CTD casts were filtered onto Whatman GF/F filters
183 (0.7 µm) which were immediately extracted with 90% acetone. Fluorescence was measured with a
184 Turner Designs 10AU fluorometer and Chl-*a* concentrations were determined after Parsons et al (1984).
185 Post-cruise HPLC analysis of pigments in 100 − 500 ml seawater samples filtered onto Whatman GF/F
186 (0.7 µm) filters were conducted at the College of Charleston Grice Marine Laboratory, Charleston, SC on
187 a Hewlett Packard 1050 system (DiTullio and Geesey, 2002).
188 Seawater samples for nutrient analyses ($NO_2^-$, $NO_3^{-2}$, $NH_4^+$ and $PO_4^{3-}$) were collected directly from
189 Niskin bottles into acid-washed, 30-mL high-density polyethylene (HDP) bottles. After three rinses,

bottles were filled to the shoulder, sealed, and frozen (−20°C). All frozen samples were transported to the Oceanic Nutrient Laboratory at USF for analysis using a Technicon Autoanalyzer II.

*2.3 Lipid extraction and analysis of intact polar lipids*

Lipids associated with the <53 µm SPM on the GFFs were Soxhlet-extracted shortly after the expedition in 2008 using dichloromethane:methanol (DCM:MeOH; 9:1 v/v) for 8 h. Extracted lipids were partitioned into DCM against 5% NaCl solution and dried over $Na_2SO_4$. Total lipid extracts (TLEs) were stored at -20°C. Soxhlet extractions, rather than for example microwave assisted Bligh-Dyer extractions, were chosen at the time because it was the only feasible way to handle the double 142mm filters. Extraction protocol surely can affect IPL distributions; as shown by Lengger et al. (2012) for smaller sediment samples.

IPL analyses by high-performance liquid chromatography-mass spectrometry (HPLC-MS) were carried out initially in 2010/2011 and again in 2015 as instrument protocols improved. In between these analyses we did not observe a notable selective loss of IPL compounds, instead we were able to detect a much larger suite of IPL structures due to improved detection and chromatographic separation techniques (Wörmer et al., 2013). The confidence in these results are supported by the analysis of IPL standards (Suppl. Table 2) that are stored at -20 °C over several years (fresh standard mixtures are typically prepared every 2 to 3 years), which do not indicate degradation of any particular IPL over time (Suppl. Fig. 1). The analysis in 2010/2011 focused on absolute concentrations of the major IPLs (for distinction between major and minor IPLs see results section). Aliquots of the TLE were dissolved in DCM/methanol (5:1 v/v) for injection on a ThermoFinnigan Surveyor HPLC system coupled to a ThermoFinnigan LCQ

211 DecaXP Plus ion-trap MS via electrospray interface (HPLC-ESI-IT-$MS^n$) using conditions described
212 previously (Sturt et al., 2004; Xie et al., 2014). Ten µL of a known TLE aliquot spiked with $C_{19}$-PC as
213 internal standard was injected onto a LiChrosphere Diol-100 column (150 × 2.1 mm, 5 µm, Alltech,
214 Germany) equipped with a guard column of the same packing material. Absolute IPL concentrations
215 were determined in positive ionization mode with automated data-dependent fragmentation of the two
216 most abundant base peak ions. Acyl moieties of glycolipids and aminolipids were identified via HPLC-
217 IT-ESI-$MS^2$ experiments in positive ionization mode, whereas phospholipid side chain composition was
218 analyzed in negative ionization mode. Details of mass spectral interpretation, and identification of fatty
219 acid moieties are described in Sturt et al. (2004) and Schubotz et al. (2009) and are exemplified in Suppl.
220 Table 3. HPLC-MS analysis is not able to differentiate between double bonds or rings, therefore in the
221 subsequent text we will refer to double bond equivalents (DBE) to include both possibilities, similarly
222 absolute chain length cannot be determined as branched and straight chain alkyl chains cannot be
223 differentiated, therefore we report total carbon atom numbers for the alkyl side chains. Assignment of
224 the betaine lipid DGTS was according to the retention time of the commercially available standard DGTS
225 (Avanti Polar Lipids, USA). The isomer DGTA, which elutes at a different retention time due to its
226 structural difference (e.g., Brandsma et al., 2012) was not observed in the HPLC-MS chromatograms.
227 For all analyses, response factors of individual IPLs relative to the injection standard $C_{19}$-PC were
228 determined using dilution series of commercially available standards (Suppl. Table 2).
229 Subsequent analyses in 2015 were used to obtain sum formulas and IPL structures based on exact
230 masses in the MS1 and MS-MS experiments and to additionally provide data on minor lipids, which were
231 below detection limit during the 2010/2011 ion trap analyses (for distinction between major and minor

232 lipids see results section). For these measurements absolute quantities could not be determined since the
233 TLE had been used for other experiments and the information on TLE amounts used was unknown;
234 therefore, these analyses are used to describe relative abundances. Analyses were performed on a Bruker
235 maXis Plus ultra-high resolution quadrupole time-of-flight mass spectrometer (Q-TOF) with an ESI
236 source coupled to a Dionex Ultimate 3000RS UHPLC. Separation of IPLs was achieved using a Waters
237 Acquity UPLC BEH Amide column as described in Wörmer et al. (2013), which resulted in better
238 chromatographic separation of compounds and higher sensitivity compared to the 2010/2011 analyses.
239 Relative proportions of compounds were quantified taking the different response factors of IPL classes
240 into account. Peak areas in extracted mass chromatograms were corrected with absolute response factors
241 determined in dilution series of commercially available standards (Suppl. Table 2). Some ions assigned
242 to either PE-AEG and PC-AEG could not be quantified individually due to co-elution of these compounds
243 and were thus quantified as one group using the mean response factor of PE- and PC-DAG. For
244 compound classes for which no standards were available, (e.g., PI-DAG, OL and the unknown aminolipids
245 AL-I and AL-II) the relative responses could not be corrected for. Assuming these compounds may
246 ionize similarly as structurally related IPLs, values may be off by a factor of 0.2 to 1.4, which is the
247 maximum range of response factors observed for the standards.
248
249 *2.4 Statistical analysis*
250 Nonmetric multidimensional scaling (NMDS) analysis was used to illustrate the relationships
251 among objects hidden in a complex data matrix (Rabinowitz, 1975) and was performed in the free software
252 R (version 3.4.3, www.r-project.org/) with *metaMDS* (vegan library, version 2.4-6) as described by

253 Wakeham et al. (2012). The datasets of relative lipid distribution and variations in carbon number and
254 double bond equivalents were standardized by Hellinger transformation using the function *decostand*,
255 while for all other variables (environmental parameters, microbial groups) absolute numbers were used.
256 The compositional dissimilarity was calculated by Euclidean distance measure. The resulting plot shows
257 the distribution of lipids and sampling depths. Microbial groups and geochemical parameters were
258 overlaid by function *envfit*. Lower stress is related to high quality of solution, and stress values ≤ 0.1
259 indicate results of good quality (Rabinowitz, 1975). Non-parametric Spearman Rank Order Correlation
260 analysis was performed on combined data of environmental variables and IPL ratios and IPL relative
261 abundances of all four stations using SigmaPlot 11.0 (Systat Software Inc., San Jose, USA).
262
263 **3. Results**
264 *3.1 Biogeochemical setting*
265 All along the transect, the thin mixed layer (upper ~20 m) was warm, ~25−28 °C, with oxygen
266 concentrations approaching air saturation at ~200 µM (Fig. 2). The euphotic zone (1% of surface
267 photosynthetically active radiation) generally ranged between 50 and 80 m depth. The thermocline was
268 abrupt at ~20-50 m, where temperatures dropped to ~15−18 °C and oxygen decreased to ~20 µM.
269 Temperatures stabilized by ~250−300 m depth at ~10−12 °C and oxygen levels were <2 µM; especially
270 at Station 8 there were spatially and temporally variable oxygen intrusions into the upper portion of the
271 OMZ. By ~600−800 m depth, a deep oxycline was observed where oxygen concentrations began to rise
272 again to ~40 µM at temperatures of ~4 °C by 1250 m. For the purposes of this discussion, the water
273 column of the ETNP was partitioned into four horizons based on oxygen content: an oxic epipelagic zone

down to the thermocline (0–50 m; 200 μM > $O_2$ > 20 μM); an upper OMZ (Station 1 and 8: 50–300 m, Station 5: 50 – 350 m, Station 2: 50–200 m; 20 μM > $O_2$ > 2 μM); the core OMZ (Station 1 and 8: 300–800 m, Station 5: 350 – 600 m Station 2: 200 – 600 m; $O_2$ < 2 μM); and a deep oxycline (Station 1 and 8 ≥ 800 m, Station 2 and 5 ≥ 600 m; $O_2$ > 2 μM) of rising $O_2$ levels (Fig. 1a). Note that sampling at stations 1 and 8 reached to 1250 m depth so SPM from >750 m depth best represents the deep oxycline.

Chl-*α* was highest in surface waters with maximum values of 1.8 μg/L at 10 m at station 5, was between 0.2 and 0.7 μg/L at station 1, 2 and 8 and decreased to values close to zero below 100 m at all stations (Fig. 2; see also Fiedler and Talley, 2006, and Pennington et al., 2006, for additional results from previous surveys). HPLC analysis of accessory pigments (Goericke et al., 2000; Ma et al., 2009) showed that picoplankton, primarily *Prochlorococcus* (indicated by divinyl chlorophyll *α*), were an important component of the photoautotrophic community, along with diatoms (fucoxanthin), especially *Rhizosolenia* at the deep fluorescence maximum at stations 1 and 5 but *Chaetoceros* at station 8, and prymnesiophytes (19'hexanoyloxyfucoxanthin and 19'butanoyloxyfucoxanthin; DiTullio and Geesey, 2002; Suppl. Table 4). High phaeopigment abundances (up to 90% of [Chl-*α* + phaeopigments]) attested to algal senescence or grazing by macro- (Wishner et al., 2013; Williams et al. 2014) and micro-zooplankton (Olson and Daly, 2013) above and into the oxycline. Primary maxima in transmissivity corresponded with the peak Chl-*α* concentrations and fluorescence maxima, but secondary transmissivity maxima between 300 and 400 m at stations 1, 5, and 8 indicated elevated particle abundances in the core of the OMZ (Fig. 2).

Nitrite ($NO_2^-$) maxima in the OMZ at all stations coincided with nitrate ($NO_3^{2-}$) deficits (Fig. 3). Ammonium ($NH_4^+$) concentrations changed little through the water column (Fig. 3). Phosphate ($PO_4^{3-}$; Fig. 3) and total dissolved nitrogen (TDN; not shown) were low (respectively, < 0.5 and < 3 μM) in the

upper 20 m of the oxic zone, but increased in the OMZ. High $PO_4^{3-}$ (up to 3.4 µM) and high TDN (up to 44.5 µM) were observed in the deep OMZ at stations 2, 5 and 8 (Fig. 3). N:P ratios were lower than the Redfield ratio (16) at all sites and depths (Fig. 3); N:P minima were lowest in surface waters (2.6 to 10 in the upper 20 m) and at ~500 m within the core OMZ and the deep oxycline at station 1 (<9).

POC and TN concentrations (< 53 µm material) were highest in the euphotic zone (POC: 20 – 100 µg/L; TN: 4 – 15 µg/L), rapidly dropping to 5 µg/L and 1 µg/L below the upper OMZ, respectively (Fig. 2; Suppl. Fig. 2). Secondary maxima for POC (~10 µg/L) and TN (~2 µg/L) within the core of the OMZ might reflect elevated microbial biomass there. Concentrations dropped in the deep oxycline to ≤3 µg/L and ≤0.5 µg/L for POC and TN, respectively.

Absolute IPL concentrations were determined by ion trap LCMS and varied between 250 and 1500 ng/L in the oxic zone and abruptly decreased more than 10-fold (to <20 ng/L) in the upper OMZ (Fig. 2). Secondary maxima in IPL concentrations (15–40 ng/L) within the OMZ at all stations roughly coincided with elevated numbers of prokaryotes (Fig. 2). IPL:POC ratios decreased with increasing depth (Fig. 2), tracking trends of POC, TN and IPL concentrations.

*3.2 Changes in IPL composition with water column depth in the ETNP*

In total, 24 IPL classes were identified in the ETNP (Fig. 4, Suppl. Fig. 3). Eleven major and thirteen minor IPL classes were detected in the QTOF analyses, which were classified according to their relative abundance: if an individual IPL comprised more than 10% of total IPLs at any depth of the four stations it was classified as a major IPL, compounds <10% were minor IPLs. Based on their head group composition IPLs were grouped into glycolipids, phospholipids or aminolipids. Figure 3 shows changes

316 in the relative abundances (as percentages of total IPLs, excluding isoprenoidal archaeal IPLs) of
317 glycolipids, phospholipids and aminolipids as well as several substitute lipid ratios, reflecting preferential
318 biosynthesis of non-phosphorus lipids to replace phospholipids under phosphate-limiting growth (cf. Van
319 Mooy et al., 2006; Popendorf, et al., 2011b; Carini et al., 2015; Bosak et al., 2016). Relative abundances
320 of non-isoprenoidal phospholipids were highest in the core OMZ between 400 and 600 m at all sites,
321 where they comprise up to 45−76% at stations 1, 2 and 5 and between 12 and 61% at station 8.
322 Phospholipid abundances were lower within the upper OMZ and oxic zone at all stations (between 4 and
323 55%) and in the deep oxycline at station 8 (<1%). Aminolipid content was highest in SPM from the
324 upper 55 m at station 5 and 8 (10 to 25%), the core OMZ at station 8 (15 to 34%) and the deep oxycline
325 at station 1 (17%). Lower aminolipid contents (2 to 11%) were observed in the oxic zone and the core
326 OMZ at stations 1 and 2, the upper OMZ at station 5 (0 to 11%) and the deep oxycline at station 8 (<2%).
327 Glycolipid abundance was >9% at all depths, with highest abundance (average 54%, max. 82%) within
328 the upper OMZ and oxic zone at all stations and the deep oxycline at station 8. Values down to 9% were
329 observed within the core OMZ.
330
331 *3.2.1 Major lipids*
332 The eleven major IPL classes included three IP-GDTs of archaeal origin: (1G-GDGT, 2G-GDGT and
333 HPH-GDGT); and eight IPLs assigned to either a bacterial or eukaryotic origin: three glycolipids (1G-
334 DAG, 2G-DAG, SQ-DAG), four phospholipids (PG-DAG, PE-DAG, PC-DAG, PE+PC-AEG) and one
335 aminolipid (DGTS). All major lipid classes were found at almost all depths at all four stations, but with
336 varying relative abundances (as % of total IPL; Fig. 4, Suppl. Table 1).

337 *Archaeal IP-GDGTs*: Relative abundances of archaeal IPL (IP-GDGTs) generally increased with
338 depth from non-detectable in surface waters to >50% of total IPLs at station 8 (bottom of core OMZ and
339 deep oxycline). Archaeal IP-GDGT abundances at stations 1 and 2 peaked at 30% (bottom of upper
340 OMZ, core OMZ and deep oxycline) but were generally <10% at station 5 (Fig. 4). At station 1 and 2,
341 1G-GDGT and 2G-GDGT were most abundant with variable amounts of HPH-GDGTs, whereas 1G-
342 GDGT and HPH-GDGT dominated archaeal IPLs at station 5 and 8 at most depths. Distributions of
343 glycosidic IPL-GDGTs obtained in the present investigation corroborate the absolute values reported by
344 (Xie et al., 2014) for stations 1 and 8: 1G-GDGT was more abundant than 2G-GDGT at station 8 when
345 compared to station 1. The core GDGTs of 1G-GDGTs and HPH-GDGTs are dominated by GDGT-0
346 and crenarchaeol (Suppl. Fig. 4), whereas 2G-GDGTs are dominated by GDGT-2 and a small amount of
347 crenarchaeol (Zhu et al., 2016)
348 *Diacylglycerol lipids*: The oxic zone and the upper OMZ were dominated (~50−80% of IPL) at all
349 sites by the diacylglycerol glycolipids, 1G-DAG, 2G-DAG and SQ-DAG (Fig. 4). In the core OMZ and
350 deep oxycline, relative amounts of 2G-DAG and SQ-DAG decreased to 4% and 12%, respectively. 1G-
351 DAG abundances were lowest in the core OMZ at all stations, but were up to 47% of total IPL in the deep
352 oxycline. Diacylglycerol phospholipids, PE-, PG- and PC-DAG, were the second most abundant IPLs.
353 Abundances of PE- and PG-DAG were highest within the upper and core OMZ, constituting >50% in the
354 core OMZ at station 1, >30% at stations 2 and 5, and 16% at station 8. PC-DAG, with average
355 abundances of 5% at stations 1, 2, 8 and 3% at station 5, did not exhibit depth-related trends. The third
356 most abundant diacylglycerol class was the betaine lipid DGTS, which was present throughout the water
357 column at average abundances of 7% at station 1, 2 and 8, and 5% at station 5.

Major diacylglycerol lipids showed changes in average number of carbon atoms and double bond equivalents (DBE) with depth (Fig. 5, Suppl. Table 5). The glycolipids and PC-DAG decreased in average carbon number by up to three carbons and decreased in DBE by up to 2 at the top of the upper OMZ and within the core OMZ compared to the oxic zone and the deep oxycline. Average carbon numbers for PE- and PG-DAG and DGTS showed an inverse trend, both generally increasing up to two carbons between the upper OMZ and the core OMZ. Changes in DBE were not as pronounced for PG-DAG and DGTS, on average 1 to 2 DBE greater in surface waters than in deeper waters, while the number of DBE increased on average with depth for PE-DAG.

*Acyl-ether glycerol lipids*: Mixed ether-ester glycerol core structures with either PE or PC head groups were observed at all stations and all depths (generally 4-12%) except for the deep oxycline at station 8.

*3.2.2 Minor lipids*

Thirteen minor IPL classes were identified, five of which were glycolipids, four phospholipids and four aminolipids. All minor lipid classes were detected at each site except for OH-DGTS which was absent at station 1. Some minor lipids were found at all depths, whereas others were restricted to specific depth zones as defined by oxygen content (Fig. 4).

*Diacylglycerol lipids:* Two minor diacylglycerol glycolipids, 1G-OH-DAG and 3G-DAG, were most abundant within the oxic zone and the upper OMZ, comprising between 2 to 15% of minor lipids on average (0.1 to 0.6% of total IPLs), but were only sporadically found within the core OMZ and deep oxycline. 1G-OH-DAG showed highest relative abundances at station 5, constituting up to 40% of minor

lipids. Four additional phospholipids with diacylglycerol core structures with the following head groups were identified: diphosphatidylglycerol (DPG), phosphatidyl-(*N*)-methylethanolamine (PME), phosphatidyl-(*N,N*)-dimethylethanolamine (PDME) and phosphatidyl inositol (PI). DPG, PME-DAG and PDME-DAG had highest relative abundances (respectively 65, 56 and 35% of minor IPL) within the upper and core OMZ, but at lower abundances within the oxic zone at all stations and in the deep oxycline at stations 1, 2 and 5. PI-DAG was most abundant in the oxic zone and the upper OMZ (up to 25% of minor IPL), but was also present in the core OMZ and the deep oxycline, except for station 8. Three types of aminolipids were observed as minor lipids. OH-DGTS with up to three hydroxyl-groups attached to the fatty acyl side chains (Suppl. Fig. 5) was observed at most depths at station 8 with an average relative abundance of 23% among the minor lipids; it was also occasionally detected at stations 2 and 5 within the oxic zone and upper OMZ. Two additional aminolipids had an undefined head group that exhibited fragmentation patterns characteristic of betaine lipids, but without established betaine head group fragments (Suppl. Fig. 6b, c). The tentatively assigned sum formula for the head group of the first unknown aminolipid (AL-I) at ca. 6.7 minutes LC retention time was $C_8H_{17}NO_3$ and for the second unknown aminolipid (AL-II) at 10.5 minutes was $C_7H_{15}NO_3$. The head group sum formula for AL-II matches that of DGCC, but the diagnostic head group fragment of m/z 252 was not detected, and furthermore, AL-II did not elute at the expected earlier retention time for DGCC. AL-I and AL-II were detected at most depths at all four stations, with average abundances of 1 to 6% of the minor lipids for AL-I and comparably higher relative abundances ranging from 16 to 36% for AL-II.

*Acyl-ether glycerol lipid*: One minor compound that eluted slightly earlier than SQ-DAG had a fragmentation pattern similar to SQ-DAG but with exact masses of the parent ion and MS-MS fragments

in both positive and negative ion mode that suggested a mixed acyl-ether glycerol core lipid structure (Suppl. Fig. 6 d, e). Tentatively assigned as SQ-AEG, this IPL was observed at most depths at all four stations with highest relative abundances of 5 to 60% of minor IPLs within the oxic zone.

*Sphingolipids*: Two types of sphingolipids were identified, monoglycosyl ceramide (1G-CER), and hydroxylated monoglycosyl ceramide (1G-OH-CER) with up to two hydroxyl groups attached to the hydrophobic side chains (Suppl Fig. 5e). Both were observed at all depths at stations 1, 2, and 5 at average relative abundances between 3 and 8% of minor IPLs, but neither was detected in the deeper part of the core OMZ or deep oxycline at station 8.

*Ornithine lipids*: Trace amounts (<4%) of ornithine lipids were detected in the core OMZ of stations 2 and 5.

*3.2.3 Statistical relationships between environmental parameters and lipid distribution*

Spearman Rank Order Correlation was used to evaluate relationships between relative lipid abundance of lipid classes and environmental parameters (Table 1). The glycolipids 2G- and SQ-DAG showed highly significant ($p<0.001$) and positive correlations with depth, fluorescence, POC, TN, temperature and Chl-$\alpha$, significant positive correlations were also observed with oxygen. Both also showed highly significant but negative correlations with phosphate and nitrate, and these overall trends were mirrored in the SQ-DAG:PG-DAG ratio. Total glycolipids (GL) and 1G-DAG only showed correlations with a few environmental parameters and total GL were only significantly positively correlated with oxygen. Most aminolipids and phospholipids did not show significant correlations with environmental parameters and any other correlations were neither strongly positive nor negative.

Relative abundances of total aminolipids and aminolipid (AL) to phospholipid (PL) ratios correlated positively with ammonium. AL:PL also correlated positively with oxygen. Relative abundance of total phospholipids and most individual phospholipids (PG-, PE-, PME-, and PDME-DAG) correlated negatively with oxygen. The only phospholipid that significantly correlated with phosphate was PDME, however, the positive correlation is not strong ($r^2$<0.4).

NMDS analysis revealed that all samples from the oxic zone had a negative loading on the NMDS2 axis along with environmental variables such as oxygen, fluorescence, TN, POC and Chl-*α*. IPLs with a strong negative loading on the NMDS2 axis (<-0.2) were 1G-OH-DAG, SQ-AEG, 2G-DAG, SQ-DAG, PI-DAG and OH-DGTS. Most samples from the core OMZ and deep oxycline had a positive loading on the NMDS2 axis, together with depth, phosphate and nitrate. IPLs that showed a strong positive loading on the NMDS2 axis (>0.2) were PDME-DAG, 2G-GDGT, DPG, PME-DAG and HPH-GDGT. Almost all environmental variables had low *p*-values (<0.001), indicating highly significant fitted vectors with the exception of temperature, salinity, ammonium and nitrate. Highest goodness of fit statistic was observed with oxygen ($r^2$=0.54), followed by phosphate ($r^2$=0.48) and then fluorescence ($r^2$=0.46).

## 4. Discussion

The moderate primary productivity in surface waters of the ETNP, intense microbial degradation of particulate organic matter exported to the thermocline, and restricted midwater oxygen replenishment produce the strong, shallow (~20 m deep) oxycline and a ~500 m thick OMZ with dissolved oxygen concentrations of <2 μM, not unlike other oceanic OMZs (e.g., Ulloa et al., 2012). The ETNP is dominated by picoplankton, and micro-grazers reported consuming most phytoplankton production

(Landry et al., 2011; Olsen and Daly, 2013). Peak macrozooplankton biomass was located at the thermocline, near the upper boundary of the OMZ, but a secondary biomass peak of a different zooplankton assemblage was present at the deep oxycline once $O_2$ concentrations rose to ~2 µM (Wishner et al., 2013). Shallow-water, plankton-derived particulate organic carbon is the primary food source for zooplankton in the mixed layer, upper oxycline and core OMZ, whereas deep POC, some of which might have been produced by microbes in the OMZ, is important for deep oxycline zooplankton (Williams et al., 2014). Microbial community structure and activities are typical of other OMZs (Taylor et al., 2001; Lin et al., 2006; Woebken et al., 2007; Wakeham et al., 2007; 2012). Cell numbers of total prokaryotes were highest in the euphotic layer and decreased with depth at the thermocline but rose again within the core OMZ (Podlaska et al., 2012). Elevated rates of chemoautotrophy, measured by dark dissolved inorganic carbon (DIC) assimilation, were observed at several depths in the OMZ and in the lower oxycline. Transfer of chemoautotrophically-fixed carbon into zooplankton food webs is also evident (Williams et al., 2014). Bacteria dominate the prokaryotic community at all stations. Nitrifying bacteria constituted 3-7% of total DAPI-positive prokaryotes in surface waters; sulfate-reducing bacteria (17 and 34% of total prokaryotes), planctomycetes (up to 24% of total prokaryotes), and anammox bacteria (<1% of prokaryotes) in the upper OMZ and deep oxycline might be associated with anoxic microzones within particle aggregates even at low dissolved oxygen concentrations (Woebken et al., 2007; Carolan et al., 2015). Archaeal cell abundances peaked at the start of the upper OMZ at all stations (up to 37% of total prokaryotes at station 2), within the core OMZ at station 2 (up to 54% of total detected cells) and within the deep oxycline at station 5 and 8 (around 25%; Fig. 2e). Crenarchaeota/thaumarchaeota represented ~20% of prokaryotes throughout the water column, generally being highest in the lower OMZ and deep

463 oxycline, and at stations 2 and 5 just above the secondary Chl-*a* maxima at ~75 m. Euryarchaeota were
464 16-20% of total prokaryotes, especially in waters above the OMZ.

465 Total IPL concentrations that were over 50 times higher in the surface waters than at deeper depths
466 coincided with high Chl-*α* concentrations, reflecting the importance of phototrophic sources to the IPL
467 pool above the thermocline. Below the thermocline, IPL concentrations generally track trends in
468 microbial cell abundances, and elevated IPL concentrations in the upper and core OMZ coincide with
469 elevated nitrite concentrations. The rapid decrease in IPL concentrations below ~100 m probably results
470 from a combination of a dearth of potential source organisms and the decomposition of sinking detrital
471 lipids (Harvey et al., 1986; Matos and Pham-Thi, 2009). IPL concentration decreases below the euphotic
472 zone are well established (Van Mooy et al., 2006; Schubotz et al., 2009; Van Mooy and Fredricks, 2010;
473 Popendorf et al., 2011b; Wakeham et al., 2012). We believe that the diverse molecular compositions and
474 shifts in relative abundances of IPLs with changing geochemistry reflect a complex biological community
475 structure and their ecophysiologic adaptation throughout the water column.

476

477 *4.1 Provenance of IPLs in the ETNP*

478 Variations in IPL distributions and head group and core lipid compositions reflect the biogeochemical
479 stratification of the water column. Below we discuss potential sources of and possible physiological
480 roles for IPLs in the different zones.

481

482 *4.1.1 Oxic zone*

483 The glycosyldiacylglycerides that dominate the IPL composition in oxic surface waters, 1G-DAG,

2G-DAG and SQ-DAG, are major constituents of photosynthetic thylakoid and chloroplast membranes (Wada and Murata, 1998; Siegenthaler, 1998) and are therefore generally assigned to photosynthetic algae or cyanobacteria (Van Mooy et al., 2006; Popendorf et al., 2011b). These are also the likely predominant sources in our study, however, notably 1G-DAG may also be synthesized by heterotrophic bacteria (Popendorf et al., 2011a; Carini et al., 2015; Sebastian et al., 2016). In the oxic zone, 1G- and 2G-DAG are predominantly comprised of $C_{16}$ and $C_{18}$ fatty acids with zero to 5 double bond equivalents polyunsaturated acid (PUFA) combinations such as $C_{16:4}/C_{18:3}$, $C_{16:4}/C_{18:4}$, $C_{18:3}/C_{16:2}$, $C_{18:4}/C_{14:0}$ and $C_{18:5}/C_{14:0}$ (Suppl. Table 5, Fig. 5). These are characteristic of eukaryotic algae (Brett and Müller-Navarra, 1997; Okuyama et al., 1993), such as diatoms and prymnesiophytes that are the major eukaryotic phytoplankton in the ETNP. SQ-DAG biosynthesized by cyanobacteria do not contain PUFA, but instead predominantly contain combinations of $C_{14:0}$, $C_{16:0}$, and $C_{16:1}$ fatty acids (e.g., Siegenthaler, 1998), yielding shorter chain lengths and a lower average number of double bonds (0.5 to 1) than the other glycolipids as observed at the ETNP (Fig. 5). Betaine lipids (DGTS) in surface waters of the ETNP are comprised of $C_{14}$, $C_{16}$, $C_{18}$ and $C_{20}$ with multiple unsaturations or rings (on average 1.5 to 3 double bond equivalents) and are also likely phytoplankton derived (Dembitsky, 1996; Popendorf et al., 2011a).

PC-DAG with fatty acyl combinations of $C_{22:6}$ and $C_{20:5}$ long-chain PUFA and $C_{16:0}$ fatty acids (Suppl. Table 5) in surface waters also point to primarily eukaryotic algal sources. PG-DAG is the only phospholipid in cyanobacteria and thylakoid membranes of eukaryotic phototrophs (Wada and Murata, 1998). Heterotrophic bacteria are an additional source for PG-DAG since it can be a major phospholipid in bacterial membranes (Goldfine, 1984). PE-DAG is a minor phospholipid in eukaryotic algae (e.g., Dembitsky et al., 1996) but is common in membranes of bacteria (Oliver and Colwell, 1973; Goldfine,

1984) and is biosynthesized by heterotrophic marine bacteria (Popendorf et al., 2011a). Lower average number of double bond equivalents in PG- and PE-DAG (<2) in the upper water column of the ETNP are consistent with a bacterial origin (Fig. 5).

Oxic ETNP waters contain PE- and PC-based phospholipids with mixed acyl and ether core lipids (AEG), which are often referred to as 1-*O*-monoalkyl glycerol ethers (MAGE) if detected as core lipids. PE-AEG have been described in some sulfate-reducing bacteria (Rütters et al., 2001), which in the oxic zone or OMZ of the ETNP would require anoxic microzones in fecal pellets or aggregates (e.g., Bianchi et al., 1992; Shanks and Reeder, 1993). In the ETNP, MAGE-based phospholipids were 1 to 30% of total IPLs. MAGE, detected as core lipids in surface waters of the Southern Ocean and eastern South Atlantic are thought to be breakdown products of IP-AEGs of aerobic bacterial origin (Hernandez-Sanchez et al., 2014), but culturing experiments have yet to confirm this conclusion. Similarly, aerobic bacteria (possibly cyanobacteria) are likely sources for SQ-AEG, since sulfoquinovosyl is a diagnostic headgroup found in cyanobacteria, although, again, these lipids have not been reported in cultured cyanobacteria. Other minor phospholipids in the euphotic zone include PI-DAG and DPG. They are minor components in several marine algae (Dembitsky, 1996) and bacteria (Morita et al., 2010; Diervo et al., 1975; Mileykovskaya and Dowhan, 2009). Bacteria may also be the source of the low detected levels of *N*-methylated phospholipids PME-DAG and PDME-DAG (Goldfine and Ellis, 1964). 3G-DAG comprised of $C_{14}$, $C_{16}$ and $C_{18}$ fatty acids with up to six double bond equivalents is another minor IPL detected in the euphotic zone at all stations except for station 5. It has been found in some plants (Hölzl and Dörmann, 2007) and some anaerobic gram-positive bacteria (Exterkate and Veerkamp, 1969), which could both be probable sources in the oxic euphotic zone of the ETNP.

526 The sphingolipid, 1G-CER, consists of a sphingosine backbone linked to a fatty acid via an amide
527 bond and was a minor component in the oxic zone (<5% of IPL) at all stations (Fig. 4). Glycosidic
528 ceramides occur in eukaryotic algae such as the coccolithophore *Emiliania huxleyi* (Vardi et al., 2009).
529 We also detected 1G-OH-CER with up to 2 hydroxylations in the core lipid structure (Suppl. Fig. 5).
530 Multiple-hydroxylated sphingoid bases are potential markers of viral infection and cell death in at least
531 some marine phytoplankton, notably *E. huxleyi* (Vardi et al., 2009). We did not, however, find mass
532 spectral evidence for the presence of viral polyhydroxylated 1G-CER, as described by Vardi et al. (2009)
533 and therefore rather suggest that eukaryotic algal cells are potential sources for the 1G-CER (Lynch and
534 Dunn et al., 2004) in surface waters of the ETNP. We also detected hydroxylated glycolipids (1G-OH-
535 DAG) and aminolipids (OH-DGTS) with up to two hydroxyl-groups or one hydroxyl group combined
536 with an epoxy or keto function attached to the acyl groups (Suppl. Fig. 5). The addition of hydroxyl
537 groups or general oxidation of fatty acids in plants, algae and yeast is a defense mechanism and response
538 to oxidative stress (Kato et al., 1984; Andreou et al., 2009). Hydroxy fatty acids, for example, are
539 intermediates in oxidative degradation of fatty acids (Lehninger, 1970), and since they are constituents of
540 structural biopolymers of many microorganisms (Ratledge and Wilkinson, 1988), they are present in
541 marine particulate matter (e.g., Wakeham, 1999), likely derived from membrane constituents of Gram-
542 negative bacteria, the most abundant bacteria in seawater (Rappé and Giovannoni, 2000).
543
544 *4.1.2 Upper OMZ*
545 Glycolipid abundance varied between 15 to 80% of total IPL within the upper OMZ below the
546 thermocline/oxycline. SQ-DAG and 2G-DAG exhibited strong decreases in relative and absolute

abundance below 125 m at all stations consistent with the decrease in their phototrophic biomass. Number of carbon atoms in the core lipid chains and number of double bond equivalents of glycolipids showed considerable variations within the upper OMZ (Fig. 5), indicating a different assemblage of source organisms compared to the oxic zone. Likewise, decreasing carbon numbers and double bond equivalents for PC-DAG and DGTS combined with a dominance by $C_{14}$, $C_{16}$ and $C_{18}$ saturated and monounsaturated fatty acids (Suppl. Table 5) supports a shift from eukaryotic to bacterial sources. This suggests the diverse proteobacteria in the upper OMZ may biosynthesize non-phosphorus substitute IPLs. 1G-DAG or DGTS are known to replace phospholipids, primarily PE-DAG and PC-DAG under phosphorus limited growth (Geske et al., 2012; Carini et al., 2015; Sebastian et al., 2016; Yao et al., 2015), including at the phosphate concentrations of 2 to 2.5 μM in the upper OMZ. Sulfate-reducing proteobacteria, which comprise up to 10% of the total bacteria in the ETNP (Podlaska et al., 2012) may be candidate organisms for this phospholipid to glycolipid replacement (Bosak et al., 2016). Structures of minor IPLs, AL-I and AL-II were not fully elucidated (see Suppl. Fig. 6) and their origins remain uncertain. PME- and PDME-DAG, DPG, 1G-CER and 1G-OH-CER within the upper OMZ are consistent with previous reports of their production by (unidentified) bacteria near redox boundaries in other stratified water bodies (Schubotz et al., 2009; Wakeham et al., 2012).

Archaeal IPLs with glycosidic headgroups and tetraether core structures (1G- and 2G-GDGT) comprised a greater proportion of the overall IPL pool within the upper OMZ than in surface waters. Analysis of these same samples by Xie et al. (2014) first reported that concentrations of glycosidic GDGTs peak in the ETNP roughly at depths where nitrite maxima are observed. IP-GDGTs with the hexose-phosphate-hexose (HPH) headgroups and the core GDGT crenarchaeol (Suppl. Fig. 4) of thaumarchaeota

(Schouten et al., 2008; Elling et al., 2017) were most abundant at depths of nitrate maxima at all ETNP stations, as they are in other oxygen-deficient water columns (e.g., Pitcher et al., 2011; Lengger et al., 2012; Schouten et al., 2012; Sollai et al., 2015), although they were present at greater depths in the ENTP as well. The microbial enumerations by Podlaska et al. (2012) had shown previously that thaumarchaeota (referred to as crenarchaeota) and euryarchaeota constitute almost equal amounts to <10% of total cell number in the upper OMZ of the ETNP. It is also possible that uncultured marine Group II euryarchaeota are additional sources for glycosidic GDGTs as has been suggested previously (Lincoln et al., 2014; Zhu et al., 2016).

*4.1.3 Core OMZ and deep oxycline*

IPL distributions in the core OMZ and at the deep oxycline of the ETNP that were notably different from the oxic zone and the upper OMZ are consistent with *in-situ* microbial origins. We choose to discuss the core OMZ and deep oxycline together because, although oxygen concentrations are beginning to rise in the deep oxycline, IPL compositions in both zones are similar and likely reflect similar biogeochemical sources. Phospholipid abundance at all stations generally increased to over 50% (except for station 8) at the expense of glycolipids. PE and PG-DAG are the most abundant phospholipids in the core OMZ, along with PC-DAG and PE- and PC-AEG, DPG. PME and PDME-DAG are all common lipids in α-, γ- and some β-proteobacteria (Oliver and Colwell, 1973; Goldfine, 1984) that are present in the OMZ (Podlaska et al., 2012). Changes in phospholipids chain length and number of double bond equivalents further support *in-situ* IPL production (Fig. 5). Fatty acid combinations for phospholipids were dominated by saturated $C_{14:0}$, $C_{15:0}$ and $C_{16:0}$ and monounsaturated $C_{16:0}$ $C_{17}$ and $C_{18:0}$ (Suppl. Table

5); PUFA were generally of reduced abundance, and odd-numbered fatty acids increased in proportion. In the case of PUFA, even though they may be biosynthesized by piezophilic aerobic deep-sea bacteria (DeLong and Yayanos,1986, Fang et al. 2003; Valentine and Valentine, 2004), either the microaerophilic bacteria in the deep OMZ of the ETNP do not produce PUFA or these labile fatty acids are rapidly degraded *in-situ* (DeBaar et al., 1983; Prahl et al., 1984; Neal et al., 1986).

Among glycolipids, 1G-DAG was most abundant at the deep OMZ/oxycline at stations 1 and 8; here 1G-DAG abundance actually increases over that of shallower depths. Carbon number and number of double bond equivalents for glycolipids are again distinct from the surface waters, with on average 1 to 2 carbon atoms shorter chain lengths and 1 to 3 fewer double bonds (Fig. 5), supporting the notion that at least some of these glycolipids are biosynthesized *in-situ* and not simply exported from the surface waters. In particular, SQ-DAG in the core OMZ/oxycline contained odd-carbon numbered fatty acids (e.g., $C_{15:0}/C_{16:0}$ and $C_{14:0}/C_{15:0}$) different from the cyanobacterial SQ-DAG in surface waters (Suppl. Table 5). Some Gram-positive bacillus and firmicutes biosynthesize 1G, 2G- and SQ-DAG (Hölzl and Dörmann, 2007) and 1G-, 2G- and SQ-DAG in deeply buried Wadden Sea sediments are attributed to anaerobic bacteria (Seidel et al., 2012). However, Gram-positive bacteria are generally not abundant in seawater.

The core OMZ/deep oxycline are particularly enriched in archaeal GDGT, notably 1G-GDGT and HPH-GDGT, with predominantly GDGT-0 and crenarchaeol as core lipids (Suppl. Fig. 4). At stations 1 and 8 where sampling penetrated below ~800 m depth, 1G-GDGT and HPH-GDGT constitute up to ~60% and ~22%, respectively, of total IPL. Significantly, the elevated abundances of 1G-GDGT and HPH-GDGT at the bottoms of the sampling depth profiles in the deep oxycline of stations 1 and 8 correspond to depths at which ammonium concentrations are higher than shallower in the core OMZ (Fig. 2).

610 Remineralization at the deep-oxycline might provide additional ammonium to drive thaumarchaeotal
611 ammonium oxidation and production of archaeal IPLs.
612
613 *4.2 Factors influencing IPL distribution in the ENTP*
614 *4.2.1 Factors affecting structural diversity of the core lipid composition*
615 IPL in the ETNP display considerable diversity not only in the headgroup but also core lipid types,
616 from diacylglycerol lipids with varying number of carbon atoms (likely chain lengths) and zero to multiple
617 double bond equivalents (likely reflecting the number of unsaturations), with or without hydroxylations
618 to mixed ether/ester glycerolipids, sphingolipids and ornithine lipids. Statistical analysis provides aids
619 in illuminating influences of environmental factors and microbial community structure on the lipid
620 composition in the water column of the ETNP. Changes in core alkyl lipid chain length and degree of
621 unsaturation are often associated with temperature (Neidleman, 1987), even at the range of temperatures
622 of the ETNP water column. However, NMDS analysis did not yield any strong correlations between
623 temperature and number of carbon atoms in the side chains or double bond equivalents of the major IPL
624 classes ($r^2 < 0.02$, Suppl. Table 6), nor with other environmental parameters (r2 < 0.3, Suppl. Table 6).
625 Instead, changing biological sources may play a decisive role in determining number of carbon atoms and
626 double bond equivalents in the ETNP. For instance, long-chain PUFAs in surface waters are mainly
627 synthesized by phytoplankton, while in deeper waters some bacteria may biosynthesize these PUFAs.
628 The degree of hydroxylation in the acyl side chains also did not show any clear link to specific
629 environmental factors, although, both 1G-OH-CER and OH-DGTS had negative loadings on the NMDS-
630 2 axis indicating a higher abundance of these compounds in oxic samples. It is possible that hydroxylated

631 IPLs play a role during oxidative stress and/or are involved in other defense mechanisms (Kato et al.,
632 1984; Andreou et al., 2009).

633 Mixed ether-acyl lipids have been reported in various oceanic settings (Hernandez-Sanchez et al.,
634 2014). In our study, there was no noticeable correlation between PE- and PC-AEG and depth or oxygen
635 concentrations (Fig. 6). Ornithine lipids were strongly negatively loaded on the NMDS-1 axis, but none
636 of the measured environmental parameters could account for this negative loading (Fig. 6). Therefore,
637 it remains unclear what factor(s) ultimately determine their distribution. Likewise, there were no
638 significant correlations between the sphingolipid 1G-CER and any environmental parameter. Since
639 ether-acyl lipids, ornithine lipids and sphingolipids play many functional roles in biological systems, their
640 variable distribution within the water column reflect most likely the diversity of microbes inhabiting the
641 dynamic oxygen regime of the ETNP.

642

643 *4.2.2 Factors influencing head group composition*

644 NMDS analysis of normalized IPL composition and quantitative microbial data (abundance of α, β,
645 γ, ε-proteobacteria, sulfate-reducing bacteria δ-proteobacteria, planctomycetes, crenarchaeota including
646 thaumarchaeota and euryarchaeota) did not yield any high goodness of fit statistic ($r^2 < 0.3$; Suppl. Table
647 6) that would clearly delineate specific prokaryotic sources for the various IPL. This absence of
648 statistical correlation would result if neither the IPL compositions of SPM nor the structure and lipid
649 composition of the prokaryotic community were sufficiently unique to strongly distinguish the
650 biogeochemical zones. Indeed, although there are depth-related differences in IPL composition of SPM
651 and prokaryotic community, there is considerable overlap. Therefore, instead of trying to elucidate

652 specific IPL sources, we here query the affect environmental factors such as temperature, nutrient or
653 oxygen concentrations may have on the IPL compositions in the ENTP, and by analogy to natural marine
654 settings in general. Most the major and minor glycolipids were loaded negatively on the NMDS2 axis,
655 as were oxygen, fluorescence, Chl-$\alpha$, POC and TN (Fig. 6). A notable exception was 1G-DAG which
656 had only a slightly negative loading on the NMDS-2 axis. These relationships (loadings) roughly reflect
657 the vertical distribution of IPLs in the water column of the ETNP. Glycolipids, particularly 2G-DAG
658 and SQ-DAG, were most abundant in the euphotic oxic zone characterized by high oxygen concentration
659 and moderate primary productivity, dominated by phytoplankton, primarily cyanobacteria (high POC, TN
660 and elevated Chl-$\alpha$ and fluorescence). Spearman Rank Order Correlations confirm these observations,
661 including the lack of significant correlations between 1G-DAG and depth or any other environmental
662 parameter. One explanation is that 1G-DAG originates from assorted sources throughout the water
663 column independent of any single environmental variable. Similarly, PC-DAG, PG-DAG, and DGTS
664 did not correlate with any of the tested environmental variables, because their compositions are relatively
665 homogeneous across all biogeochemical zones. PE-, PME- and PDME-DAG, and DPG, on the other
666 hand, that became more prevalent within the core OMZ, and at deeper depths where oxygen concentrations
667 decrease and nutrient ($NO_3^-$ and $PO_4^{3-}$) concentrations were elevated due to organic matter
668 remineralization, gave positive loadings with these environmental parameters on the NDMS2 axis.
669 Archaeal IPLs showed positive loadings on the NMDS2 axis, consistent with the increasing importance
670 of archaeal abundance with depth and at reduced oxygen concentrations.
671
672 *4.2.3 Links between substitute lipid ratios and nutrient concentrations*

673 SQ-DAG and PC-DAG are often the most abundant respective glycolipids and phospholipids in the
674 surface ocean (Popendorf et al., 2011a,b), including the Eastern Tropical South Pacific (Van Mooy and
675 Fredricks, 2010). The abundance of SQ-DAG in the surface waters of the ETNP (18-50% of total IPL)
676 is thus not unusual. In the ETNP, however, PC-DAG was comparably minor (3-13% of total IPL).
677 Instead, DGTS was abundant at some stations, up to ~20% of major IPL at station 5. SQ-DAG and
678 DGTS serve similar biochemical functions as the phospholipids PG-DAG and PC-DAG, respectively, due
679 to similar ionic charges at physiological pH. The former may be preferentially biosynthesized by
680 phytoplankton and some bacteria as substitute lipids for PG-DAG and PC-DAG when phosphate starved
681 (Benning, 1993; Van Mooy et al., 2006, 2009). Likewise, 1G-DAG, glycuronic acid diacylglycerol
682 (GADG) and ornithine lipids may substitute for PE-DAG in marine bacteria (e.g., chemoheterotrophic α-
683 proteobacteria of the SAR11 clade of *Pelagibacter* sp.: Carini et al., 2015; the sulfate reducing bacterium,
684 *Desulfovibrio alaskensis*: Bosak et al., 2016). In oligotrophic surface waters of the Sargasso Sea ($PO_4^{3-}$
685 <10 nM) ratios of SQ-DAG:PG-DAG and DGTS:PC-DAG are high (4 to 13) compared to the same ratios
686 (3) in the phosphate replete South Pacific ($PO_4^{3-}$ >100 nM), consistent with cyanobacteria synthesizing
687 phosphorus-free substitute lipids to maintain growth in response to phosphorus deprivation (Van Mooy et
688 al., 2009). At the ETNP, SQ-DAG:PG-DAG ratios ranged between 1 and 10 within the upper 100-200
689 m along the transect and were <1 deeper into the OMZ (Fig. 3). DGTS:PC-DAG ratios in the ETNP
690 were quite variable, ranging between 0.4 and 2.4 at most depths, but with notable spikes (>30) within the
691 oxic zone at station 5, within the upper core OMZ at station 2 and 8 and in the lower portion of the core
692 OMZ at station 8. 1G-DAG:PE-DAG ratios where highly variable (0.2 to 945) and were highest within
693 the upper OMZ at station 2, 5 and 8 and within the deep oxycline at station 8, where 1G-DAG:PE ratios

range between 290 and 945 (Fig. 3). To test the substitute lipid hypothesis for the ETNP, we performed a Spearman Rank Order Correlation analysis of known substitute lipid ratios as well as total aminolipid (AL) to phospholipid (PL) and total glycolipid (GL) to PL ratios with nutrient concentrations and other environmental parameters. Only SQ-DAG:PG-DAG was significantly correlated with phosphate (-0.56, $p<0.001$) but also correlated with other parameters, such as depth (-0.76, $p<0.001$) and oxygen concentration (0.58, $p<0.001$). These correlations reflect the elevated SQ-DAG:PG-DAG ratios (2-8) in the surface waters and upper OMZ (Fig. 3) and support the notion that SQ-DAG might serve as a substitute lipid in both surface waters and the OMZ when phosphate concentrations are in the low micromolar range (~0.1-0.4 μM in surface waters; ~2-3.5 μM in the OMZ). Other proposed substitute lipid ratios, DGTS:PC-DAG (Van Mooy et al., 2009) and 1G-DAG:PE-DAG (Carini et al., 2015), did not correlate with nutrient concentrations in the water column of the ETNP but rather showed highly variable distributions. Similarly, AL:PL ratios did not exhibit strong relationships with any environmental parameter, and GL:PL ratios showed similar but less pronounced trends as SQ-DAG:PG-DAG ratios. Overall, we observed no correlation between these substitute lipid ratios and phosphate concentration in the ETNP. We propose that non-phosphorus IPL within the OMZ of the ETNP originate from bacteria growing under low micromolar concentrations of phosphate. Indeed, the culture experiments of Bosak et al. (2016) demonstrated that the sulfate reducer, *Desulfovibrio alaskensis*, begins to replace most of its membrane phospholipids with 1G-DAG, glycuronic acid diacylglycerol and ornithine lipids even at phosphate concentrations as high as 20 μM.

## 5. Conclusions

715 The water column of the ETNP is characterized by a diverse suite of intact polar lipids. IPL
716 distributions reflect the dynamic nature of the biological community in the ETNP, with light and oxygen
717 as primary determinants, from fully oxygenated euphotic surface waters to an aphotic strong oxygen
718 minimum zone at mid-depth. Highest concentrations of IPLs (250 – 1500 ng/L) in oxygenated surface
719 waters zone results from abundant phototrophic eukaryotic and cyanobacterial sources above the OMZ.
720 Secondary peaks in IPL concentration (12 – 56 ng/L) within the core of the OMZ mirror elevated
721 abundances of heterotrophic and chemoautotrophic bacteria and archaea under low oxygen conditions.
722 Glycolipids derived from photoautotrophs generally accounted for more than 50% of total IPLs in the
723 euphotic zone (< 200 m, oxic and upper OMZ zones), but bacterial phospholipids were more abundant
724 (avg. 40%) in the OMZ and deep oxycline layers. Archaeal GDGTs were abundant within the OMZ and
725 deep oxycline, consistent with elevated archaeal abundances there. Variations in major fatty acid
726 constituents within IPL classes with acyl core moieties show that biological source(s) for the different IPL
727 were distinct in each depth/oxygen-content horizon. Nevertheless, microbial sources for many of the
728 detected lipids remain unclear and therefore potentially unique ecophysiological adaptations these lipids
729 may represent remain to be explored.

730 The presence of the glycolipid, monoglycosyl diacylglycerol (1G-DAG), and the betaine lipid,
731 diacylglyceryl homoserine (DGTS), both with varying fatty acid compositions, within all biogeochemical
732 zones, and especially in the OMZ, indicates that these canonical phototrophic markers are not only
733 biosynthesized in surface waters, but may indeed be produced in the aphotic water column and by a much
734 larger host of organisms than previously thought. Since 1G-DAG and DGTS can be biosynthesized by
735 various bacteria to replace phospholipids under phosphorus limited growth, we suggest that they serve as

non-phosphorus substitute lipids for some microorganisms in the OMZ. The presence of these substitute lipids at micromolar concentrations of phosphate of the ETNP suggests that the paradigm of substitute lipid biosynthesis being restricted to the $PO_4^{3-}$-depleted oligotrophic surface ocean may need to be re-evaluated.

**Author contribution**

SGW collected the samples. SGW, FS and KUH designed the study. SX and FS measured and processed the data. JSL and FS performed statistical analyses. FS and SGW wrote the paper with input from SX, KUH and JSL.

**Competing interests**

The authors declare that they have no conflict of interest.

**Acknowledgments**

We are grateful to the captain and the crew of R/V *Seward Johnson*, to K. Daly and K. Wishner as co-chief scientists, and to the U.S. National Science Foundation for supporting the cruise. H. Albrecht, B. Olsen and S. Habtes helped with PM sampling. We thank K. Fanning and R. Masserini (University of South Florida) for providing their nutrient results; C. Flagg (Stony Brook) processed CTD hydrographic data; Jay Brandes and Mary Richards (Skidaway Institute) conducted the POC and TN analyses; B. Olson and K. Daly (University of South Florida) provided ship-board Chl-*a* analyses; and G. DeTullio (College of Charleston) conducted HPLC analyses of pigments. Lab supplies and analytical infrastructure for

lipid analyses was funded by the Deutsche Forschungsgemeinschaft (DFG, Germany) through the Cluster of Excellence/Research Center MARUM. The UHPLC-QTOF instrument was granted by the DFG, Germany through grants Inst 144/300-1. S. Xie was funded by the China Scholarship Council, F. Schubotz by the Zentrale Forschungsförderung of the University of Bremen, and U.S. National Science Foundation grant OCE-0550654 to S. G. Wakeham supported this project. SGW also acknowledges a Fellowship from the Hanse-Wissenschaftskolleg (Hanse Institute for Advanced Studies) in Delmenhorst, Germany.

**References**

Andreou, A., Brodhun, F., Feussner, I.: Biosynthesis of oxylipins in non-mammals, Progr. Lip. Res., 48, 148-170, 2009.

Bale, N. J., Hopmans, E. C., Schoon, P. L., de Kluijver, A., Downing, J. A., Middelburg, J. J., Sinninghe Damsté, J. S. and Schouten, S.: Impact of trophic state on the distribution of intact polar lipids in surface waters of lakes. Limnol. Oceanogr., 61, 1065–1077, 2016.

Basse, A., Zhu, C., Versteegh, G.J.M., Fischer, G., Hinrichs, K.-U., and Mollenhauer, G.: Distribution of intact and core tetraether lipids in water column profiles of suspended particulate matter off Cape Blank, NW Africa, Org. Geochem., 72, 1-13, 2014.

Benning, C., Beatty, J. T., Prince, R. C., and Somerville C. R.: The sulfolipid sulfoquinovosyldiacylglycerol is not required for photosynthetic electron transport in Rhodobacter sphaeroides but enhances growth under phosphate limitation, Proc. Natl. Acad. Sci. USA, 90, 1561–1565, 1993.

778 Bianchi, M., Marty, D., Teyssié, J.-L., and Fowler, S. W.: Strictly aerobic and anaerobic bacteria
779 associated with sinking particulate matter and zooplankton fecal pellets, Mar. Ecol. Press Ser., 88, 55-
780 60, 1992.
781 Bosak, T., Schubotz, F., de Santiago-Torio, A., Kuehl, J. V., Carlson, H. K., Watson, N., Daye, M.,
782 Summons, R. E., Arkin, A. P., and Deutschbauer A. M.: System-wide adaptations of *Desulfovibrio*
783 *alaskensis* G20 to phosphate-limited conditions, PLoS ONE 11, e0168719, 2016.
784 Brandsma, J., Hopmans, E. C., Philippart, C. J. M., Veldhuis, M. J. W., Schouten, S., and Sinninghe
785 Damste, J. S.: Low temporal variation in the intact polar lipid composition of North Sea coastal marine
786 water reveals limited chemotaxonomic value, Biogeosciences, 9, 1073–1084, 2012.
787 Brett, M. T., and Müller-Navarra, D. C.: The role of highly unsaturated fatty acids in aquatic foodweb
788 pro- cesses, Freshw. Biol., 38, 483–499, 1997.
789 Carini P., Van Mooy B. A. S., Thrash J. C., White A., Zhao Y., Campbell E. O., Fredricks H. F., and
790 Giovannoni S. J.: SAR11 lipid renovation in response to phosphate starvation. Proc. Natl. Acad. Sci.
791 USA, 112, 7767–7772, 2015.
792 Carolan, M.T., Smith, J.M., and Beman, J.M.: Transcriptomic evidence for microbial sulfur cycling in the
793 eastern tropical North Pacific oxygen minimum zone. Front. Microbiol. 6, 334, 2015.
794 Cass, C. J., and Daly, K. L.: Ecological characteristics of eucalanoid copepods of the eastern tropical
795 North Pacific Ocean: Adaptations for life within a low oxygen system, J. Exp. Mar. Biol. Ecol., 468,
796 118-129, 2015.
797 Cavan, E. L., Trimmer, M., Shelley, F., Sanders, R.: Remineralization of particulate organic carbon in an
798 ocean oxygen minimum zone, Nat. Comm., 8, 14847, 2016.

799 Codispoti, L. A., and Richards, F. A.: An analysis of the horizontal regime of denitrification in the eastern
800 tropical North Pacific. Limnology and Oceanography 21, 379-388, 1976.
801 DeBaar, H. J. W., Farrington, J. W. and Wakeham, S. G.: Vertical flux of fatty acids in the North Atlantic
802 Ocean, J. Mar. Res., 41, 19-41, 1983.
803 DeLong, E. F. and Yayanos, A.: Biochemical function and ecological significance of novel bacterial lipids
804 in deep-sea procaryotes, Appl. Environ. Mirobiol., 51, 730-737, 1986.
805 Dembitsky, V.: Betaine ether-linked glycerolipids: Chemistry and biology, Progr. Lip. Res., 35, 1-51,
806 1996.
807 Diervo, A. J. and Reynolds, J. W.: Phospholipid composition and cardiolipin synthesis in fermentative
808 and nonfermentative marine bacteria, J. Bacteriol. 123, 294-301, 1975.
809 DiTullio, G., and Geesey, M. E.: Photosynthetic Pigments in Marine Algae and Bacteria. In: G Bitton (ed),
810 Encyclopedia of Environmental Microbiology, vol. 5, Wiley, pp 2453-2470, 2002.
811 Elling, F. J., Könneke, M., Mußmann, M., Greve, A., and Hinrichs, K.-U.: Influence of temperature, pH,
812 and salinity on membrane lipid composition and TEX86 of marine planktonic thaumarchaeal isolates,
813 Geochim. Cosmochim. Acta, 171, 238-255, 2015.
814 Elling, F. J., Könneke, M., Nicol, G. W., Stieglmeier, M., Bayer, B., Spieck, E., La Torre, De J. R., Becker,
815 K. W., Thomm, M., Prosser, J. I., Herndl, G. J., Schleper, C., and Hinrichs, K.-U. Chemotaxonomic
816 characterisation of the thaumarchaeal lipidome, Environ. Microbiol. 10, 1080, 2017.
817 Ertefai, T., Fisher, M., Fredricks, H. and Lipp, J.: Vertical distribution of microbial lipids and functional
818 genes in chemically distinct layers of a highly polluted meromictic lake, Org. Geochem., 39, 1572-
819 1588, 2008.

820 Exterkate, F. A., and Veerkamp, J. H.: Biochemical changes in Bifidobacterium bifidum var.
821 Pennsylvanicus after cell wall inhibition. I. Composition of lipids, Biochim. Biophys. Acta, 176, 65–
822 77, 1969.
823 Fang, J., Kato, C., Sato, T., Chan, O., and McKay, D.: Biosynthesis and dietary uptake of polyunsaturated
824 fatty acids by piezophilic bacteria. Comp. Biochem. Physiology Part B, 137 455–46, 2004.
825 Fiedler, P. C., and Talley, L. D.: Hydrography of the eastern tropical Pacific: A review. Progr. Oceanogr.,
826 69, 143-180, 2006.
827 Franck, V. M., Smith, G. J., Bruland, K. W., and Brzezinski, M. A.: Comparison of size-dependent carbon,
828 nitrate and silicic acid uptake rates in high- and low-iron waters. Limnol. Oceanogr., 50, 825-838,
829 2005.
830 Geiger, O., González-Silva, N., López-Lara, I. M., and Sohlenkamp, C.: Amino acid-containing
831 membrane lipids in bacteria, Progr. Lip. Res., 49, 46–60, 2010.
832 Geiger, O., Röhrs, V., Weissenmayer, B., Finan, T. M., and Thomas-Oates, J. E.: The regulator gene phoB
833 mediates phosphate stress-controlled synthesis of the membrane lipid diacylglyceryl-N,N,N-
834 trimethylhomoserine in Rhizobium (Sinorhizobium) meliloti, Mol. Microbiol., 32, 63–73, 1999.
835 Geske, T., Dorp vom, K., Dörmann, P., and Hölzl G.: Accumulation of glycolipids and other non-
836 phosphorous lipids in Agrobacterium tumefaciens grown under phosphate deprivation, Glycobiol., 23,
837 69–80, 2012.
838 Goericke, R., Olson, R. J., and Shalapyonok, A.: A novel niche for Prochlorococcus sp. in low-light
839 suboxic environments in the Arabian Sea and the Eastern Tropical North Pacific, Deep Sea Res. I, 47,
840 1183-1205, 2000.

841 Goldfine, H.: Bacterial membranes and lipid packing theory, J. Lip. Res., 25, 1501–1507, 1984.
842 Goldfine, H., and Ellis, M. E.: N-methyl groups in bacterial lipids, J. Bacteriol., 87, 8–15, 1964.
843 Gruber, N.: The marine nitrogen cycle: overview and challenges, in: Nitrogen in the marine environment,
844 Eds. DG Capone, DA Bronk, MR Mulholland, EJ Carpenter, Burlington, MA, USA: Academic, 1-50,
845 2008.
846 Harvey, R. H., Fallon R. D., and Patton, J. S.: The effect of organic matter and oxygen on the degradation
847 of bacterial membrane lipids in marine sediments, Geochim. Cosmochim. Acta, 50, 795-804, 1986.
848 Hernandez-Sanchez, M. T., Homoky, W. B., and Pancost, R. D.: Occurrence of 1-O-monoalkyl glycerol
849 ether lipids in ocean waters and sediment, Org. Geochem. 66, 1–13, 2014.
850 Hölzl, G., and Dörmann, P.: Structure and function of glycoglycerolipids in plants and bacteria, Progr.
851 Lip. Res. 46, 225–243, 2007.
852 Hurley, S. J., Elling, F. J., Könneke, M., Buchwald, C., Wankel, S. D., Santoro, A. E., Lipp, J. S., Hinrichs,
853 K.-U., and Pearson, A.: Influence of ammonia oxidation rate on thaumarchaeal lipid composition and
854 the TEX86 temperature proxy, Proc. Natl. Acad. Sci. USA, 113, 7762-7767, 2016.
855 Kalvelage, T., Lavik, G., Jensen, M. M., Revsbech, N. P., Löscher, C., Schunck, H., Desai, D. K., Hauss,
856 H., Kiko, R., Holtappels, M., LaRoche, J., Schmitz, R. A., Graco, M. I., and Kuypers, M. M. M:
857 Aerobic microbial respiration in oceanic oxygen minimum zones, PLoS ONE, 10(7):e0133526, 2015.
858 Karstensen, J., Stramma L., and Visbeck M.: Oxygen minimum zones in the eastern tropical Atlantic and
859 Pacific oceans, Progr. Oceanogr., 77, 331-350, 2008.
860 Kato, T., Yamaguchi, Y., Hirano, T., and Yokoyama, T.: Unsaturated hydroxy fatty acids, the self
861 defensive substances in rice plant against rice blast disease, Chem. Let., 409-412, 1984.

862 Keeling, R. F., Körtzinger, A., and Gruber N.: Ocean deoxygenation in a warming world, Annu. Rev.
863 Marine. Sci., 2, 199–229, 2010.
864 Kharbush, J. J., Allen, A. E., Moustafa, A., Dorrestein, P.C., Aluwihare, L. I.: Intact polar diacylglycerol
865 biomarker lipids isolated from suspended particulate organic matter accumulating in an
866 ultraoligotrophic water column, Org. Geochem., 100, 29-41, 2016.
867 Lam, P. and Kuypers, M. M. M.: Microbial nitrogen cycling processes in oxygen minimum zones, Annu.
868 Rev. Marine. Sci., 3, 317–345, 2011.
869 Landry, M. R., Selph, K. E., Taylor, A.G., Décima, M., Balch, W. M., and Bidigare R. R.: Phytoplankton
870 growth, grazing and production balances in the HNLC equatorial Pacific, Deep Sea Res. I, 58, 524-
871 535, 2011.
872 Lavín, M. F., Fiedler, P. C., Amador, J. A., Balance, L. T., Färber-Lorda, J., Mestas-Nuñez, A. M.: A
873 review of eastern tropical Pacific oceanography: Summary, Progr. Oceanogr., 69, 391-398, 2006.
874 Lee C., and Cronin C.: Particulate amino acids in the sea: Effects of primary productivity and biological
875 decomposition, J. Mar. Res., 42, 1075-1097, 1984.
876 Lehninger A. L.: Oxidation of fatty acids, in: Biochemistry, New York: Worth, 417-432, 1970.
877 Lengger, S. K., Hopmans, E. C., Sinninghe Damsté, J. S., and Schouten, S.: Comparison of extraction and
878 work up techniques for analysis of core and intact polar tetraether lipids from sedimentary
879 environments, Org. Geochem., 47, 34–40, 2012.
880 Lin, X., Wakeham, S. G., Putnam, I. F., Astor, Y. M., Scranton, M. I., Chistoserdov, A. Y., and Taylor, G.
881 T.: Comparison of vertical distributions of prokaryotic assemblages in the anoxic Cariaco Basin and
882 Black Sea by use of fluorescence in situ hybridization, Appl. Environ. Microbiol., 72, 2679-2690,

2006.

Lincoln, S. A., Wai, B., Eppley, J. M., Church, M. J., Summons, R. E. and DeLong, E. F.: Planktonic Euryarchaeota are a significant source of archaeal tetraether lipids in the ocean, Proc. Natl. Acad. Sci. USA, 111, 9858–9863, 2014.

Lynch, D. V., and Dunn, T. M.: An introduction to plant sphingolipids and a review of recent advances in understanding their metabolism and function, New Phytol., 161, 677-702, 2004.

Ma, Y., Zeng, Y., Jiao, N., Shi, Y., and Hong, N.: Vertical distribution and phylogenetic composition of bacteria in the Eastern Tropical North Pacific Ocean, Microbiol. Res., 164, 624-663, 2009.

Maas, A. E., Frazar, S. L., Outram, D.M., Seibel, B. A., and Wishner, K. F.: Fine-scale vertical distributions of macroplankton and micronekton in the Eastern Tropical North Pacific in association with an oxygen minimum zone, J Plankt. Res., 36, 1557-1575, 2014.

Martin, J. H., Knauer, G. A., Karl, D. M., and Broenkow, W. W.: VERTEX: carbon cycling in the northeast Pacific, Deep-Sea Research 34, 267-285, 1987.

Matos, A. R., and Pham-Thi, A.-T.: Lipid deacylating enzymes in plants: Old activities, new genes. Plant Physiol. and Biochem. 47, 491-503, 2009.

Meador, T. B., Gagen, E. J., Loscar, M. E., Goldhammer, T., Yoshinaga, M. Y., Wendt, J., Thomm, M., and Hinrichs, K.-U.: Thermococcus kodakarensis modulates its polar membrane lipids and elemental composition according to growth state and phosphate availability, Front. Microbiol., 5:10, doi:10.3389/fmicb.2014.00010, 2014.

Mileykovskaya, E., and Dowhan, W.: Cardiolipin membrane domains in prokaryotes and eukaryotes, Biochim. Biophys. Acta 1788, 2084–2091, 2009.

Morita, Y. S., Yamaryo-Botte, Y., and Miyanagi, K.: Stress-induced synthesis of phosphatidylinositol 3-phosphate in mycobacteria, J. Biol. Chem. 285, 16643-16650, 2010.

Neal, A. C., Prahl, F. G., Eglinton, G., O'Hara, S. C. M., and Corner, E. D. S.: Lipid changes during a planktonic feeding sequence involving unicellular algae, Elminius Nauplii and Adult Calanus, J. Mar. Biol. Assoc. UK, 66, 1-13, 1986.

Neidleman, S. L.: Effects of temperature on lipid unsaturation: Biotechnology and Genetic Engineering Reviews, 5:1, 245-268, 1987.

Oliver, J. D., and Colwell, R. R.: Extractable lipids of gram-negative marine bacteria: Phospholipid composition, J. Bacteriol. 114, 897-908, 1973.

Olson, M. B., and Daly, K. L.: Micro-grazer biomass, composition and distribution across prey resource and dissolved oxygen gradients in the far eastern tropical north Pacific Ocean, Deep Sea Res. I, 75, 28-38, 2014.

Okuyama, H., Kogame, K., and Takeda, S.: Phylogenetic significance of the limited distribution of octadecapentaenoic acid in prymnesiophytes and photosynthetic dinoflagellates, Proc. NIPR Symp. Polar Biol., 6, 21–26, 1993.

Parsons, T. R., Takahashi, M., and Hargrave B. (Eds.): Biological Oceanographic Processes, 3rd ed., Pergamon Press, NY, 1984.

Paulmier, A., and Ruiz-Pino, D.: Oxygen minimum zones (OMZs) in the modern ocean, Progr. Oceanogr. 80, 113-128, 2009.

Pennington, J. T., Mahoney, K. L., Kuwahara, V. S., Kolber, D. D., Clienes, R., Chavez, F. P.: Primary production in the eastern tropical Pacific: A review, Progr. Oceanogr., 69, 285-317, 2006.

925 Pitcher, A., Villanueva, L., Hopmans, E. C., Schouten, S., Reichart, G.-J. and Sinninghe Damsté, J. S.:
926 Niche segregation of ammonia-oxidizing archaea and anammox bacteria in the Arabian Sea oxygen
927 minimum zone, ISME J., 5, 1896–1904, 2011.
928 Podlaska, A., Wakeham, S. G., Fanning, K. A., and Taylor, G. T.: Microbial community structure and
929 productivity in the oxygen minimum zone of the eastern tropical North Pacific, Deep-Sea Res. Part I,
930 66, 77–89, 2012.
931 Popendorf, K., Lomas, M., and Van Mooy, B.: Microbial sources of intact polar diacylglycerolipids in the
932 Western North Atlantic Ocean, Org. Geochem. 42, 803-811, 2011a.
933 Popendorf, K. J., Tanaka, T., Pujo-Pay, M., Lagaria, A., Courties, C., Conan, P., Oriol, L., Sofen, L. E.,
934 Moutin, T., and Van Mooy, B. A. S.: Gradients in intact polar diacylglycerolipids across the
935 Mediterranean Sea are related to phosphate availability, Biogeosci. 8, 3733–3745, 2011b.
936 Prahl, F. G., Eglinton, G., Corner, E. D. S., O'Hara, D. C. M., and Forsberg, T. E. V.: Changes in plant
937 lipids during passage through the gut of Calanus, J. Mar. Biol. Assoc. UK, 1984.
938 Rabinowitz, G. B.: An introduction to nonmetric multidimensional scaling, Amer. J. Polit. Sci., 343-90,
939 1975.
940 Rappé, M. S., and Giovannoni, S. J.: The uncultured microbial majority, Annu. Rev. Microbiol., 57, 369-
941 394, 2003.
942 Rojas-Jiménez, K., Sohlenkamp, C., Geiger, O., Martínez-Romero, E., Werner, D., and Vinuesa, P.: A
943 ClC chloride channel homolog and ornithine-containing membrane lipids of rhizobium tropici
944 CIAT899 are involved in symbiotic efficiency and acid tolerance, Mol. Plant-Microbe Interact., 18,
945 1175–1185, 2005.

946 Rush, D., Wakeham, S. G., Hopmans, E. C., Schouten, S., and Damsté, J. S. S.: Biomarker evidence for
947 anammox in the oxygen minimum zone of the Eastern Tropical North Pacific, Org. Geochem., 53,
948 80–87, 2012.
949 Rütters, H., Sass, H., Cypionka, H., and Rullkötter, J.: Monoalkylether phospholipids in the sulfate-
950 reducing bacteria Desulfosarcina variabilis and Desulforhabdus amnigenus, Arch. Microbiol., 176,
951 435–442, 2011.
952 Schouten, S., Pitcher, A., Hopmans, E. C., Villanueva, L., Van Bleijswijk, J., and Sinninghe Damsté, J.
953 S.: Intact polar and core glycerol dibiphytanyl glycerol tetraether lipids in the Arabian Sea oxygen
954 minimum zone: I. Selective preservation and degradation in the water column and consequences for
955 the TEX86, Geochim. Cosmochim. Acta, 98, 228–243, 2012.
956 Schubotz, F., Wakeham, S. G., Lipp, J., Fredricks, H. F., and Hinrichs, K.-U.: Detection of microbial
957 biomass by intact polar membrane lipid analysis in the water column and surface sediments of the
958 Black Sea, Environ. Microbiol., 11, 2720-2734, 2009.
959 Sebastian, M., Smith, A. F., González, J. M., Fredricks, H. F., Van Mooy, B., Koblížek, M., Brandsma,
960 J., Koster, G., Mestre, M., Mostajir, B., Pitta, P., Postle, A. D., Sánchez, P., Gasol, J. M., Scanlan, D.
961 J., and Chen, Y.: Lipid remodelling is a widespread strategy in marine heterotrophic bacteria upon
962 phosphorus deficiency, ISME J, 10, 968–978, 2016.
963 Seibel, B.A.: Critical oxygen levels and metabolic suppression in oceanic oxygen minimum zones, J. Exp.
964 Biol., 214, 326-336, 2011.
965 Seidel, M., Graue, J., Engelen, B., Köster, J., Sass, H., and Rullkötter, J.: Advection and diffusion
966 determine vertical distribution of microbial communities in intertidal sediments as revealed by

967 combined biogeochemical and molecular biological analysis, Org. Geochem., 52, 114–129, 2012.
968 Shanks, A. L., and Reeder, M. L.: Reducing microzones and sulfide production in marine snow. Marine
969 Ecology Press Series 96, 43-47, 1993.
970 Siegenthaler P.-A.: Molecular organization of acyl lipids in photosynthetic membranes of higher plants,
971 in: Lipids in Photosynthesis, Siegenthaler, P.-A., and Murata, N. (Eds). Dordrecht, the Netherlands:
972 Kluwer Academic Publishers, 119–144, 1998.
973 Sohlenkamp, C., López-Lara, I. M., and Geiger, O.: Biosynthesis of phosphatidylcholine in bacteria, Progr.
974 Lip. Res., 42, 115–162, 2003.
975 Sollai, M., Hopmans, E. C., Schouten, S., Keil, R. G., and Sinninghe Damsté, J.S.: Intact polar lipids of
976 Thaumarchaeota and anammox bacteria as indicators of N cycling in the eastern tropical North Pacific
977 oxygen-deficient zone, Biogeosci., 12, 4833-4864, 2015.
978 Stevens H., and Ulloa, O.: Bacterial diversity in the oxygen minimum zone of the eastern tropical South
979 Pacific, Environ. Microbiol., 10, 1244–1259, 2008.
980 Stramma, L., Johnson, G. C., Sprintall, J., and Mohrholz, V.: Expanding Oxygen-Minimum Zones in the
981 Tropical Oceans, Science, 320, 655-658, 2008.
982 Stramma, L., Schmidtko, S., Levin, L. A., and Johnson, G. C.: Ocean oxygen minima expansions and their
983 biological impacts, Deep Sea Res. I, 57, 587-595, 2010.
984 Sturt, H. F., Summons, R. E., Smith, K.E., Elvert, M., Hinrichs, K.-U.: Intact polar membrane lipids in
985 prokaryotes and sediments deciphered by high-performance liquid chromatography/electrospray
986 ionization multistage mass spectrometry - new biomarkers for biogeochemistry and microbial ecology,
987 Rapid Comm. Mass Spec., 18, 617-628, 2004.

988 Taylor, G. T., Iabichella, M., Ho, T.-Y., Scranton, M. I., Thunell, R. C., Muller-Karger, F., and Varela R.:
989 Chemoautotrophy in the redox transition zone of the Cariaco Basin: A significan midwater source of
990 organic carbon production, Limol. Oceanogr., 46, 148-163, 2001.
991 Tiano, L., Garcia-Robledo, E., Dalsgaard, T., Devol, A. H., Ward, B. B., Ulloa, O., Canfield, D. E., and
992 Revsbech, N. P.: Oxygen distribution and aerobic respiration in the north and south eastern tropical
993 Pacific oxygen minimum zones, Deep Sea Res. I, 94, 173-183, 2014.
994 Turich, C., and Freeman, K. H.: Archaeal lipids record paleosalinity in hypersaline systems, Org.
995 Geochem. 42, 1147-1157, 2011.
996 Ulloa, O., Canfield, D., DeLong, E. F., Letelier, R. M., and Stewart, F. J.: Microbial oceanography of
997 anoxic oxygen minimum zones, Proc. Natl. Acad. Sci., USA 109, 15996-16003, 2012.
998 Valentine, R. C., and Valentine, D. L.: Omega-3 fatty acids in cellular membranes: a unified concept,
999 Progr. Lip. Res. 43, 383–402, 2004.
1000 Van Mooy, B. A. S., and Fredricks, H. F.: Bacterial and eukaryotic intact polar lipids in the eastern
1001 subtropical South Pacific: Water-column distribution, planktonic sources, and fatty acid composition,
1002 Geochim. Cosmochim. Acta, 74, 6499–6516, 2010.
1003 Van Mooy, B. A. S., Fredricks, H. F., Pedler, B. E., Dyhrman, S. T., Karl, D. M., Koblížek, M., Lomas,
1004 M. W., Mincer, T. J., Moore, L. R., Moutin, T., Rappé, M. S., and Webb, E. A.: Phytoplankton in the
1005 ocean use non-phosphorus lipids in response to phosphorus scarcity, Nature, 458, 69–72, 2009.
1006 Van Mooy, B. A. S., Rocap, G., Fredricks, H. F., Evans, C. T., and Devol, A. H.: Sulfolipids dramatically
1007 decrease phosphorus demand by picocyanobacteria in oligotrophic marine environments, Proc. Natl.
1008 Acad. Sci. USA, 103, 8607–8612, 2006.

Vardi, A., Van Mooy, B. A. S., Fredricks, H. F., Popendorf, K. J., Ossolinski, J. E., Haramty, L., and Bidle, K. D.: Viral glycosphingolipids induce lytic infection and cell death in marine phytoplankton, Science, 326, 861-865, 2009.

Wada, H., and Murata, N.: Membrane Lipids in cyano- bacteria, in: Lipids in Photosynthesis: Structure, Function and Genetics, Siegenthaler, P., and Murata, N. (Eds), Dordrecht, the Netherlands: Kluwer Academic Publishers, 65–81, 1998.

Wakeham, S. G., Turich, C., Schubotz, F., Podlaska, A., Li, X. N., Varela, R., Astor, Y., Sáenz, J. P., Rush, D., Sinninghe Damsté, J. S., Summons, R. E., Scranton, M. I., Taylor, G. T., and Hinrichs, K.-U.: Biomarkers, chemistry and microbiology show chemoautotrophy in a multilayer chemocline in the Cariaco Basin, Deep Sea Res. Part I, 63, 133–156, 2012.

Wakeham, S. G., Amann, R., Freeman, K. H., Hopmans, E. C., Jørgensen, B. B., Putnam, I. F., Schouten, S., Sinninghe Damsté, J. S., Talbot, H. M., and Woebken, D.: Microbial ecology of the stratified water column of the Black Sea as revealed by a comprehensive biomarker study, Org. Geochem., 38, 2070–2097, 2007.

Wakeham. S. G.: Monocarboxylic, dicarboxylic and hydroxy acids released by sequential treatments of suspended particles and sediments of the Black Sea, Org. Geochem. 30, 1059-1074, 1999.

Wakeham, S. G.: Reduction of stenols to stanols in particulate matter at oxic-anoxic boundaries in sea water, Nature, 342, 787-790, 1989.

Wakeham, S. G., and Canuel, E. A.: Organic geochemistry of particulate matter in the eastern tropical North Pacific Ocean: Implications for particle dynamics, J. Mar. Res., 46, 182-213, 1988.

Wakeham, S. G.: Steroid geochemistry in the oxygen minimum zone of the eastern tropical North Pacific

Ocean, Geochim. Cosmochim. Acta, 51, 3051-3069, 1987.

Williams, R. L., Wakeham, S., McKinney, R., Wishner, K. F.: Trophic ecology and vertical patterns of carbon and nitrogen stable isotopes in zooplankton from oxygen minimum zone regions, Deep Sea Res. I, 90 36-47, 2014.

Wishner, K. F., Outram, D. M., Seibel, B. A., Daly, K. L., and Williams, R. L.: Zooplankton in the eastern tropical north Pacific: Boundary effects of oxygen minimum zone expansion, Deep Sea Res. I, 79, 122-140, 2013.

Wishner, K. F., Gelfman, C., Gowing, M. M., Outram, D. M., Rapien, M., and Williams, R. L.: Vertical zonation and distributions of calanoid copepods through the lower oxycline of the Arabian Sea oxygen minimum zone, Progr. Oceanogr., 78, 163-191, 2008.

Woebken, D., Fuchs, B. M., Kuypers, M. M. M, and Aman, R.: Potential interactions of particle-associated anammox bacteria with bacterial and archaeal partners in the Namibian upwelling system, Appl. Environ. Microbiol., 73, 4648-4657, 2007.

Wörmer, L., Lipp, J. S., Schröder, J. M., and Hinrichs, K.-U.: Application of two new LC-ESI-MS methods for improved detection of intact polar lipids (IPLs) in environmental samples, Org. Geochem. 59, 10–21, 2013.

Wright, J. J., Konwar, K. M., and Hallam, S. J: Microbial ecology of expanding oxygen minimum zones, Nat. Rev. Microbiol. 10, 381-394, 2012.

Xie, S., Liu, X.-L., Schubotz, F., Wakeham, S. G., and Hinrichs K.-U.: Distribution of glcerol ether lipids in the oxygen minimum zone of the Easter Tropical North Pacific Ocean, Org. Geochem. 71, 60–71, 2014.

Yao, M., Elling, F. J., Jones, C., Nomosatryo, S., Long, C. P., Crowe, S. A., Antoniewicz, M. R., Hinrichs, K.-U., and Maresca, J. A.: Heterotrophic bacteria from an extremely phosphate-poor lake have conditionally reduced phosphorus demand and utilize diverse sources of phosphorus, Environ. Microbiol. 18, 656–667, 2015.

Zavaleta-Pastor, M., Sohlenkamp, C., Gao, J. L., Guan, Z., Zaheer, R., Finan, T. M., Raetz, C. R. H., López-Lara, I. M., and Geiger, O.: Sinorhizobium meliloti phospholipase C required for lipid remodeling during phosphorus limitation, Proc. Natl. Acad. Sci. USA, 107, 302–307, 2010.

Zhang, Y.-M., and Rock, C. O.: Membrane lipid homeostasis in bacteria, Nat. Rev. Microbiol., 6, 222–233, 2008.

Zhu, C., Wakeham, S. G., Elling, F. J., Basse, A., Mollenhauer, G., Versteegh, G. J. M., Könneke, M., and Hinrichs, K.-U.: Stratification of archaeal membrane lipids in the ocean and implications for adaptation and chemotaxonomy of planktonic archaea, Environ. Microbiol. 18, 4324-4336, 2016.

## Tables

**Table 1.** Spearman Rank Order Correlation coefficients (r) for data combined from all four stations. Only significant correlations, where $p < 0.05$ (highly significant $p < 0.001$, in bold), are presented.

| | Glycolipids | | | | | | Aminolipids | | | | Phospholipids | | | | | |
|---|---|---|---|---|---|---|---|---|---|---|---|---|---|---|---|---|
| | % GL | % 1G | % 2G | % SQ | GL:PL | SQ:PG | % AL | % DGTS | AL:PL | DGTS:PC | % PL | % PC | % PG | % PE | % PME | % PDME |
| Depth | -0.32 | | **-0.7** | **-0.67** | -0.41 | **-0.76** | | | | | | | | | | |
| Fluorescence | | | **0.63** | **0.67** | | **0.65** | | | | | | | | | | |
| POC | | | **0.61** | **0.6** | | **0.6** | | | | | | | | | | |
| TN | | | **0.66** | **0.62** | | **0.63** | | | | | | | | | | |
| Oxygen | **0.57** | 0.3 | **0.48** | 0.35 | **0.55** | **0.58** | | | 0.36 | | **-0.49** | | -0.38 | -0.33 | -0.46 | -0.52 |
| Temperature | 0.3 | | **0.52** | **0.63** | 0.39 | **0.69** | | | | | | | | | | |
| Chl a | 0.35 | | **0.72** | **0.71** | 0.42 | 0.78 | | | | | | | | | | -0.33 |
| Phosphate | | | **-0.62** | **-0.53** | -0.4 | **-0.56** | | | | | | | | | | 0.36 |
| Nitrate | | | **-0.53** | **-0.49** | | -0.38 | | | | | | | | | | |
| Nitrite | | -0.33 | | | | | | | | | | | | | 0.3 | |
| Ammonium | | | | | | | 0.41 | 0.42 | 0.35 | 0.4 | | | | | | |
| N:P | | | -0.3 | -0.32 | | | | | | | | | -0.36 | | | |

Abbreviations: GL – glycolipids, 1G – monoglycosyl, 2G – diglycosyl, SQ – sulfoquinovosyl, PL – phospholipids, AL – aminolipids, DGTS – diacylglyceryl trimethyl homoserine, PC – phosphatidyl choline, PG – phosphatidyl glycerol, PE – phosphatidyl ethanolamine, PME – phosphatidyl methyl-ethanolamine, PDME – phosphatidyl dimethyl-ethanolamine

**Figures**

**Figure 1.** a) Map of ETNP with R/V *Seward Johnson* (November 2007) cruise sampling stations investigated in this study.

**Figure 2.** Depth profiles of (a) oxygen and temperature, (b) chlorophyll-$\alpha$ and transmissivity, (c) particulate organic matter (POC) and C:N, (d) intact polar lipid (IPL) to POC ratio and IPL concentration, and (e) absolute cell abundance and relative proportions of archaeal cells (data from Podlaska et al. (2012)). C:N (SPM) is total carbon over total nitrogen of the solid phase collected by water filtration. Note that C:N, POC and IPL/POC are only analyzed for <53 μm particle fraction. Also depicted are the different geochemical zones in the water column.

**Figure 3.** Depth profiles of (a) nitrate, nitrite, and ammonium, (b) phosphate and N:P, (c) total non-archaeal (non-isoprenoidal) phospholipids, glycolipids and (d) aminolipids shown as percent of total intact polar lipids and ratios of non-phospholipids to phospholipids for DGTS to PC-DAG (e) SQ-DAG to PG-DAG, (e), and 1G-DAG to PE-DAG. Also depicted are the different geochemical zones in the water column.

**Figure 4.** Relative abundance of (a) major and (b) minor IPLs at sampled depths of stations 1, 2, 5, and 8 in the ETNP. Major IPLs are defined as those comprising more than 10% of total IPLs (minor compounds comprised less than 10%) at more than one depth horizon at the four stations. Also depicted are the different geochemical zones in the water column.

**Figure 5.** Changes in average carbon atoms (CA) and number of double bond equivalents (DB) of the alkyl side chains of major IPLs detected at stations 1, 2, 5 and 8 in the ETNP.

**Figure 6.** Nonmetric multidimensional scaling (NMDS) ordination plot assessing the relationship between IPL biomarkers, sampling depths and geochemical parameters in the ETNP (stress=0.125). Squares represent the water depth of each sample and are color-coded according to the defined geochemical zonation. Filled circles stand for lipid distribution of major IPLs and open circles for minor IPLs on the ordination. Vector lines of geochemical parameters are weighted by their p-values with each NMDS axis.

fig01

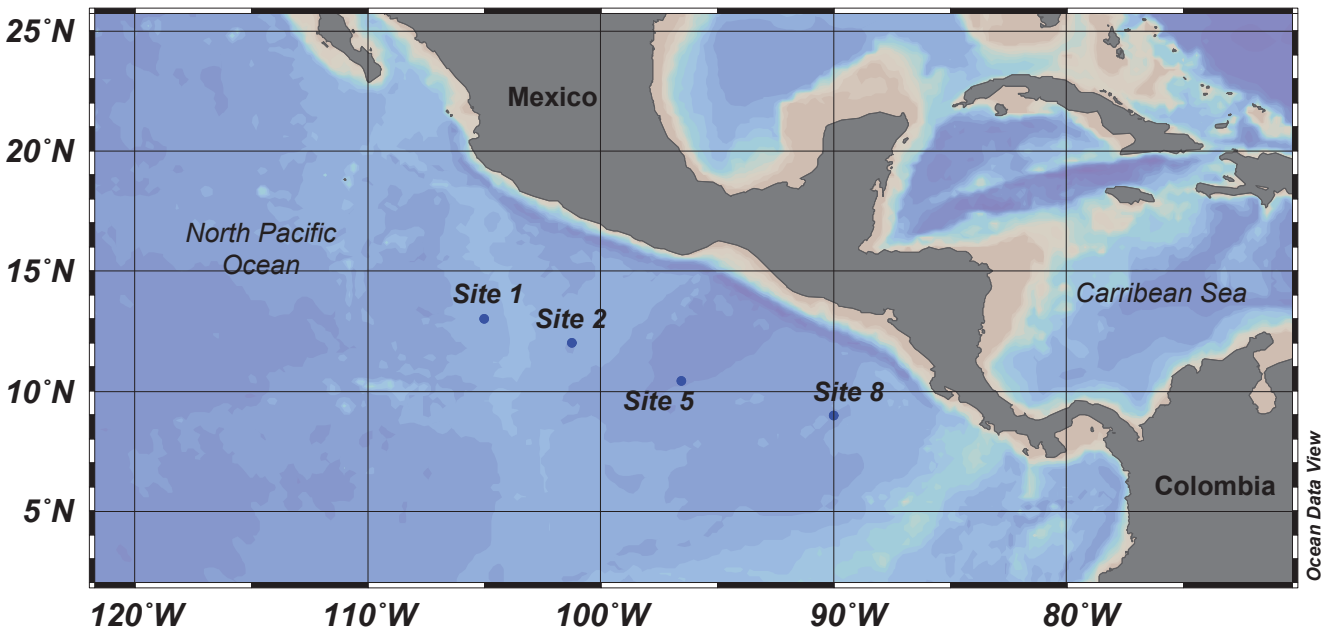
25˚N
20˚N
15˚N
10˚N
5˚N
120˚W
110˚W
100˚W
90˚W
80˚W
Mexico
North Pacific Ocean
Carribean Sea
Colombia
Site 1
Site 2
Site 5
Site 8
Ocean Data View

fig02

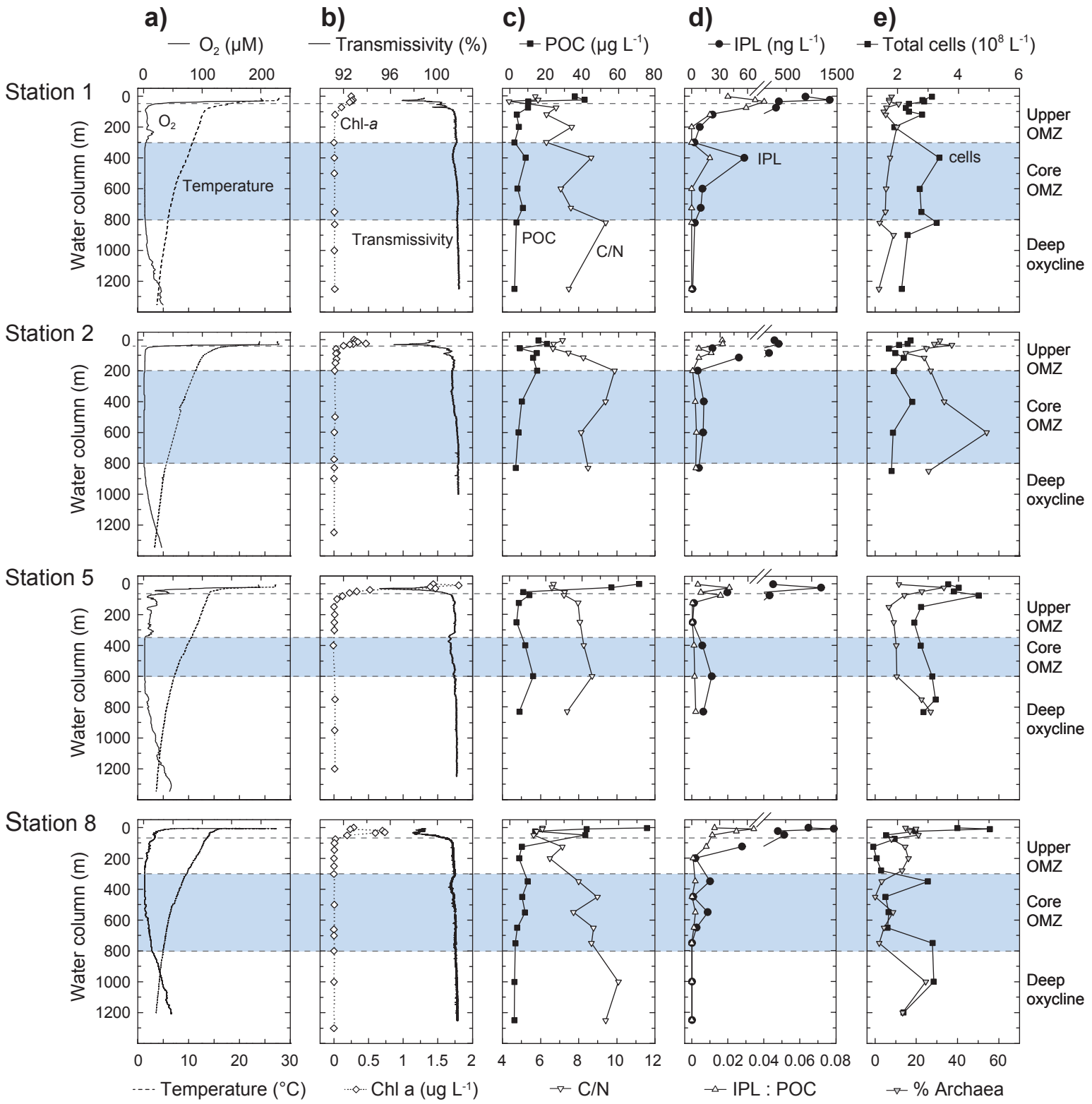
a)
b)
c)
d)
e)
O2 (µM)
Transmissivity (%)
POC (µg L-1)
IPL (ng L-1)
Total cells (10^8 L-1)
Station 1
Station 2
Station 5
Station 8
Water column (m)
O2
Temperature
Chl-a
Transmissivity
POC
C/N
IPL
cells
Upper OMZ
Core OMZ
Deep oxycline
Temperature (°C)
Chl a (ug L-1)
C/N
IPL : POC
% Archaea

fig03

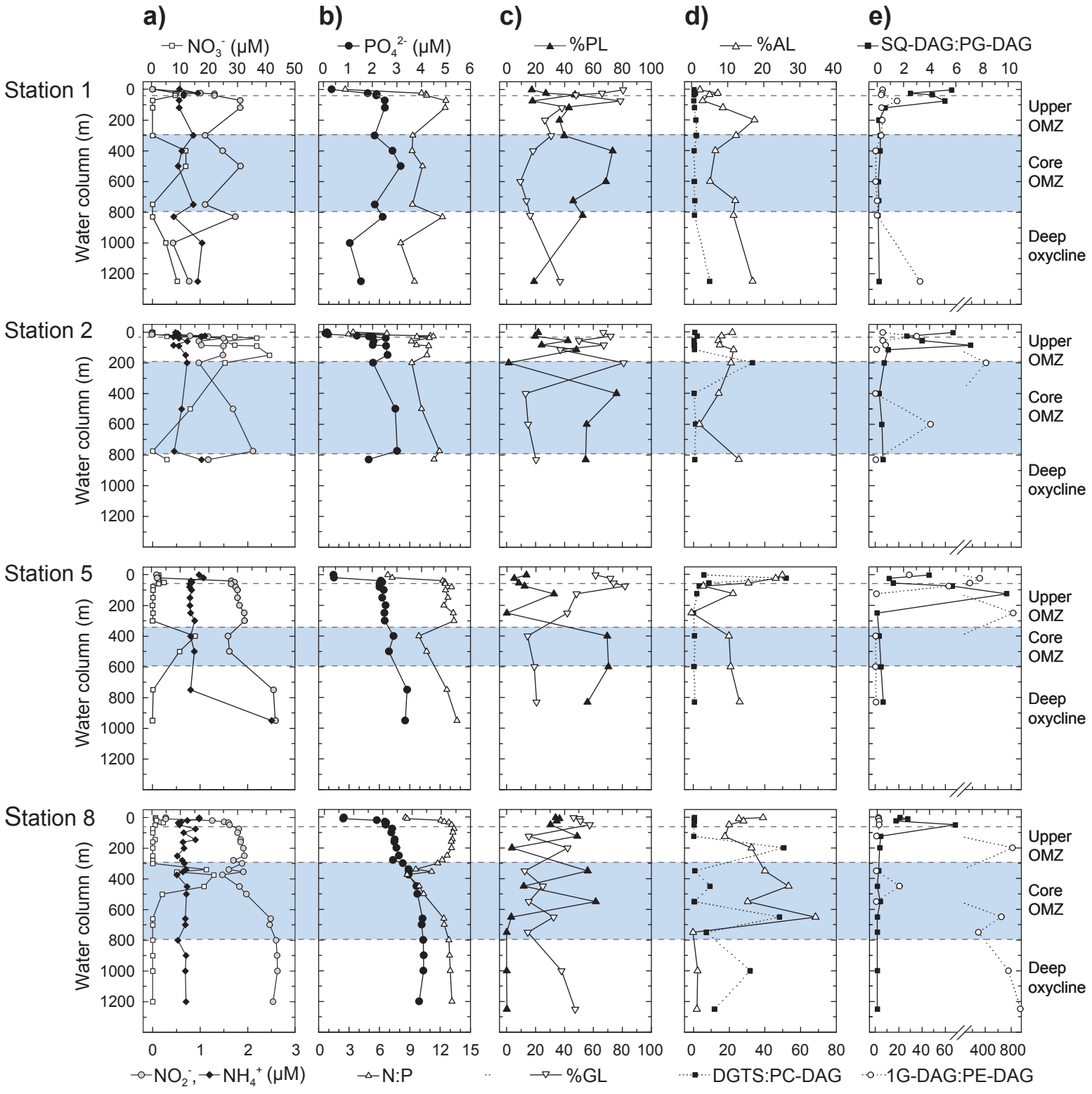


Figure 3

fig04

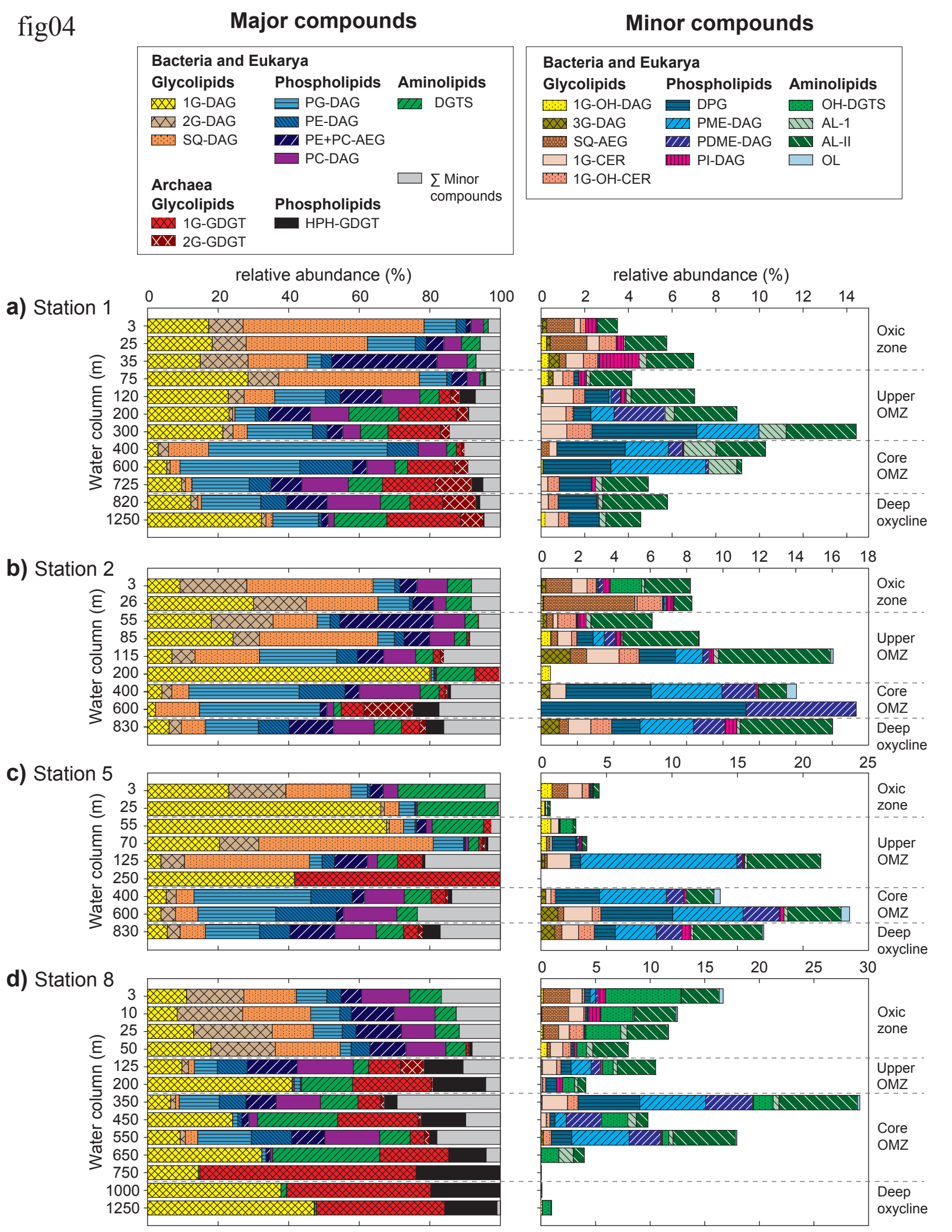
Major compounds
Minor compounds
Bacteria and Eukarya
Glycolipids
1G-DAG
2G-DAG
SQ-DAG
Phospholipids
PG-DAG
PE-DAG
PE+PC-AEG
PC-DAG
Aminolipids
DGTS
∑ Minor compounds
Archaea
Glycolipids
1G-GDGT
2G-GDGT
Phospholipids
HPH-GDGT
Bacteria and Eukarya
Glycolipids
1G-OH-DAG
3G-DAG
SQ-AEG
1G-CER
1G-OH-CER
Phospholipids
DPG
PME-DAG
PDME-DAG
PI-DAG
Aminolipids
OH-DGTS
AL-1
AL-II
OL
relative abundance (%)
relative abundance (%)
a) Station 1
b) Station 2
c) Station 5
d) Station 8
Water column (m)
Oxic zone
Upper OMZ
Core OMZ
Deep oxycline

fig05

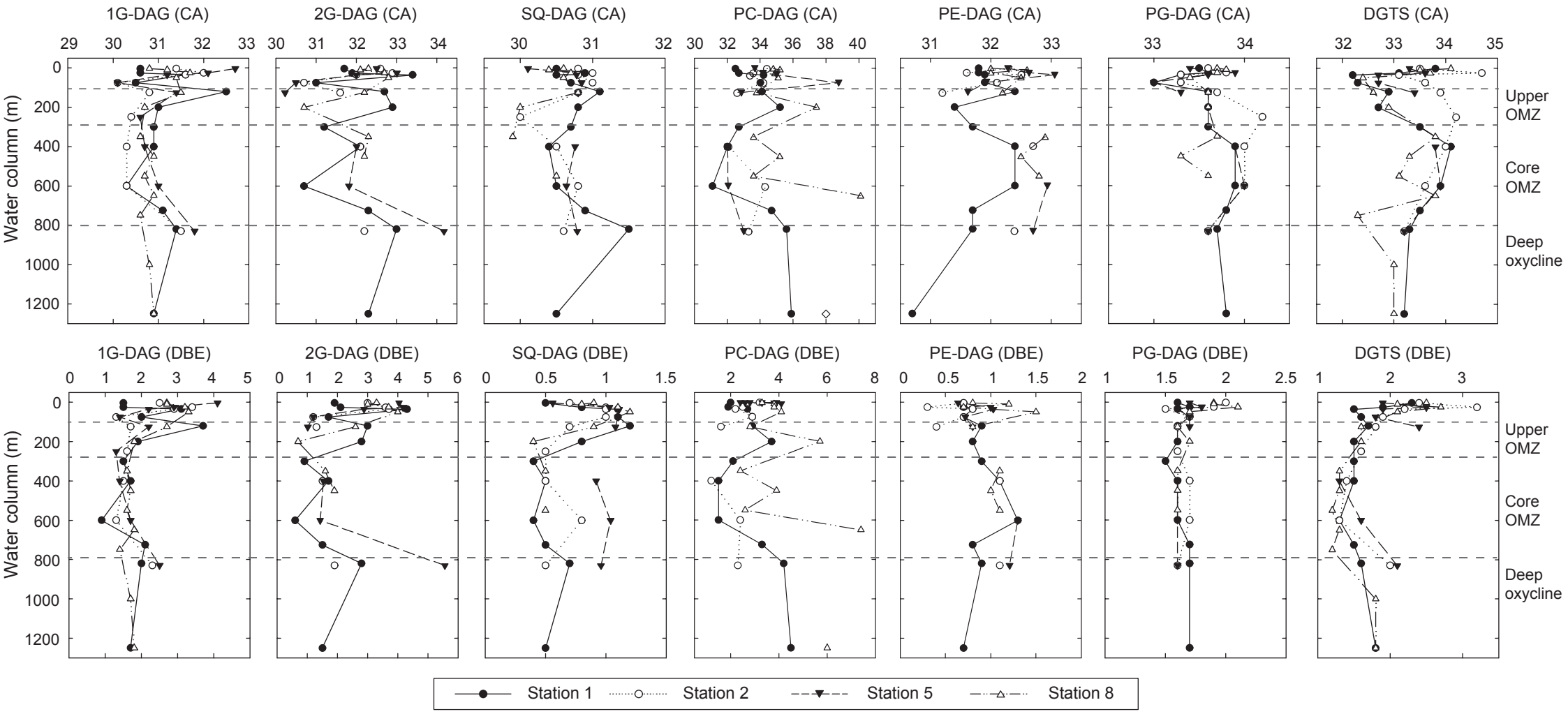
1G-DAG (CA)
2G-DAG (CA)
SQ-DAG (CA)
PC-DAG (CA)
PE-DAG (CA)
PG-DAG (CA)
DGTS (CA)
1G-DAG (DBE)
2G-DAG (DBE)
SQ-DAG (DBE)
PC-DAG (DBE)
PE-DAG (DBE)
PG-DAG (DBE)
DGTS (DBE)
Water column (m)
Upper OMZ
Core OMZ
Deep oxycline
Station 1
Station 2
Station 5
Station 8

fig06

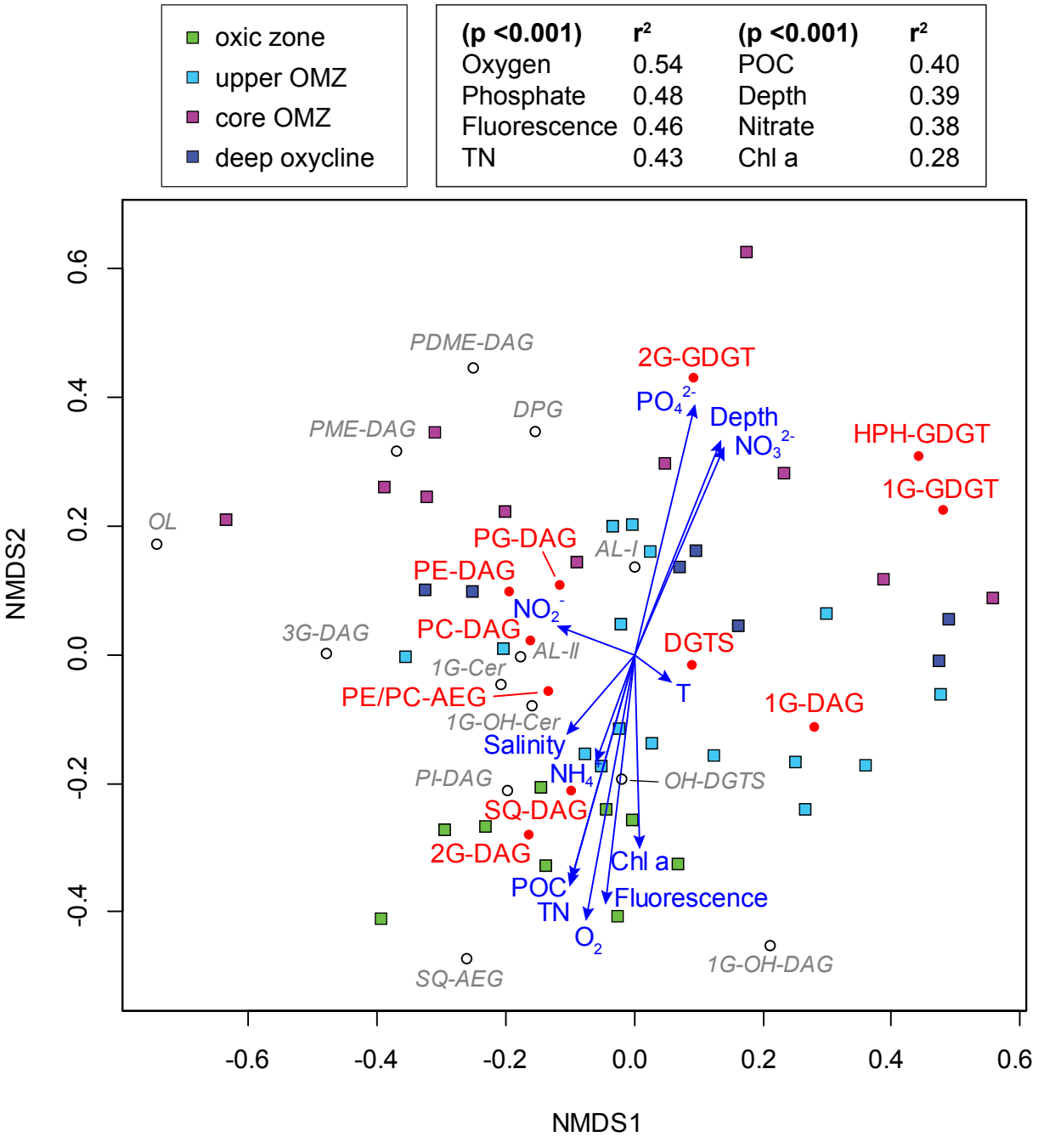
oxic zone
upper OMZ
core OMZ
deep oxycline
(p <0.001) r²
Oxygen 0.54
Phosphate 0.48
Fluorescence 0.46
TN 0.43
(p <0.001) r²
POC 0.40
Depth 0.39
Nitrate 0.38
Chl a 0.28
PDME-DAG
2G-GDGT
PO4 2-
DPG
Depth
PME-DAG
NO3 2-
HPH-GDGT
1G-GDGT
OL
PG-DAG
AL-I
PE-DAG
NO2 -
3G-DAG
PC-DAG
AL-II
DGTS
1G-Cer
T
PE/PC-AEG
1G-DAG
1G-OH-Cer
Salinity
NH4
PI-DAG
OH-DGTS
SQ-DAG
2G-DAG
Chl a
POC
Fluorescence
TN
O2
SQ-AEG
1G-OH-DAG
NMDS1
NMDS2
-0.6
-0.4
-0.2
0.0
0.2
0.4
0.6

**Intact polar lipids in the water column of the Eastern Tropical North Pacific: Abundance and structural variety of non-phosphorus lipids**

Florence Schubotz [1*], Sitan Xie [1,¶], Julius S. Lipp [1], Kai-Uwe Hinrichs [1], Stuart G. Wakeham[2]

[1]MARUM Center for Marine Environmental Sciences and Department of Geosciences, University of Bremen, 28359 Bremen, Germany

[2]Skidaway Institute of Oceanography, Savannah, GA 31411, USA

[¶]Current address: Wai Gao Qiao Free Trade Zone, 200131 Shanghai, China

[*]Corresponding author. MARUM, University of Bremen, Leobener Str. 13, Room 1070, 28359 Bremen, Germany. Tel: +49-421-218-65724. Fax: +49-421-218-65715. E-mail: schubotz@uni-bremen

**Suppl. Table 1.** Relative abundance of detected intact polar lipids (IPL) at all four stations (1, 2, 5 and 8) in the Eastern Tropical North Pacific, t.a. - trace amonts, n.d. - not detected. For IPL abbreviations refer to main text.

| | | | | Relative Abundance (%) | | | | | | | | | | | | | | | | | | | | | | |
|---|---|---|---|---|---|---|---|---|---|---|---|---|---|---|---|---|---|---|---|---|---|---|---|---|---|---|
| Station | Depth (m) | Water filtered (L) | Total IPL (ng/L) | 1G-DAG | 2G-DAG | SQ-DAG | DGTS | PE+PC-AEG | PE-DAG | PC-DAG | PG-DAG | DPG | 3G-DAG | SQ-DEG | 1G-Cer | AL-1 | AL-II | OL | PME-DAG | PDME-DAG | PI-DAG | 1G-OH-DAG | 1G-OH-Cer | OH-DGTS | 1G-GDGT | 2G-GDGT | HPH-GDGT |
| 1 | 3 | 575 | 882.3 | 17.4 | 9.8 | 51.2 | 1.3 | 1.4 | 2.8 | 3.5 | 9.0 | 0.0 | 0.2 | 1.3 | 0.3 | t.a. | 0.9 | n.d. | n.d. | n.d. | 0.5 | 0.1 | 0.2 | n.d. | n.d. | n.d. | n.d. |
| 1 | 25 | 193 | 1357.8 | 18.4 | 9.6 | 34.3 | 5.3 | 4.9 | 3.2 | 5.0 | 13.5 | 0.0 | 0.2 | 1.7 | 0.6 | 0.1 | 1.9 | n.d. | n.d. | n.d. | 0.3 | 0.3 | 0.8 | n.d. | n.d. | n.d. | n.d. |
| 1 | 35 | 1636 | 361.6 | 15.0 | 13.5 | 16.7 | 2.4 | 29.8 | 3.0 | 8.5 | 4.0 | 0.1 | 0.5 | 0.3 | 0.8 | 0.3 | 2.2 | n.d. | n.d. | n.d. | 1.8 | 0.4 | 0.7 | n.d. | n.d. | n.d. | n.d. |
| 1 | 75 | 1013 | 304.0 | 28.5 | 8.7 | 39.8 | 0.9 | 4.2 | 1.5 | 3.7 | 7.7 | 0.2 | 0.2 | n.d. | 0.4 | 0.2 | 1.9 | n.d. | n.d. | n.d. | 0.4 | 0.3 | 0.5 | n.d. | 0.2 | 0.1 | 0.4 |
| 1 | 120 | 1347 | 22.3 | 22.9 | 4.5 | 8.6 | 5.5 | 11.8 | 4.2 | 10.7 | 14.4 | 1.1 | 0.1 | n.d. | 1.4 | 0.2 | 2.9 | n.d. | 0.1 | 0.4 | 0.3 | n.d. | 0.5 | n.d. | 3.3 | 2.6 | 4.5 |
| 1 | 200 | 1578 | 8.4 | 23.2 | 1.0 | 0.7 | 14.0 | 11.9 | 3.8 | 10.9 | 5.7 | 0.8 | n.d. | n.d. | 1.1 | 0.4 | 2.9 | n.d. | 1.1 | 2.3 | n.d. | n.d. | 0.3 | n.d. | 16.4 | 3.2 | 0.3 |
| 1 | 300 | 1337 | 2.9 | 21.4 | 2.9 | 4.0 | 7.8 | 4.5 | 4.1 | 4.9 | 18.5 | 4.8 | n.d. | n.d. | 1.2 | 1.2 | 3.2 | n.d. | 2.8 | n.d. | n.d. | n.d. | 1.2 | n.d. | 14.9 | 2.6 | n.d. |
| 1 | 400 | 1300 | 56.4 | 3.1 | 2.9 | 11.3 | 2.7 | 0.0 | 8.8 | 8.1 | 50.6 | 3.1 | n.d. | 0.4 | 0.4 | 1.5 | 2.3 | n.d. | 2.0 | 0.6 | 0.1 | n.d. | n.d. | n.d. | 1.4 | 0.8 | n.d. |
| 1 | 600 | 1748 | 11.4 | 5.6 | 0.9 | 2.8 | 3.5 | 3.9 | 15.1 | 8.0 | 33.9 | 3.1 | n.d. | n.d. | n.d. | 1.3 | 0.2 | n.d. | 4.3 | 0.1 | n.d. | 0.1 | n.d. | n.d. | 13.3 | 3.8 | n.d. |
| 1 | 725 | 800 | 9.7 | 9.8 | 1.0 | 1.9 | 9.6 | 8.7 | 6.1 | 13.2 | 16.2 | 1.5 | n.d. | n.d. | 0.3 | 0.3 | 2.1 | n.d. | n.d. | n.d. | 0.2 | n.d. | 0.5 | n.d. | 14.9 | 10.4 | 3.2 |
| 1 | 820 | 1571 | 3.3 | 12.3 | 2.0 | 1.1 | 8.4 | 11.4 | 7.3 | 15.1 | 16.8 | 1.8 | n.d. | n.d. | 0.3 | 0.2 | 3.0 | n.d. | n.d. | n.d. | 0.1 | n.d. | 0.5 | n.d. | 9.3 | 9.4 | 1.2 |
| 1 | 1250 | 1374 | 0.8 | 32.4 | 1.3 | 1.9 | 14.9 | 1.9 | 0.8 | 1.6 | 13.0 | 1.4 | n.d. | n.d. | 0.6 | 0.3 | 1.6 | n.d. | n.d. | n.d. | n.d. | 0.2 | 0.5 | n.d. | 21.0 | 6.3 | 0.3 |
| 2 | 3 | 1071 | 266.2 | 9.3 | 18.9 | 35.7 | 6.8 | 4.8 | 1.4 | 8.6 | 6.2 | 0.1 | 0.2 | 1.4 | 0.8 | 0.2 | 2.5 | t.a. | n.d. | 0.3 | 0.4 | t.a. | 0.5 | 1.7 | 0.0 | n.d. | n.d. |
| 2 | 6 | 1166 | 349.6 | 30.1 | 14.9 | 20.3 | 7.2 | 5.9 | 0.8 | 3.5 | 9.0 | 0.1 | t.a. | 5.0 | 0.1 | 0.0 | 1.0 | n.d. | 0.1 | n.d. | 0.4 | 0.1 | 1.4 | t.a. | 0.0 | n.d. | n.d. |
| 2 | 55 | 1647 | 21.9 | 18.1 | 17.5 | 12.4 | 3.7 | 26.5 | 2.8 | 8.9 | 3.6 | 0.1 | 0.2 | 0.4 | 0.3 | 0.3 | 3.4 | t.a. | t.a. | n.d. | 0.4 | 0.1 | t.a. | n.d. | 0.3 | n.d. | n.d. |
| 2 | 85 | 1435 | 160.0 | 24.3 | 7.5 | 33.5 | 3.5 | 7.3 | 2.7 | 7.1 | 4.7 | 0.9 | t.a. | 0.4 | 0.8 | 0.1 | 4.2 | t.a. | 0.6 | 0.6 | 0.3 | 0.5 | 0.3 | n.d. | 0.6 | 0.2 | 0.0 |
| 2 | 115 | 1517 | 50.0 | 7.0 | 6.6 | 18.2 | 5.0 | 7.4 | 5.8 | 9.1 | 21.9 | 2.0 | 1.6 | 0.9 | 1.8 | 0.3 | 6.2 | 0.1 | 1.5 | 0.3 | 0.3 | n.d. | 1.1 | n.d. | 2.1 | 1.0 | n.d. |
| 2 | 200 | 193 | 6.0 | 80.0 | 0.0 | 0.4 | 10.8 | 0.2 | 0.2 | 0.3 | 0.7 | 0.0 | n.d. | n.d. | n.d. | n.d. | n.d. | n.d. | n.d. | n.d. | n.d. | 0.5 | n.d. | n.d. | 6.8 | 0.0 | n.d. |
| 2 | 400 | 1725 | 12.6 | 4.2 | 2.8 | 4.8 | 5.4 | 4.1 | 13.0 | 17.2 | 31.2 | 4.7 | 0.5 | n.d. | 0.9 | n.d. | 1.6 | 0.5 | 3.9 | 1.9 | 0.1 | n.d. | n.d. | n.d. | 1.7 | 0.7 | 1.0 |
| 2 | 600 | 1476 | 11.8 | 2.4 | 0.0 | 12.5 | 2.1 | 1.9 | 0.1 | 1.9 | 34.1 | 11.3 | n.d. | n.d. | n.d. | n.d. | 0.0 | 0.0 | n.d. | 6.1 | n.d. | n.d. | n.d. | n.d. | 6.5 | 13.8 | 7.5 |
| 2 | 830 | 1397 | 7.2 | 6.2 | 3.5 | 6.8 | 7.7 | 12.5 | 8.7 | 11.5 | 15.0 | 1.6 | 1.0 | 0.5 | 1.2 | 0.2 | 5.1 | 0.0 | 2.9 | 1.7 | 0.6 | n.d. | 1.1 | n.d. | 5.1 | 1.8 | 5.1 |
| 5 | 3 | 223 | 244.4 | 23.1 | 16.1 | 18.4 | 24.6 | 3.8 | 0.8 | 4.1 | 4.6 | 0.1 | n.d. | 1.2 | 1.1 | t.a. | 0.4 | n.d. | n.d. | n.d. | 0.1 | 0.8 | 0.5 | 0.1 | n.d. | n.d. | n.d. |

| | | | | | | | | | | | | | | | | | | | | | | | | | | | |
|---|---|---|---|---|---|---|---|---|---|---|---|---|---|---|---|---|---|---|---|---|---|---|---|---|---|---|---|
| 5 | 25 | 128 | 1187.6 | 66.1 | 1.0 | 4.1 | 22.9 | 0.0 | 0.2 | 0.4 | 4.5 | 0.0 | n.d. | n.d. | 0.0 | 0.2 | 0.2 | n.d. | n.d. | n.d. | 0.1 | 0.3 | n.d. | n.d. | n.d. | n.d. | n.d. |
| 5 | 35 | 1683 | 38.1 | 67.7 | 0.7 | 4.0 | 14.5 | 2.8 | 0.4 | 1.7 | 3.3 | 0.0 | n.d. | n.d. | 0.6 | n.d. | 0.2 | n.d. | t.a. | n.d. | 0.0 | 0.8 | n.d. | 1.0 | 2.2 | n.d. | n.d. |
| 5 | 75 | 995 | 174.8 | 20.5 | 11.0 | 49.3 | 2.9 | 0.2 | 0.3 | 0.9 | 8.6 | 1.8 | t.a. | 0.2 | 0.2 | t.a. | 0.3 | t.a. | 0.1 | 0.2 | 0.2 | 0.4 | n.d. | t.a. | 1.1 | 0.8 | 0.8 |
| 5 | 125 | 1289 | 2.3 | 3.9 | 6.7 | 35.3 | 5.6 | 9.3 | 3.6 | 2.8 | 3.6 | 0.8 | 0.2 | 0.2 | 1.8 | 0.2 | 5.6 | n.d. | 11.9 | 0.4 | 0.1 | 0.1 | n.d. | t.a. | 7.1 | n.d. | 0.8 |
| 5 | 250 | 1362 | 1.1 | 41.7 | 0.0 | 0.0 | 0.0 | 0.0 | 0.1 | 0.0 | 0.0 | 0.0 | n.d. | n.d. | n.d. | n.d. | n.d. | n.d. | n.d. | n.d. | n.d. | n.d. | n.d. | n.d. | 58.3 | n.d. | n.d. |
| 5 | 400 | 1365 | 11.2 | 5.4 | 2.8 | 5.0 | 7.7 | 3.4 | 11.8 | 11.3 | 33.0 | 3.4 | 0.4 | n.d. | 0.4 | 0.1 | 2.1 | 0.5 | 5.1 | 1.3 | 0.1 | n.d. | 0.3 | n.d. | 4.0 | 0.8 | 1.1 |
| 5 | 600 | 968 | 21.4 | 3.9 | 4.2 | 6.3 | 5.8 | 2.1 | 17.1 | 15.1 | 22.0 | 5.5 | 1.3 | 0.4 | 2.2 | 0.3 | 4.1 | 0.7 | 5.4 | 2.8 | 0.4 | n.d. | 0.7 | n.d. | 0.0 | n.d. | 0.0 |
| 5 | 830 | 1595 | 12.4 | 5.7 | 3.6 | 7.2 | 7.7 | 12.8 | 8.6 | 11.6 | 15.4 | 1.6 | 1.0 | 0.5 | 1.3 | 0.2 | 5.3 | 0.1 | 3.1 | 2.0 | 0.7 | n.d. | 1.2 | n.d. | 4.1 | 1.3 | 5.1 |
| 8 | 3 | 387 | 955.4 | 11.2 | 16.2 | 14.9 | 9.0 | 5.8 | 4.0 | 13.6 | 8.6 | 0.5 | t.a. | 2.4 | 1.1 | t.a. | 3.5 | 0.3 | 0.5 | 0.2 | 0.7 | 0.2 | 0.2 | 6.9 | 0.0 | n.d. | 0.0 |
| 8 | 10 | 309 | 1458.8 | 8.5 | 18.5 | 19.2 | 6.0 | 12.1 | 3.2 | 11.6 | 8.3 | 0.2 | 0.1 | 2.5 | 1.4 | 0.1 | 3.8 | 0.1 | t.a. | 0.1 | 1.1 | n.d. | 0.2 | 3.0 | 0.0 | n.d. | n.d. |
| 8 | 25 | 1648 | 348.7 | 13.2 | 22.2 | 11.6 | 6.8 | 12.9 | 3.9 | 9.5 | 8.2 | 0.0 | 0.1 | 1.4 | 1.0 | 0.6 | 3.7 | 0.1 | 0.1 | n.d. | t.a. | 0.1 | 1.3 | 3.2 | 0.0 | n.d. | n.d. |
| 8 | 50 | 887 | 474.4 | 18.0 | 18.3 | 18.4 | 5.7 | 10.2 | 5.3 | 11.3 | 3.1 | 0.2 | 0.1 | 0.3 | 1.1 | 0.6 | 3.2 | n.d. | n.d. | n.d. | 0.3 | 0.5 | 0.7 | 0.9 | 0.8 | 0.2 | 0.7 |
| 8 | 125 | 1231 | 54.2 | 9.8 | 1.9 | 1.7 | 4.4 | 14.1 | 8.5 | 15.8 | 6.5 | 0.9 | t.a. | 0.1 | 1.3 | 0.4 | 3.5 | t.a. | 1.9 | 0.8 | 0.2 | n.d. | 0.4 | 1.0 | 9.1 | 6.7 | 11.0 |
| 8 | 200 | 1698 | 3.8 | 41.1 | 0.2 | 0.3 | 14.5 | n.d. | t.a. | 0.3 | 1.8 | 1.0 | n.d. | n.d. | 0.1 | 0.3 | 0.7 | n.d. | n.d. | n.d. | 0.5 | n.d. | 0.3 | 1.1 | 22.3 | 0.4 | 15.0 |
| 8 | 350 | 1633 | 19.5 | 6.7 | 1.3 | 1.1 | 10.5 | 8.5 | 7.5 | 12.6 | 11.3 | 5.6 | 0.1 | n.d. | 2.3 | 0.5 | 7.2 | 0.2 | 6.0 | 4.3 | 0.1 | n.d. | 1.0 | 1.8 | 6.5 | 1.0 | 3.6 |
| 8 | 450 | 1440 | 1.5 | 24.2 | 0.0 | n.d. | 22.6 | 2.1 | 1.2 | 2.4 | 1.5 | 0.5 | n.d. | n.d. | 0.5 | 0.8 | 1.1 | n.d. | 1.1 | 3.2 | n.d. | n.d. | 0.3 | 2.4 | 22.8 | 0.9 | 12.7 |
| 8 | 550 | 1251 | 17.2 | 9.4 | 1.4 | 3.5 | 8.7 | 9.4 | 11.4 | 15.5 | 15.1 | 1.9 | 0.2 | n.d. | n.d. | 0.4 | 5.8 | 0.1 | 5.3 | 2.9 | 0.2 | n.d. | 0.7 | 0.6 | 4.0 | 1.4 | 2.1 |
| 8 | 650 | 1633 | 5.1 | 32.4 | n.d. | n.d. | 30.4 | 1.2 | 0.1 | 0.6 | 1.2 | 0.0 | n.d. | n.d. | n.d. | 1.3 | 1.0 | n.d. | n.d. | n.d. | n.d. | n.d. | n.d. | 1.6 | 19.5 | 0.1 | 10.5 |
| 8 | 750 | 1926 | 0.1 | 14.5 | n.d. | n.d. | 0.4 | n.d. | 0.1 | 0.1 | n.d. | n.d. | n.d. | n.d. | n.d. | n.d. | t.a. | n.d. | n.d. | n.d. | n.d. | n.d. | n.d. | n.d. | 61.2 | n.d. | 23.8 |
| 8 | 1000 | 1633 | 0.1 | 37.9 | n.d. | n.d. | 1.6 | n.d. | 0.1 | 0.1 | n.d. | n.d. | n.d. | n.d. | n.d. | n.d. | 0.1 | n.d. | n.d. | n.d. | n.d. | n.d. | n.d. | n.d. | 40.7 | n.d. | 19.8 |
| 8 | 1250 | 1417 | 0.1 | 47.3 | n.d. | n.d. | 0.6 | n.d. | 0.1 | 0.1 | n.d. | n.d. | n.d. | n.d. | n.d. | n.d. | t.a. | n.d. | n.d. | n.d. | n.d. | 0.1 | n.d. | 0.8 | 36.3 | 0.0 | 14.9 |

**Suppl. Table 2.** List of commercially available standards used to determine response factors of intact polar lipids (IPL) in this study. For absolute quantification by HPLC-ion trap-MS the response factor was evaluated relative to the injection standard C19:0 PC-DAG. For determining relative abundances of IPLs via HPLC-QTOF-MS (see methods in the main text), the absolute responses of the individual standards were used. For IPL abbreviations refer to main text.

| Short ID | Full Name | Fatty acid distribution | Company | Used for IPL class (HPLC-ion trap-MS) | Used for IPL class (HPLC-QTOF-MS) |
|---|---|---|---|---|---|
| 16:0 PE-DAG | 1,2-dipalmitoyl-sn-glycero-3-phosphoethanolamine | 16:0/16:0 | Avanti Polar Lipids, USA | PE-DAG, PME-DAG, PDME-DAG | PE-DAG |
| 16:0 PC-DAG | 1,2-dipalmitoyl-sn-glycero-3-phosphocholine | 16:0/16:0 | Avanti Polar Lipids, USA | PC-DAG | PC-DAG |
| 19:0 PC-DAG | 1,2-dinonadecanoyl-sn-glycero-3-phosphocholine | 19:0/19:0 | Avanti Polar Lipids, USA | | internal standard for all IPLs |
| 16:0 PME-DAG | 1,2-dipalmitoyl-sn-glycero-3-phosphoethanolamine-N-methyl | 16:0/16:0 | Avanti Polar Lipids, USA | | PME-DAG |
| 16:0 PDME-DAG | 1,2-dipalmitoyl-sn-glycero-3-phosphoethanolamine-N,N-dimethyl | 16:0/16:0 | Avanti Polar Lipids, USA | | PDME-DAG |
| 16:0 PG-DAG | 1,2-dipalmitoyl-sn-glycero-3-phospho-(1'-rac-glycerol) | 16:0/16:0 | Avanti Polar Lipids, USA | PG-DAG, SQ-DAG, DPG | PG-DAG, SQ-DAG |
| 16:1 DPG | 1',3'-bis(1,2-dipalmitoleoyl-sn-glycero-3-phospho)-glycerol | 16:1/16:1/16:1/16:1 | Avanti Polar Lipids, USA | | DPG |
| 1Glc-DAG | 1,2-diacyl-3-O-(a-D-glucopyranosyl)-sn-glycerol (E.coli) | 18:1/16:0, 18:1/16:1, 16:1/16:0, 18:1/18:1 | Avanti Polar Lipids, USA | 1G-DAG | 1G-DAG |
| 2G-DAG | Digalactosyldiacylglcyerol (plant, hydrogenated) | 18:0/18:0, 18:0/16:0 | Avanti Polar Lipids, USA | 2G-DAG | 2G-DAG |
| DGTS | 1,2-dipalmitoyl-sn-glycero-3-O-4'-[N,N,N-trimethyl)-homoserine | 16:0/16:0 | Avanti Polar Lipids, USA | DGTS | DGTS |
| C18 1G-CER | D-galactosyl-b-1,1'-N-stearoyl-D-erythro-sphingosine | d18:1/18:0 | Avanti Polar Lipids, USA | 1G-CER | 1G-CER |
| 1G-GDGT-PG | Main phospholipid of Thermoplasma acidophilum (>95% pure) | | Matreya LLC, USA | HPH-GDGT, 1G-GDGT, 2G-GDGT | HPH-GDGT, 1G-GDGT, 2G-GDGT |

**Suppl. Table 3.** Examples of HPLC-MS fragmentation patterns (MS2) in positive ionization mode for select major ions (MS1) of intact polar lipids (IPLs) detected in this study.

| IPL | MS1 (pos ion mode)<br>Select major ions (m/z) | MS2 (pos ion mode)<br>Neutral loss (Da) | MS2 (pos ion mode)<br>Select diagnostic ions (m/z) |
|---|---|---|---|
| ***Glycolipids*** | | | |
| 1G-DAG | 766.546, 718.546, 716.531 $[M+NH_4]^+$ | Hexose plus $NH_3$ (179.079) | 335.258, 305.211, 313.277, 285.245 |
| 1G-OH-DAG | 732.526, 730.510 $[M+NH_4]^+$ | Hexose plus $NH_3$ (179.079) | 313.277, 285.245 |
| 2G-DAG | 936.662, 934.646, 882.615, 880.599 $[M+NH_4]^+$ | Two hexoses plus $NH_3$ (341.132) | 339.291, 337.274, 313.277, 285.245 |
| SQ-DAG | 812.555, 784.524, 782.508, 756.493 $[M+H]^+$ | Sulfoquinovosyl (261.052) | 313.277, 313.277, 311.258, 285.245 |
| SQ-AEG | 824.592, 798.576 $[M+H]^+$ | Sulfoquinovosyl (261.052) | 339.291 |
| 1G-CER | 748.572, 734.557 $[M+H]^+$ | Hexose plus $H_2O$ (180.063) | 294.279 (LCB) |
| 1G-OH-CER | 780.598, 766.583, 752.567 $[M+H]^+$ | Hexose plus $H_2O$ (180.063) | 294.279 (LCB) |
| 1G-GDGT | 1481.402, 1471.324 $[M+NH_4]^+$ | Hexose plus $NH_3$ (179.079) | 1302.323, 1292.44 |
| 2G-GDGT | 1639.424 $[M+NH_4]^+$ | Two hexoses plus $NH_3$ (341.132) | 1298.291 |
| HPH-GDGT | 1723.421, 1713.343 $[M+NH_4]^+$ | Hexose plus $NH_3$ (179.079), hexose (162.053) | 1544.342, 1382.289, 1534.264, 1372.211 |
| ***Phospholipids*** | | | |
| PE-DAG | 730.538, 718.538, 704.522, 678.507 $[M+H]^+$ | Phosphoethanolamine (141.019) | DAG fragments |
| PE-AEG | 706.575, 702.543 $[M+H]^+$ | Phosphoethanolamine (141.019) | |
| PC-DAG | 806.569, 780.554, 746.569, 706.538 $[M+H]^+$ | - | 184.073, DAG fragments |
| PC-AEG | 746.606 742.575, 716.559 $[M+H]^+$ | - | 184.073 |
| PG-DAG | 766.559, 764.544, 762.528 $[M+NH_4]^+$ | Phosphoglycerol plus $NH_3$ (189.040) | DAG fragments |
| DPG | 1404.990, 1380.990, 1352.959, 1338.943 $[M+NH_4]^+$ | - | DAG fragments |
| PME-DAG | 732.554, 718.538, 692.522 $[M+H]^+$ | Phosphomethylethanolamine (155.035) | DAG fragments |
| PDME-DAG | 732.554, 730.538, 704.522 $[M+H]^+$ | Phosphodimethylethanolamine (169.050) | DAG fragments |
| PI-DAG | 902.575, 900.560 $[M+NH_4]^+$ | Phosphoinositol plus $NH_3$ (277.056) | DAG fragments |

| | | | |
|---|---|---|---|
| ***Aminolipids*** | | | |
| DGTS | 764.640, 760.609, 736.609, 732.577 $[M+H]^+$ | - | 498.382, 480.371, 474.382, 456.237, 236.149 |
| OH-DGTS | 754.619, 746.557 $[M+H]^+$ | - | 512.358, 494.351, 476.340, 496.366, 478.357, 236.149 |
| OL | 693.614, 653.583 $[M+H]^+$ | - | 115.087 |
| AL-I | 842.650, 814.619, 742.619 $[M+H]^+$ | - | 558.378, 514.409 |
| AL-II | 800.603, 728.603, 700.572 $[M+H]^+$ | - | 562.374, 544.365, 490.374, 472.364 |

**Suppl. Table 4.** Absolute concentrations of pigments detected in surface waters of the Eastern Tropical North Pacific at stations 1, 5 and 8.

Concentration (ng/L)

| Station | Depth (m) | MgDVP | Chl c2 | Chl c1 | Per | 19-But | Fuco | Neo | Prasino | Viola | 19-Hex | DD | Cis-fuco | Allo | DT | Zeax | Lutein | Lutein Late | 8-Apo | Croco | DV Chl a | Chl a | Chl c2 Like | a-Car | b-Car | Chl c3 | Chl b | c-MVP | Sum Ph-ide | Ph-ide 2 | Ph-ide 3 | Ph-tin |
|---|---|---|---|---|---|---|---|---|---|---|---|---|---|---|---|---|---|---|---|---|---|---|---|---|---|---|---|---|---|---|---|---|
| 1 | 3 | 2.64 | 7.55 | 0.00 | 0.00 | 4.77 | 4.74 | 0.00 | 0.00 | 0.00 | 14.60 | 3.24 | 0.00 | 0.00 | 0.00 | 109.7 | 1.53 | 0.00 | 18.46 | 0.00 | 69.51 | 125.76 | 0.00 | 10.94 | 4.02 | 7.91 | 30.08 | 0.00 | 0.00 | 0.00 | 0.00 | 5.35 |
| 1 | 9 | 4.07 | 3.91 | 0.00 | 0.00 | 5.69 | 4.95 | 0.00 | 0.00 | 0.00 | 15.94 | 3.79 | 0.00 | 0.00 | 0.00 | 136.6 | 1.05 | 3.97 | 15.21 | 0.00 | 74.43 | 123.91 | 0.00 | 13.97 | 6.14 | 4.08 | 28.25 | 0.00 | 0.00 | 0.00 | 0.00 | 6.61 |
| 1 | 16 | 4.84 | 15.00 | 0.00 | 2.49 | 8.66 | 6.83 | 0.75 | 0.00 | 0.00 | 23.91 | 3.31 | 0.00 | 0.00 | 0.00 | 90.62 | 0.00 | 9.54 | 14.95 | 0.00 | 87.95 | 148.73 | 2.24 | 14.79 | 4.19 | 12.87 | 36.40 | 0.91 | 0.38 | 0.00 | 0.38 | 9.29 |
| 1 | 29 | 8.08 | 32.27 | 0.00 | 1.75 | 16.59 | 38.92 | 1.17 | 1.58 | 0.53 | 42.64 | 4.18 | 0.00 | 1.47 | 0.00 | 60.07 | 0.00 | 1.59 | 17.28 | 3.23 | 91.55 | 293.10 | 2.80 | 47.24 | 3.23 | 43.08 | 136.8 | 0.00 | 55.53 | 10.81 | 44.72 | 23.40 |
| 1 | 51 | 25.23 | 20.58 | 11.20 | 0.00 | 6.46 | 8.73 | 0.85 | 3.49 | 0.00 | 15.57 | 1.14 | 0.00 | 1.41 | 0.00 | 37.65 | 0.00 | 0.00 | 17.22 | 4.03 | 132.9 | 148.47 | 6.44 | 105.9 | 0.00 | 14.95 | 238.3 | 2.70 | 68.71 | 14.21 | 54.50 | 35.86 |
| 1 | 71 | 17.78 | 102.6 | 0.00 | 0.00 | 15.65 | 246.1 | 0.00 | 0.00 | 63.51 | 63.10 | 14.01 | 10.36 | 0.00 | 0.00 | 19.87 | 0.00 | 0.00 | 18.67 | 4.29 | 21.58 | 931.31 | 16.29 | 103.0 | 17.00 | 276.1 | 79.45 | 15.18 | 333.2 | 79.38 | 253.8 | 101.6 |
| 5 | 0 | 0.00 | 192.1 | 0.00 | 12.99 | 187.8 | 270.1 | 6.43 | 0.00 | 0.00 | 240.8 | 51.14 | 0.00 | 5.60 | 3.52 | 62.41 | 0.00 | 8.06 | 15.56 | 0.00 | 8.76 | 1352.2 | 15.66 | 5.56 | 14.05 | 152.7 | 100.1 | 14.63 | 52.93 | 10.79 | 42.14 | 33.16 |
| 5 | 25 | 6.79 | 181.5 | 0.00 | 23.55 | 156.3 | 279.2 | 0.00 | 9.86 | 0.00 | 224.5 | 33.02 | 0.00 | 5.25 | 0.00 | 38.49 | 0.00 | 7.04 | 15.96 | 0.00 | 0.00 | 1319.5 | 9.27 | 0.00 | 12.44 | 184.3 | 81.11 | 17.59 | 73.68 | 0.00 | 73.68 | 54.97 |
| 5 | 30 | 5.13 | 148.8 | 0.00 | 20.79 | 97.17 | 230.6 | 2.41 | 21.46 | 0.00 | 253.4 | 21.60 | 0.00 | 7.45 | 0.00 | 16.37 | 0.00 | 7.06 | 15.74 | 15.57 | 0.00 | 1234.4 | 7.25 | 8.25 | 9.26 | 206.5 | 95.88 | 26.30 | 128.5 | 35.16 | 93.40 | 58.44 |
| 5 | 50 | 4.82 | 39.66 | 0.00 | 0.00 | 4.68 | 19.93 | 0.00 | 0.00 | 0.00 | 48.81 | 0.00 | 0.00 | 0.00 | 0.00 | 6.07 | 0.00 | 0.00 | 16.28 | 0.00 | 17.57 | 229.27 | 0.00 | 0.00 | 16.58 | 59.42 | 85.63 | 7.91 | 0.00 | 0.00 | 0.00 | 5.26 |
| 8 | 3 | 3.66 | 10.30 | 0.00 | 3.92 | 14.61 | 13.04 | 1.97 | 0.00 | 0.00 | 48.72 | 10.54 | 0.00 | 0.00 | 0.36 | 78.80 | 1.56 | 1.97 | 12.95 | 0.03 | 39.71 | 229.12 | 3.18 | 10.15 | 6.56 | 8.44 | 42.99 | 1.70 | 11.39 | 10.84 | 0.55 | 8.17 |
| 8 | 8 | 3.63 | 16.05 | 0.00 | 4.67 | 17.55 | 14.94 | 2.50 | 0.00 | 0.00 | 59.27 | 12.54 | 0.00 | 0.00 | 0.00 | 83.38 | 1.92 | 2.35 | 14.36 | 0.00 | 43.07 | 256.61 | 3.82 | 10.76 | 5.78 | 12.57 | 50.16 | 0.00 | 14.53 | 14.25 | 0.29 | 14.02 |
| 8 | 15 | 4.40 | 18.75 | 0.00 | 4.43 | 18.17 | 15.02 | 2.45 | 0.00 | 0.00 | 59.63 | 11.33 | 0.00 | 0.00 | 0.05 | 82.00 | 1.91 | 2.28 | 15.11 | 0.00 | 45.50 | 249.58 | 3.88 | 10.53 | 4.98 | 16.99 | 51.01 | 2.54 | 14.66 | 12.49 | 2.17 | 10.26 |
| 8 | 22 | 3.55 | 21.55 | 0.00 | 4.87 | 26.04 | 12.62 | 3.15 | 0.00 | 0.00 | 62.91 | 8.31 | 0.00 | 0.00 | 0.00 | 55.30 | 1.80 | 2.31 | 14.78 | 0.00 | 40.34 | 239.20 | 3.83 | 12.16 | 3.06 | 24.03 | 62.93 | 3.13 | 16.03 | 13.40 | 2.63 | 10.65 |
| 8 | 28 | 8.16 | 34.03 | 1.20 | 6.15 | 39.75 | 15.38 | 4.55 | 1.98 | 0.00 | 81.30 | 7.41 | 0.00 | 8.13 | 0.00 | 132.0 | 3.21 | 2.78 | 15.05 | 3.23 | 104.3 | 325.87 | 3.53 | 40.16 | 3.58 | 36.93 | 135.7 | 4.95 | 23.00 | 16.64 | 6.36 | 20.17 |
| 8 | 36 | 9.75 | 46.13 | 0.00 | 9.39 | 46.60 | 19.96 | 5.58 | 3.74 | 0.00 | 85.55 | 7.43 | 0.00 | 6.35 | 0.00 | 179.4 | 2.51 | 3.07 | 16.39 | 5.07 | 171.8 | 410.98 | 3.59 | 73.91 | 5.26 | 52.45 | 213.1 | 6.05 | 29.87 | 18.78 | 11.09 | 34.61 |
| 8 | 51 | 15.21 | 27.88 | 0.00 | 11.44 | 24.12 | 34.07 | 5.41 | 5.15 | 0.00 | 55.41 | 6.82 | 0.00 | 3.44 | 0.00 | 92.29 | 0.00 | 1.98 | 16.50 | 5.72 | 157.3 | 316.46 | 9.21 | 114.1 | 6.78 | 34.50 | 250.4 | 5.53 | 56.84 | 30.00 | 26.84 | 44.70 |
| 8 | 70 | 4.90 | 9.97 | 0.00 | 2.89 | 6.10 | 7.30 | 0.80 | 0.37 | 0.00 | 26.00 | 1.61 | 0.00 | 1.69 | 0.00 | 7.67 | 0.00 | 0.96 | 15.45 | 1.48 | 18.44 | 117.73 | 0.00 | 18.98 | 0.00 | 13.62 | 61.13 | 3.72 | 7.39 | 3.96 | 3.43 | 6.78 |
| 8 | 0 | 10.84 | 37.93 | 0.00 | 8.34 | 19.02 | 10.52 | 2.97 | 0.00 | 0.00 | 70.72 | 9.44 | 0.00 | 0.00 | 0.00 | 115.4 | 3.21 | 2.95 | 14.47 | 0.00 | 68.20 | 280.17 | 4.31 | 19.80 | 7.23 | 62.74 | 66.98 | 2.75 | 13.96 | 3.60 | 10.35 | 6.93 |
| 8 | 8 | 8.71 | 26.02 | 0.00 | 9.92 | 26.58 | 11.05 | 4.33 | 0.00 | 0.00 | 91.62 | 12.79 | 0.00 | 0.00 | 0.00 | 145.1 | 3.84 | 3.63 | 15.33 | 17.41 | 85.10 | 337.85 | 5.44 | 19.81 | 6.96 | 29.75 | 82.22 | 3.53 | 16.36 | 10.98 | 5.38 | 13.84 |
| 8 | 15 | 3.91 | 16.41 | 0.00 | 6.50 | 23.06 | 9.86 | 3.50 | 0.00 | 0.00 | 77.40 | 10.31 | 0.00 | 1.00 | 0.00 | 92.79 | 1.66 | 3.03 | 15.80 | 0.36 | 59.86 | 277.69 | 4.32 | 15.46 | 5.37 | 17.11 | 70.49 | 2.77 | 18.44 | 18.44 | 0.00 | 13.64 |
| 8 | 22 | 4.94 | 37.27 | 0.00 | 7.67 | 47.25 | 12.27 | 4.76 | 0.00 | 0.00 | 94.68 | 7.68 | 0.00 | 4.44 | 0.00 | 49.99 | 2.10 | 3.49 | 15.42 | 0.00 | 19.44 | 359.89 | 5.32 | 8.21 | 3.48 | 45.18 | 100.2 | 5.54 | 4.38 | 3.93 | 0.45 | 12.13 |
| 8 | 36 | 9.30 | 31.81 | 0.00 | 6.37 | 60.45 | 32.80 | 4.85 | 2.32 | 0.00 | 62.93 | 6.48 | 0.00 | 2.79 | 0.00 | 47.77 | 0.00 | 2.61 | 14.82 | 0.14 | 59.68 | 365.47 | 3.08 | 27.08 | 2.72 | 43.56 | 131.7 | 5.68 | 7.47 | 5.87 | 1.60 | 16.81 |
| 8 | 51 | 11.20 | 28.60 | 0.00 | 2.88 | 23.59 | 38.55 | 4.25 | 4.48 | 0.00 | 37.61 | 4.76 | 0.00 | 2.40 | 0.00 | 71.85 | 0.00 | 1.53 | 17.44 | 4.84 | 147.4 | 278.60 | 8.48 | 138.1 | 0.00 | 34.34 | 270.8 | 4.81 | 45.38 | 16.85 | 28.53 | 45.95 |

**Suppl. Table 5.** Fatty acyl combinations (number of carbon atoms and double bond equivalents, DBE, in the alkyl side chains) of the major groups of intact polar lipids and their relative abundance at different depths within the water column of the Eastern Tropical North Pacific.

| | | | | | Rel. Abundance (%) | | | | | | | |
|---|---|---|---|---|---|---|---|---|---|---|---|---|
| | | | | | Oxic | | Upper OMZ | | Core OMZ | | Deep Oxycline | |
| IPL | *m/z* (pos mode) | Carbon atoms | DBE | FA combination | Mean | SD | Mean | SD | Mean | SD | Mean | SD |
| 1G-DAG | 788.531 | 36 | 8 | 18:4/18:4 | 1.86 | 1.03 | 3.55 | 4.15 | 0.74 | 0.50 | 1.10 | 0.24 |
| | 786.515 | 36 | 9 | 18:4/18:5 | 6.05 | 7.89 | 1.72 | 1.67 | 0.84 | 0.87 | 1.52 | 0.31 |
| | 774.609 | 34 | 1 | | 2.69 | 1.99 | 1.48 | 1.36 | 2.59 | 1.93 | 2.96 | 1.06 |
| | 766.546 | 34 | 5 | | 1.17 | 0.82 | 1.74 | 1.31 | 1.11 | 0.47 | 3.43 | 3.63 |
| | 762.515 | 34 | 7 | 18:3/16:4 | 5.07 | 3.61 | 1.59 | 1.00 | 2.20 | 1.52 | 2.70 | 0.61 |
| | 746.578 | 32 | 1 | | 3.82 | 5.24 | 3.59 | 2.09 | 4.53 | 1.78 | 4.54 | 0.71 |
| | 732.562 | 31 | 1 | | 2.09 | 2.55 | 2.02 | 1.51 | 2.96 | 1.93 | 2.43 | 1.72 |
| | 720.562 | 30 | 0 | 16:0/14:0 | 6.98 | 10.09 | 5.76 | 2.92 | 7.15 | 3.49 | 6.99 | 0.86 |
| | 718.546 | 30 | 1 | 16:1/14:0 | 27.91 | 10.70 | 40.79 | 11.46 | 49.59 | 5.41 | 39.07 | 3.42 |
| | 716.531 | 30 | 2 | 16:2/14:0 | 10.59 | 7.40 | 11.90 | 5.88 | 7.93 | 2.21 | 7.74 | 2.53 |
| | 692.531 | 28 | 0 | | 4.79 | 2.82 | 2.97 | 1.30 | 4.48 | 1.18 | 3.71 | 1.20 |
| | 690.515 | 28 | 1 | | 3.83 | 2.61 | 4.54 | 2.48 | 3.18 | 1.18 | 2.45 | 1.35 |
| 2G-DAG | 948.568 | 36 | 9 | | 2.11 | 1.62 | 1.18 | 1.35 | 0.41 | 0.50 | 4.10 | 6.60 |
| | 936.662 | 34 | 1 | 18:1/16:0 | 5.27 | 2.43 | 4.50 | 4.54 | 13.94 | 1.86 | 11.00 | 5.92 |
| | 934.646 | 34 | 2 | 18:2/16:0 | 6.68 | 2.86 | 2.87 | 2.77 | 7.43 | 3.02 | 9.11 | 4.42 |
| | 932.631 | 34 | 3 | 18:3/16:0 | 4.94 | 1.71 | 2.45 | 1.91 | 2.95 | 1.75 | 4.93 | 1.89 |
| | 930.615 | 34 | 4 | | 3.15 | 1.65 | 1.66 | 1.62 | 1.54 | 0.89 | 3.37 | 1.14 |
| | 928.599 | 34 | 5 | 18:3/16:2 | 4.11 | 1.86 | 1.64 | 1.22 | 1.43 | 0.93 | 6.93 | 9.29 |
| | 926.584 | 34 | 6 | | 3.12 | 1.66 | 1.61 | 1.56 | 1.36 | 0.91 | 2.28 | 1.57 |
| | 924.568 | 34 | 7 | 18:3/16:4 | 4.90 | 2.40 | 1.73 | 1.78 | 1.20 | 0.80 | 2.75 | 0.39 |
| | 908.631 | 32 | 1 | 18:1/14:0 ; 16:1/16:0 | 5.03 | 2.49 | 13.67 | 12.27 | 23.54 | 5.07 | 15.29 | 4.20 |
| | 906.615 | 32 | 2 | | 2.20 | 0.92 | 3.52 | 4.42 | 2.89 | 1.71 | 3.42 | 0.84 |
| | 902.584 | 32 | 4 | 18:4/14:0 | 5.45 | 2.91 | 1.14 | 2.07 | 0.78 | 0.68 | 0.76 | 0.94 |
| | 900.568 | 32 | 5 | 18:5/14:0 | 4.76 | 2.10 | 4.25 | 13.38 | 0.17 | 0.49 | 0.63 | 1.27 |
| | 898.552 | 32 | 6 | | 4.19 | 7.62 | 0.27 | 0.42 | 0.00 | 0.00 | 0.00 | 0.00 |
| | 882.615 | 30 | 0 | 16:0/14:0 | 13.49 | 6.98 | 17.20 | 7.58 | 15.68 | 1.76 | 9.10 | 7.37 |
| | 880.599 | 30 | 1 | 16:1/14:0 | 9.95 | 3.90 | 24.46 | 11.88 | 16.88 | 2.52 | 9.50 | 6.58 |
| | 878.584 | 30 | 2 | 16:2/14:0 | 2.71 | 2.54 | 5.21 | 4.96 | 0.09 | 0.26 | 0.00 | 0.00 |
| | 854.584 | 28 | 0 | | 3.82 | 2.91 | 3.17 | 3.47 | 2.73 | 4.45 | 1.72 | 3.44 |
| SQ-DAG | 838.571 | 34 | 1 | 18:1/16:0 | 1.97 | 1.08 | 2.83 | 3.36 | 4.98 | 4.57 | 8.52 | 7.97 |
| | 836.555 | 34 | 2 | | 4.02 | 2.38 | 1.70 | 1.63 | 1.02 | 1.23 | 1.64 | 1.90 |

| | | | | | | | | | | | | |
|---|---|---|---|---|---|---|---|---|---|---|---|---|
| | 834.540 | 34 | 3 | | 3.22 | 1.71 | 0.56 | 0.72 | 0.44 | 0.87 | 1.24 | 1.43 |
| | 812.555 | 32 | 0 | 16:0/16:0 ; 15:0/14:0 | 9.15 | 3.10 | 4.46 | 3.78 | 9.29 | 4.07 | 12.60 | 3.12 |
| | 810.540 | 32 | 1 | 16:1/16:0 | 7.29 | 2.63 | 11.61 | 6.09 | 12.53 | 2.50 | 10.36 | 4.74 |
| | 808.524 | 32 | 2 | 16:1/16:1 | 5.23 | 3.07 | 11.49 | 7.09 | 6.69 | 3.79 | 5.43 | 4.34 |
| | 784.524 | 30 | 0 | 16:0/14:0 | 26.72 | 5.24 | 24.93 | 16.07 | 30.45 | 3.33 | 30.89 | 3.33 |
| | 782.508 | 30 | 1 | 16:1/14:0 | 15.90 | 6.46 | 31.16 | 11.93 | 13.75 | 4.21 | 12.69 | 4.69 |
| | 780.493 | 30 | 2 | 16:2/14:0 | 4.95 | 3.47 | 2.81 | 4.28 | 7.29 | 11.51 | 0.47 | 0.54 |
| | 756.493 | 28 | 0 | 14:0/14:0 | 16.24 | 6.46 | 6.84 | 5.26 | 13.57 | 11.15 | 13.66 | 9.59 |
| PG-DAG | 806.591 | 37 | 2 | | 1.59 | 2.88 | 1.88 | 2.51 | 3.07 | 1.23 | 2.63 | 1.39 |
| | 792.575 | 36 | 2 | 18:1/18:1 | 9.81 | 5.61 | 7.12 | 3.44 | 9.78 | 3.67 | 7.69 | 0.25 |
| | 780.575 | 35 | 1 | | 1.55 | 2.32 | 3.48 | 2.67 | 4.22 | 1.57 | 3.26 | 0.62 |
| | 778.559 | 35 | 2 | 18:1/17:1 ; 19:1/16:1 | 3.26 | 2.46 | 10.69 | 6.95 | 13.26 | 2.11 | 11.05 | 0.62 |
| | 766.559 | 34 | 1 | 18:1/16:0 | 12.32 | 2.78 | 8.63 | 8.75 | 7.21 | 2.63 | 7.00 | 0.45 |
| | 764.544 | 34 | 2 | 18:2/16:0 | 21.87 | 10.62 | 18.84 | 8.87 | 19.50 | 4.17 | 25.57 | 4.49 |
| | 762.528 | 34 | 3 | 18:3/16:0 | 15.03 | 9.19 | 2.67 | 3.22 | 3.78 | 1.34 | 3.78 | 0.32 |
| | 752.544 | 33 | 1 | 17:1/15:0 | 7.52 | 4.63 | 13.03 | 5.80 | 16.60 | 2.27 | 14.65 | 3.77 |
| | 738.528 | 32 | 1 | 16:1/16:0 | 11.41 | 4.41 | 11.43 | 5.08 | 10.84 | 3.29 | 10.11 | 1.45 |
| | 736.512 | 32 | 2 | 16:1/16:1 | 13.19 | 3.79 | 19.08 | 12.58 | 9.77 | 2.20 | 10.42 | 0.80 |
| | 710.497 | 30 | 1 | | 2.31 | 1.41 | 3.09 | 1.76 | 1.76 | 1.22 | 3.84 | 0.17 |
| PE-DAG | 730.538 | 32 | 2 | 18:1/17:1 | 12.02 | 9.37 | 19.53 | 13.16 | 23.32 | 7.97 | 19.51 | 11.03 |
| | 718.538 | 34 | 1 | 18:1/16:0 | 7.28 | 6.14 | 6.44 | 7.72 | 11.29 | 5.49 | 9.85 | 6.57 |
| | 716.522 | 34 | 2 | 18:1/16:1 ; 17:1/17:1 | 3.78 | 3.64 | 2.91 | 2.90 | 9.97 | 8.36 | 3.83 | 2.93 |
| | 704.522 | 33 | 1 | 17:1/16:0 | 22.14 | 14.88 | 16.16 | 8.54 | 13.55 | 2.63 | 10.32 | 6.89 |
| | 702.507 | 33 | 2 | | 1.32 | 1.33 | 1.79 | 2.25 | 2.05 | 1.35 | 4.12 | 5.50 |
| | 690.507 | 32 | 1 | 16:1/16:0 | 6.93 | 10.80 | 5.53 | 7.05 | 7.11 | 4.76 | 8.29 | 10.09 |
| | 688.491 | 32 | 2 | | 2.26 | 4.02 | 3.14 | 10.46 | 3.16 | 3.63 | 0.48 | 0.97 |
| | 678.507 | 31 | 0 | 16:0/15:0 | 33.48 | 20.83 | 23.89 | 15.41 | 10.07 | 4.24 | 15.60 | 11.12 |
| | 676.491 | 31 | 1 | | 3.82 | 3.31 | 2.83 | 2.43 | 3.07 | 1.10 | 1.66 | 1.85 |
| | 674.476 | 31 | 2 | | 0.09 | 0.30 | 0.02 | 0.07 | 0.04 | 0.11 | 0.00 | 0.00 |
| | 664.491 | 30 | 0 | 16:0/14:0 | 1.54 | 2.69 | 8.02 | 8.30 | 6.76 | 2.37 | 11.74 | 4.36 |
| | 662.476 | 30 | 1 | | 1.57 | 1.44 | 2.74 | 5.83 | 1.92 | 1.77 | 2.72 | 4.35 |
| | 650.476 | 29 | 0 | 15:0/14:0 | 2.61 | 2.09 | 6.66 | 5.43 | 6.50 | 3.55 | 10.94 | 8.75 |
| | 648.460 | 29 | 1 | | 0.08 | 0.19 | 0.14 | 0.34 | 0.04 | 0.11 | 0.00 | 0.00 |
| | 636.460 | 28 | 0 | | 1.08 | 1.54 | 0.21 | 0.49 | 1.17 | 0.88 | 0.95 | 1.44 |
| PC-DAG | 878.575 | 44 | 12 | 22:6/22:6 | 3.87 | 3.27 | 6.12 | 11.60 | 3.83 | 7.70 | 2.29 | 3.39 |
| | 852.560 | 42 | 11 | 22:6/20:5 | 1.87 | 1.60 | 2.90 | 3.11 | 3.55 | 6.04 | 4.79 | 5.74 |
| | 822.601 | 39 | 5 | | 1.59 | 1.12 | 1.50 | 1.49 | 0.67 | 0.93 | 1.47 | 1.35 |
| | 806.569 | 38 | 6 | 22:6/16:0 | 20.28 | 7.02 | 19.69 | 16.84 | 13.97 | 11.29 | 36.10 | 36.79 |
| | 788.616 | 36 | 1 | | 1.74 | 1.20 | 1.76 | 1.63 | 2.28 | 4.20 | 0.74 | 0.68 |

| | | | | | | | | | | | | |
|---|---|---|---|---|---|---|---|---|---|---|---|---|
| | 780.554 | 36 | 5 | 20:5/16:0 | 12.14 | 7.79 | 9.03 | 6.74 | 4.58 | 3.79 | 8.41 | 6.72 |
| | 776.616 | 35 | 0 | | 0.49 | 0.66 | 1.09 | 1.23 | 0.59 | 0.58 | 0.71 | 0.77 |
| | 774.601 | 35 | 1 | | 1.69 | 0.98 | 1.68 | 1.58 | 1.53 | 1.07 | 2.12 | 3.00 |
| | 760.585 | 34 | 1 | 18:1/16:0 | 6.68 | 4.39 | 5.27 | 3.65 | 8.01 | 8.70 | 2.70 | 3.23 |
| | 754.538 | 34 | 4 | | 2.73 | 1.57 | 1.86 | 2.02 | 0.76 | 0.66 | 1.15 | 1.10 |
| | 748.585 | 33 | 0 | | 1.21 | 1.18 | 1.93 | 1.89 | 1.59 | 1.36 | 1.24 | 1.20 |
| | 746.569 | 33 | 1 | | 1.85 | 3.95 | 3.18 | 3.63 | 3.88 | 2.12 | 2.66 | 2.43 |
| | 744.554 | 33 | 2 | 17:1/16:1 | 0.91 | 1.03 | 1.97 | 1.68 | 5.96 | 6.54 | 2.33 | 1.39 |
| | 734.569 | 32 | 0 | 16:0/16:0 ; 17:0/15:0 | 6.20 | 3.84 | 4.16 | 3.36 | 4.78 | 4.00 | 3.09 | 2.34 |
| | 732.554 | 32 | 1 | 16:0/16:1 | 4.83 | 2.98 | 5.96 | 3.69 | 7.15 | 3.92 | 6.15 | 3.68 |
| | 730.538 | 32 | 2 | 16:1/16:1 | 2.19 | 1.51 | 4.96 | 4.91 | 7.57 | 4.32 | 4.47 | 3.08 |
| | 720.554 | 31 | 0 | | 1.86 | 1.32 | 2.86 | 3.45 | 2.09 | 1.43 | 1.61 | 1.59 |
| | 718.538 | 31 | 1 | | 1.65 | 1.61 | 1.91 | 3.22 | 3.86 | 2.53 | 2.63 | 2.51 |
| | 716.522 | 31 | 2 | | 0.91 | 1.01 | 0.87 | 1.10 | 4.55 | 5.76 | 0.97 | 0.89 |
| | 706.538 | 30 | 0 | 16:0/14:0 | 9.35 | 2.79 | 5.68 | 4.00 | 3.29 | 1.87 | 2.53 | 2.65 |
| | 704.522 | 30 | 1 | 16:1/14:0 | 4.89 | 4.78 | 3.71 | 2.41 | 4.62 | 2.79 | 2.75 | 2.62 |
| | 702.507 | 30 | 2 | | 0.25 | 0.27 | 0.48 | 0.66 | 0.87 | 0.90 | 1.19 | 1.98 |
| | 692.522 | 29 | 0 | | 2.13 | 1.68 | 3.21 | 2.35 | 2.26 | 1.52 | 1.67 | 1.99 |
| | 690.507 | 29 | 1 | | 2.01 | 3.26 | 1.57 | 1.99 | 3.08 | 3.45 | 2.38 | 3.68 |
| | 688.491 | 29 | 2 | | 0.45 | 0.64 | 0.76 | 2.63 | 1.57 | 2.59 | 0.10 | 0.21 |
| | 678.507 | 28 | 0 | 14:0/14:0 | 6.22 | 3.39 | 5.89 | 4.62 | 3.09 | 1.68 | 3.76 | 3.82 |
| DGTS | 764.640 | 36 | 2 | 18:1/18:1 | 6.72 | 3.20 | 8.70 | 4.81 | 14.23 | 4.45 | 7.86 | 2.68 |
| | 762.624 | 36 | 3 | | 3.66 | 1.56 | 2.53 | 0.76 | 1.43 | 0.64 | 3.14 | 0.91 |
| | 760.609 | 36 | 4 | 18:2/18:2 ; 20:0/16:4 | 7.36 | 2.99 | 4.41 | 2.02 | 1.57 | 0.80 | 5.41 | 2.37 |
| | 758.593 | 36 | 5 | 18:2/18:3 | 5.12 | 2.44 | 2.89 | 1.46 | 1.45 | 0.80 | 3.96 | 1.22 |
| | 740.640 | 34 | 0 | | 1.11 | 0.39 | 2.65 | 1.48 | 4.93 | 1.81 | 1.98 | 1.10 |
| | 738.624 | 34 | 1 | 18:1/16:0 | 3.90 | 1.70 | 14.87 | 13.30 | 32.49 | 12.73 | 14.69 | 2.83 |
| | 736.609 | 34 | 2 | 18:2/16:0 | 7.44 | 3.95 | 6.57 | 1.85 | 8.60 | 0.91 | 8.33 | 2.26 |
| | 734.593 | 34 | 3 | 18:3/16:0 | 5.04 | 2.11 | 2.84 | 1.05 | 1.14 | 0.59 | 3.33 | 0.85 |
| | 732.577 | 34 | 4 | | 4.34 | 1.23 | 2.15 | 1.12 | 0.58 | 0.48 | 1.30 | 1.08 |
| | 710.593 | 32 | 1 | 18:1/14:0 | 3.94 | 1.25 | 6.92 | 2.50 | 9.60 | 4.41 | 10.54 | 2.56 |
| | 708.577 | 32 | 2 | 18:2/14:0 | 3.85 | 1.31 | 3.80 | 1.46 | 2.89 | 2.26 | 5.61 | 1.86 |
| | 706.562 | 32 | 3 | | 2.65 | 0.83 | 2.07 | 1.25 | 0.74 | 0.41 | 3.05 | 2.00 |
| | 698.593 | 31 | 0 | | 1.40 | 0.47 | 2.90 | 2.18 | 2.26 | 2.04 | 3.24 | 1.44 |
| | 684.577 | 30 | 0 | 16:0/14:0 | 3.90 | 1.45 | 3.69 | 1.69 | 2.18 | 1.75 | 3.45 | 0.77 |
| | 682.562 | 30 | 1 | 16:1/14:0 | 3.58 | 3.14 | 8.92 | 4.80 | 4.13 | 4.52 | 7.75 | 0.96 |
| | 670.562 | 29 | 0 | | 3.60 | 1.39 | 3.47 | 1.93 | 2.14 | 1.62 | 2.34 | 0.76 |
| | 656.546 | 28 | 0 | 14:0/14:0 | 9.56 | 4.74 | 6.54 | 3.47 | 4.44 | 2.18 | 4.81 | 0.46 |

**Suppl. Table 6.** Goodness of fit statistics for the NMDS analyses of normalized intact polar lipid (IPL) composition and quantitative microbial data (FISH), number of double bond equivalents (DBE) and carbon atoms in the alkyl side chains of IPLs.

| | IPL (relative abundance) | | | |
|---|---|---|---|---|
| FISH Probe | NMDS1 | NMDS2 | r2 | p |
| Alphaproteobacteria | -0.56 | -0.83 | 0.02 | 0.613 |
| Betaproteobacteria | -0.60 | -0.80 | 0.10 | 0.133 |
| Gammaproteobacteria | -0.66 | -0.76 | 0.24 | 0.004 |
| SRB | -0.42 | -0.91 | 0.33 | 0.002 |
| Epsilonproteobacteria | -0.88 | -0.47 | 0.18 | 0.022 |
| Nso | -0.94 | -0.33 | 0.18 | 0.023 |
| Anammox | -0.04 | -1.00 | 0.25 | 0.006 |
| Planctomycetes | -0.87 | -0.50 | 0.13 | 0.730 |

| | Number of DBE | | | |
|---|---|---|---|---|
| Environmental parameter | NMDS1 | NMDS2 | r2 | p |
| Depth | -0.80 | 0.59 | 0.12 | 0.081 |
| POC | 0.93 | -0.35 | 0.19 | 0.019 |
| TN | 0.95 | -0.30 | 0.20 | 0.012 |
| Phosphate | -0.90 | 0.44 | 0.12 | 0.740 |
| Nitrate | -0.51 | 0.86 | 0.07 | 0.250 |
| Nitrite | -0.57 | -0.82 | 0.14 | 0.043 |
| Ammonium | 0.67 | -0.75 | 0.06 | 0.311 |
| Salinity | 0.96 | 0.29 | 0.00 | 0.909 |
| Temperature | 0.66 | -0.76 | 0.02 | 0.686 |
| Fluorescence | 0.97 | -0.26 | 0.27 | 0.003 |
| Oxygen | 0.83 | -0.55 | 0.26 | 0.002 |
| Chl-a | 0.96 | -0.27 | 0.28 | 0.002 |

| | Number of carbon atoms | | | |
|---|---|---|---|---|
| Environmental parameter | NMDS1 | NMDS2 | r2 | p |
| Depth | 0.48 | 0.88 | 0.00 | 0.944 |
| POC | -0.14 | 0.99 | 0.05 | 0.340 |
| TN | -0.10 | 1.00 | 0.56 | 0.324 |
| Phosphate | 0.06 | -1.00 | 0.03 | 0.531 |
| Nitrate | 0.65 | -0.76 | 0.34 | 0.472 |
| Nitrite | -0.54 | -0.84 | 0.15 | 0.052 |
| Ammonium | -0.15 | 0.99 | 0.05 | 0.339 |
| Salinity | 0.94 | 1.00 | 0.01 | 0.713 |
| Temperature | -0.23 | -0.97 | 0.01 | 0.882 |
| Fluorescence | 0.04 | 1.00 | 0.05 | 0.374 |
| Oxygen | -0.12 | 0.99 | 0.09 | 0.138 |
| Chl-a | -0.01 | 1.00 | 0.16 | 0.042 |

**Suppl. Figure 1.** Fluctuations in (A) absolute and (B) relative responses of select commercially available IPL standards over time. The values represent the slope of standards measured in different concentrations (usually 100 pg to 10 ng injected on column). Standard Mix A, B and C represents newly prepared standard mixtures. The standard mix used in this study was from November 2015.

Deleted: relevant for this study

**Suppl. Figure 2.** Depth profiles of (a) total particulate nitrogen and (b) phaeophytin concentrations, at the investigated four stations in the ETNP.

**Suppl. Figure 3.** Structures of (a) bacterial/eukaryotic and (b) archaeal intact polar lipids (IPLs) observed in the ETNP. The position of the double bonds or rings and the OH-, epoxy- and keto-groups of the R' and R" side chains were not determined.

**Suppl. Figure 4.** Extracted ion chromatograms of intact polar and core GDGTs showing the ring distribution within each individual compound class. Analyses were performed by HPLC-QTOF-MS with reversed phase chromatography as described in Zhu et al., (2016). Extracted ions for HPH-GDGTs were: *m/z* 1723.421, 1721.406, 1719.390, 1717.374, 1715.359, 1713.343; for 2G-GDGT: *m/z* 1643.455, 1641.439, 1639.424, 1637.408, 1635.392, 1633.377; for 1G-GDGT: *m/z* 1481.402, 1479.386, 1477.371, 1475.355, 1473.339, 1471.324 and for core GDGTs: *m/z* 1302.323, 1300.307, 1298.291, 1296.276, 1294.2, 1292.244. The numbers denote number of rings: 0 – GDGT-0, 1 – GDGT-1, 2 – GDGT-2, 5 – crenarchaeol.

**Suppl. Figure 5.** Identification of hydroxylated aminolipids and sphingolipids in water column samples

of the ETNP. (a) HPLC-MS density map, full scan ($MS^1$), in the mass range from m/z 600 to 900 and retention time range from 7 to 9 minutes. Representative high-resolution accurate mass $MS^2$ mass spectrum showing fragmentation patterns of (b) DGTS, (c) 1OH-DGTS, (d) 3OH-DGTS and (e) 1G-2OH-CER in positive ionization mode. Typical fragments for DGTS include monoacylglycerol side chains with the head group still attached. Similar fragmentation patters are observed between DGTS, 1OH-DGTS and 3OH-DGTS with exact masses pointing to additional hydroxyl-groups attached to the fatty acyl side chains. Note, that it's possible that the dihydroxylated fatty acid, could also be an epoxy-hydroxy or keto-hydroxy acid as only one loss of water was observed in the MS2 (from fragment *m/z* 466.281 to *m/z* 448.270). Multiple fatty acid side chain combinations are possible. Fragments of 1G-2OH-CER include the glycosidic head group loss of 180 Da and two hydroxyl-group losses as well as the long chain base (LCB), *m/z* 294.279.

**Suppl. Figure 6.** Identification of aminolipids AL-I and AL-II and ester/ether-sulfoquinovosyl (SQ-AEG) in water column samples of the ETNP. (a) HPLC-MS density map, full scan ($MS^1$), in the mass range from *m/z* 600 to 900 and retention time range from 6.5 to 11.5 minutes. Representative high-resolution accurate mass $MS^2$ mass spectrum showing fragmentation patterns of (b) AL-I and (c) AL-II in positive ionization mode. Fragmentation patterns of AL-I and AL-II are very similar to DGTS (Suppl. Fig. 3) showing monoacylglycerol fragments with the amino-head group still attached. The sum formula of the AL-I headgroup matches the head group of DGCC with an extra methyl group. However, since no head group fragments were observed no further structural inference could be made. The sum formula of AL-II matches exactly the head group of DGCC, however, the DGCC-characteristic head group ion fragment

*m/z* 252.144 was not observed and no structural inference from the detected head group fragments *m/z* 132.102 and 104.107 could be made. Representative high-resolution accurate mass $MS^2$ mass spectrum showing fragmentation patterns of (d) SQ-DAG and (e) SQ-AEG in positive and negative ionization mode. Both compound classes exhibit the sulfoquinovosyl-diagnostic head group loss of 261.05 Da. However, SQ-AEG only has one fatty acyl side chain fragment, whereas SQ-DAG has two fatty acyl fragments in positive and negative ion mode. Furthermore, the exact mass of the parent ion and the fragments indicate that SQ-AEG has one oxygen less than SQ-DAG, indicating the replacement of one of the ester bonds with an ether bond.

suppl.fig01

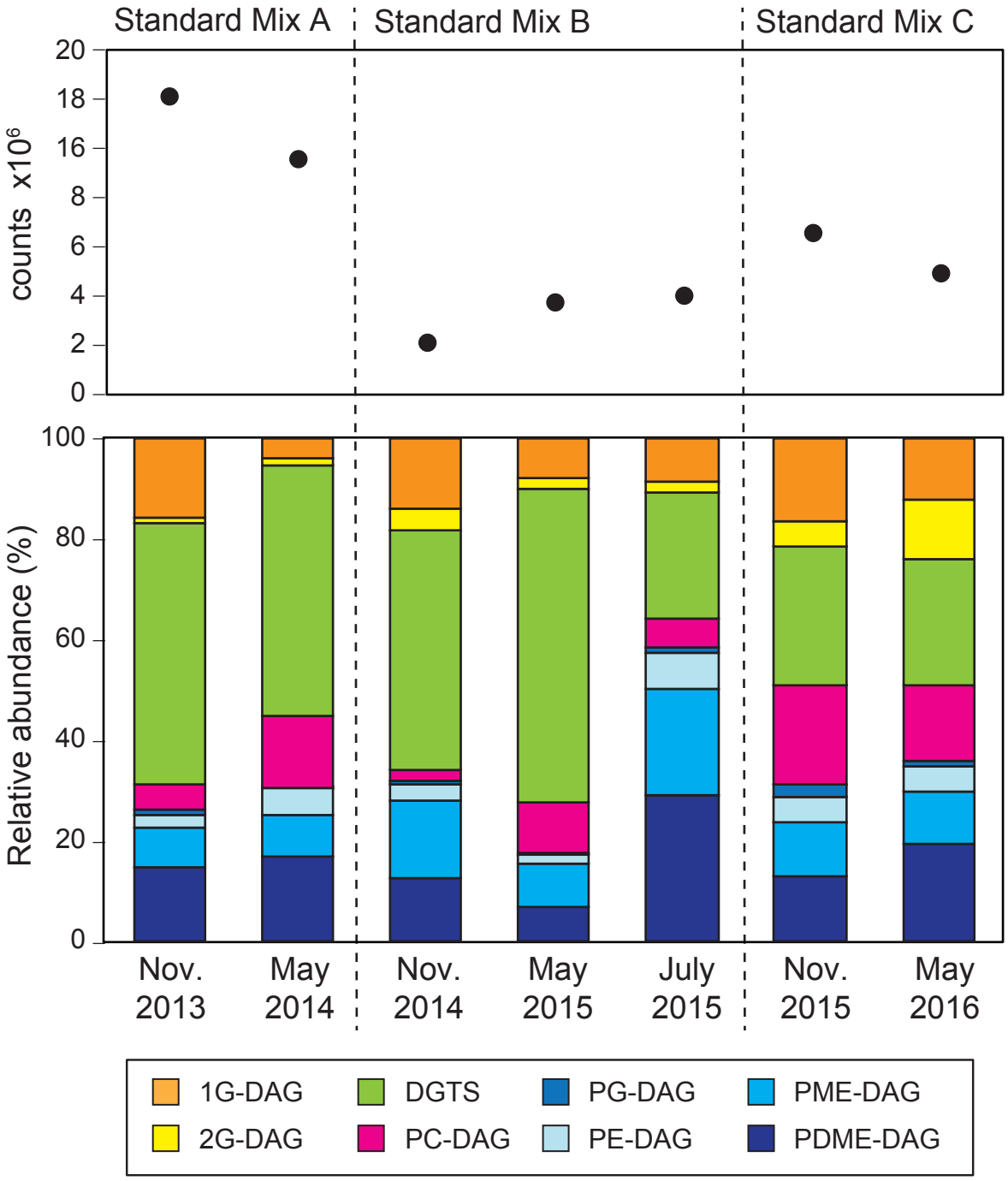
Standard Mix A
Standard Mix B
Standard Mix C
counts x10^6
20
18
16
8
6
4
2
0
Relative abundance (%)
100
80
60
40
20
0
Nov. 2013
May 2014
Nov. 2014
May 2015
July 2015
Nov. 2015
May 2016
1G-DAG
2G-DAG
DGTS
PC-DAG
PG-DAG
PE-DAG
PME-DAG
PDME-DAG

suppl.fig02

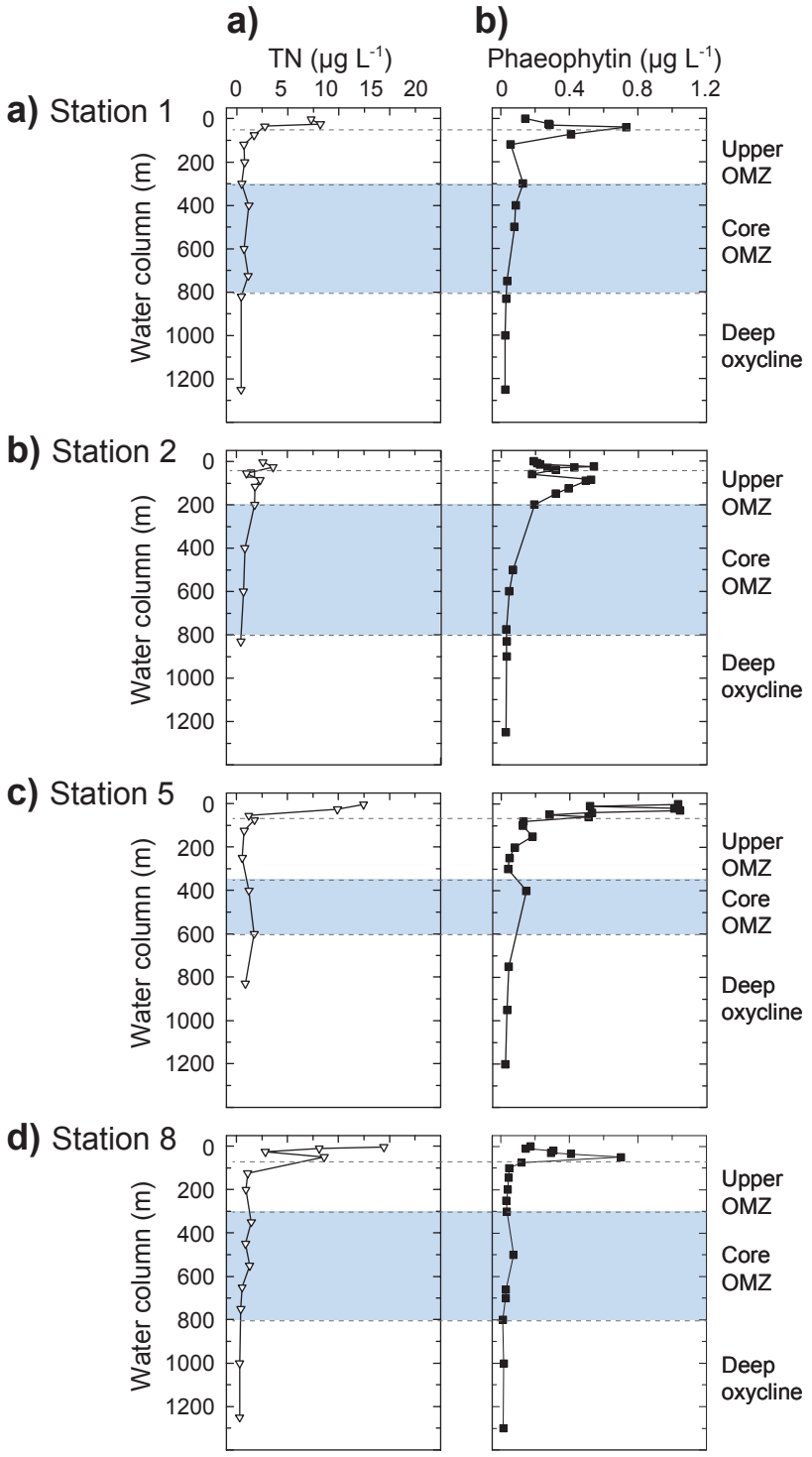
a)
b)
TN (µg L-1)
Phaephytin (µg L-1)
0 5 10 15 20
0 0.4 0.8 1.2
a) Station 1
b) Station 2
c) Station 5
d) Station 8
Water column (m)
0
200
400
600
800
1000
1200
Upper OMZ
Core OMZ
Deep oxycline

suppl.fig03

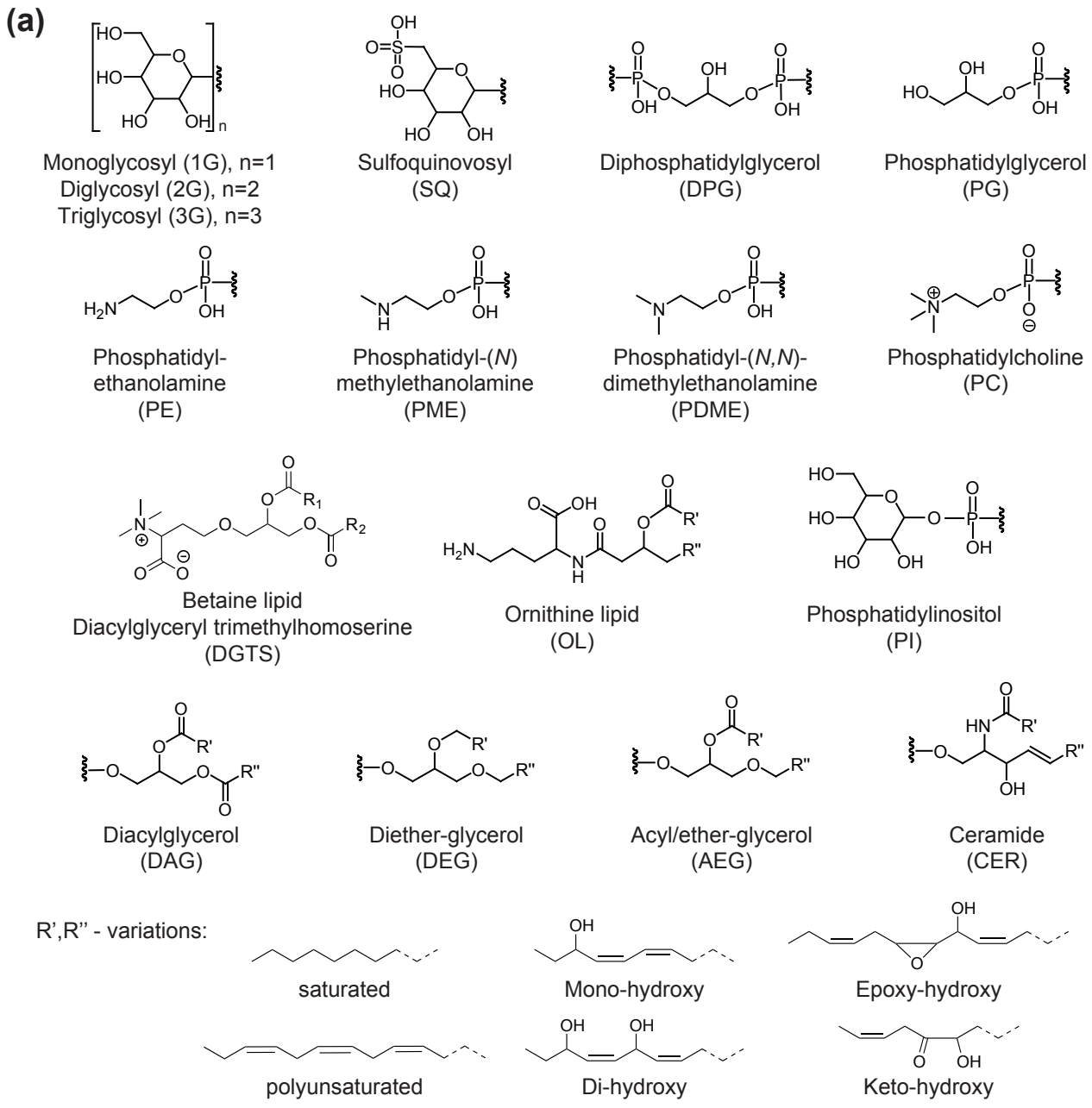
(a)
Monoglycosyl (1G), n=1
Diglycosyl (2G), n=2
Triglycosyl (3G), n=3
Sulfoquinovosyl
(SQ)
Diphosphatidylglycerol
(DPG)
Phosphatidylglycerol
(PG)
Phosphatidyl-
ethanolamine
(PE)
Phosphatidyl-(N)
methylethanolamine
(PME)
Phosphatidyl-(N,N)-
dimethylethanolamine
(PDME)
Phosphatidylcholine
(PC)
Betaine lipid
Diacylglyceryl trimethylhomoserine
(DGTS)
Ornithine lipid
(OL)
Phosphatidylinositol
(PI)
Diacylglycerol
(DAG)
Diether-glycerol
(DEG)
Acyl/ether-glycerol
(AEG)
Ceramide
(CER)
R',R'' - variations:
saturated
Mono-hydroxy
Epoxy-hydroxy
polyunsaturated
Di-hydroxy
Keto-hydroxy
(b)
1G-GDGT, n=1
2G-GDGT, n=2
HPH-GDGT
X,Y - variations:

suppl.fig04

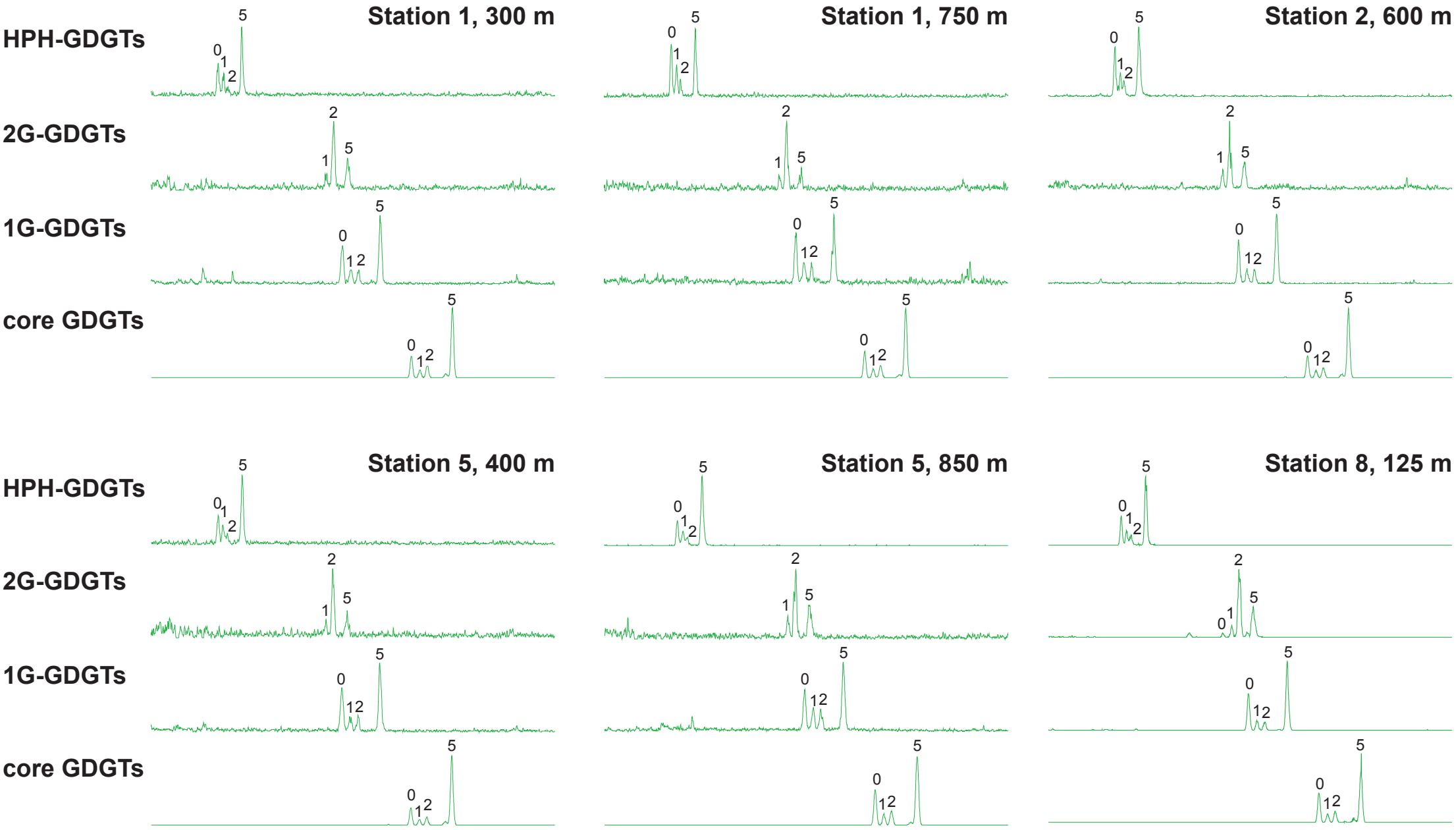
Station 1, 300 m
Station 1, 750 m
Station 2, 600 m
Station 5, 400 m
Station 5, 850 m
Station 8, 125 m
HPH-GDGTs
2G-GDGTs
1G-GDGTs
core GDGTs
0
1
2
5

suppl.fig05

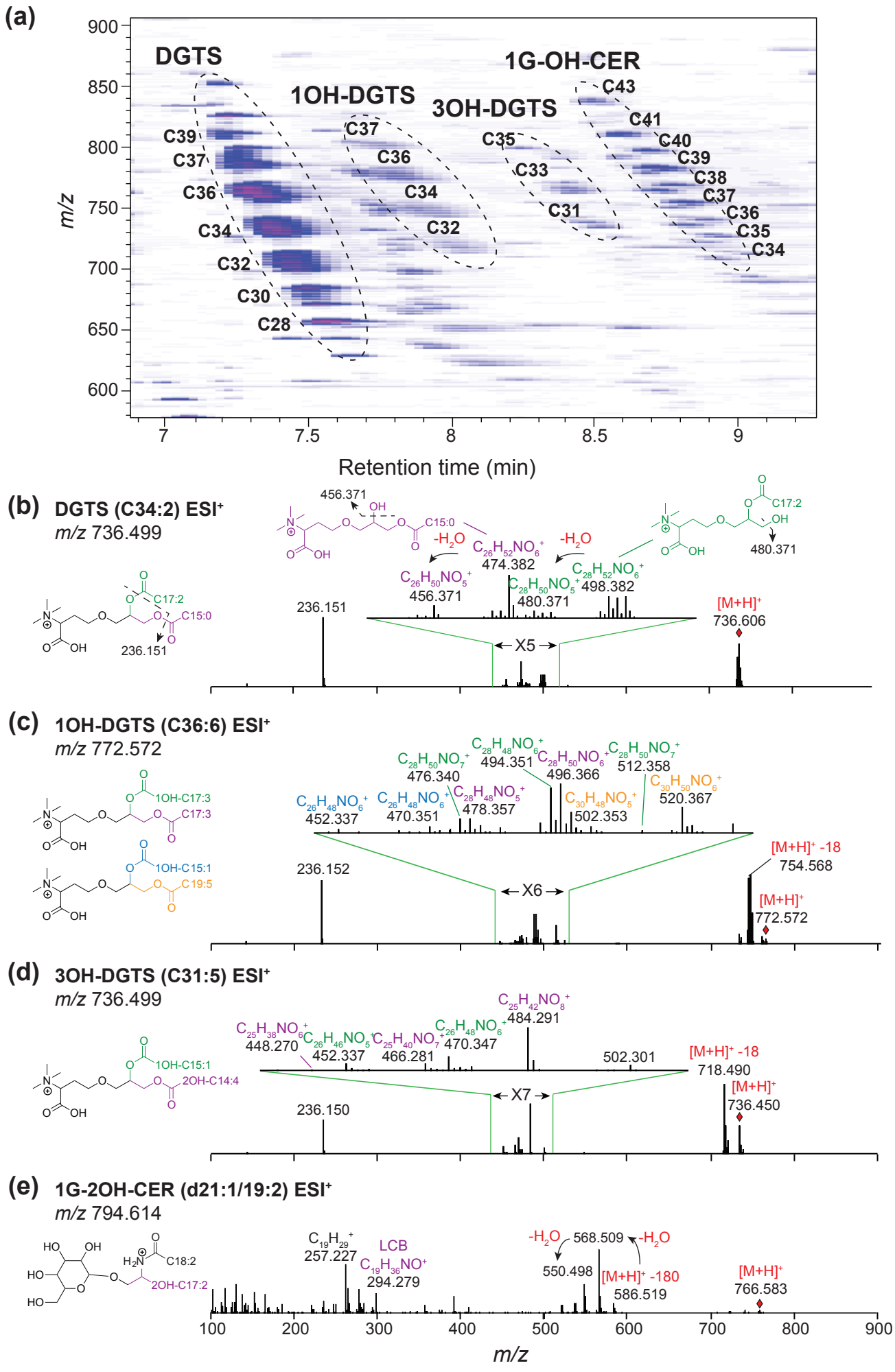
(a)
DGTS
1OH-DGTS
3OH-DGTS
1G-OH-CER
C39
C37
C36
C34
C32
C30
C28
C37
C36
C34
C32
C35
C33
C31
C43
C41
C40
C39
C38
C37
C36
C35
C34
m/z
Retention time (min)
(b) DGTS (C34:2) ESI+
m/z 736.499
C17:2
C15:0
236.151
456.371
-H2O
C26H52NO6+ 474.382
-H2O
C26H50NO5+ 456.371
C28H50NO5+ 480.371
C28H52NO6+ 498.382
480.371
236.151
X5
[M+H]+ 736.606
(c) 1OH-DGTS (C36:6) ESI+
m/z 772.572
1OH-C17:3
C17:3
1OH-C15:1
C19:5
C28H50NO7+ 476.340
C28H48NO6+ 494.351
C28H50NO6+ 496.366
C28H50NO7+ 512.358
C26H48NO6+ 452.337
C26H48NO6+ 470.351
C28H48NO5+ 478.357
C30H48NO5+ 502.353
C30H50NO6+ 520.367
236.152
X6
[M+H]+ -18 754.568
[M+H]+ 772.572
(d) 3OH-DGTS (C31:5) ESI+
m/z 736.499
1OH-C15:1
2OH-C14:4
C25H38NO6+ 448.270
C26H46NO5+ 452.337
C25H40NO7+ 466.281
C26H48NO6+ 470.347
C25H42NO8+ 484.291
502.301
236.150
X7
[M+H]+ -18 718.490
[M+H]+ 736.450
(e) 1G-2OH-CER (d21:1/19:2) ESI+
m/z 794.614
C18:2
2OH-C17:2
C19H29+ 257.227
LCB
C19H36NO+ 294.279
-H2O
568.509
-H2O
550.498
[M+H]+ -180 586.519
[M+H]+ 766.583
m/z

suppl.fig06

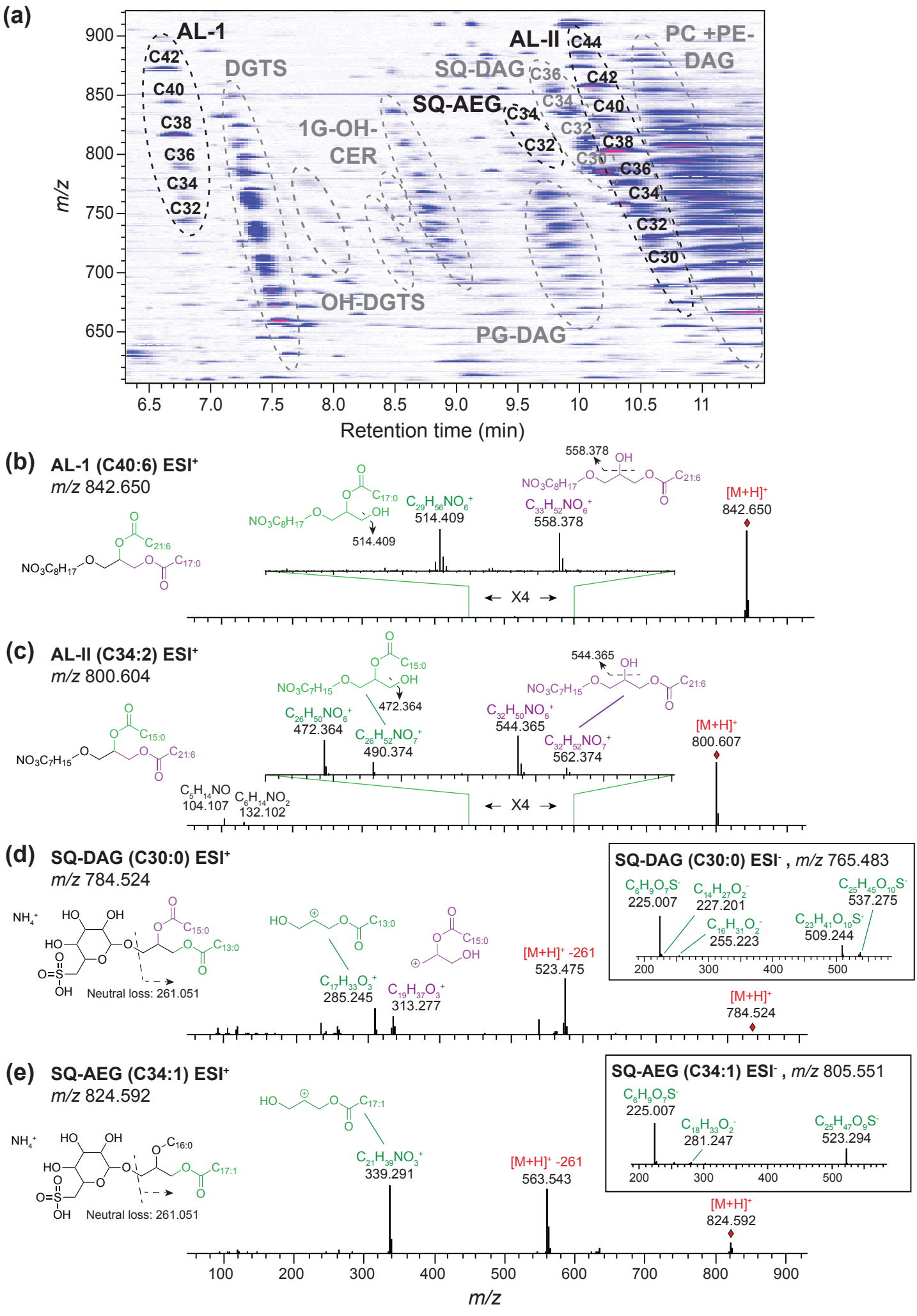
(a)
AL-1
C42
C40
C38
C36
C34
C32
DGTS
1G-OH-CER
OH-DGTS
SQ-DAG
SQ-AEG
AL-II
C44
C42
C40
C38
C36
C34
C32
C30
C36
C34
C32
PC +PE-DAG
PG-DAG
m/z
Retention time (min)
(b) AL-1 (C40:6) ESI+
m/z 842.650
514.409
558.378
842.650
X4
(c) AL-II (C34:2) ESI+
m/z 800.604
472.364
490.374
544.365
562.374
800.607
104.107
132.102
X4
(d) SQ-DAG (C30:0) ESI+
m/z 784.524
Neutral loss: 261.051
285.245
313.277
[M+H]+ -261
523.475
784.524
SQ-DAG (C30:0) ESI- , m/z 765.483
225.007
227.201
255.223
509.244
537.275
(e) SQ-AEG (C34:1) ESI+
m/z 824.592
Neutral loss: 261.051
339.291
[M+H]+ -261
563.543
824.592
SQ-AEG (C34:1) ESI- , m/z 805.551
225.007
281.247
523.294
m/z